



Universidad de Valladolid



DOCTORATE PROGRAM IN INDUSTRIAL
ENGINEERING

DOCTORAL THESIS:

**DETECTION, CLASSIFICATION AND
CHARACTERIZATION OF DEFECTS IN
PHOTOVOLTAIC MODULES THROUGH
THE USE OF THERMOGRAPHY,
ELECTROLUMINESCENCE, I-V CURVES
AND VISUAL ANALYSIS**

Presented by Sara Gallardo Saavedra
to qualify for the degree of
Doctor from the University of Valladolid

Directed by:
Luis Hernández Callejo
Óscar Duque Pérez



Universidad de Valladolid



PROGRAMA DE DOCTORADO EN INGENIERÍA
INDUSTRIAL

TESIS DOCTORAL:

**DETECCIÓN, CLASIFICACIÓN Y
CARACTERIZACIÓN DE DEFECTOS EN
MÓDULOS FOTOVOLTAICOS MEDIANTE
LA UTILIZACIÓN DE TERMOGRAFÍA,
ELECTROLUMINISCENCIA, CURVAS I-V Y
ANÁLISIS VISUALES**

Presentada por Sara Gallardo Saavedra
para optar al grado de
Doctora por la Universidad de Valladolid

Dirigida por:
Luis Hernández Callejo
Óscar Duque Pérez

A Mario

ACKNOWLEDGMENTS / AGRADECIMIENTOS

Me gustaría aprovechar esta página para expresar mi gratitud a todas las personas que han hecho posible la realización de esta tesis doctoral.

En primer lugar, quisiera dar las gracias a mis dos directores de tesis. Al Dr. Luis Hernández Callejo por su disponibilidad y dedicación, por todo lo que me ha enseñado y aconsejado, por confiar en mí y por su motivación e interés en la investigación, permitiendo a tantos estudiantes crecer, desarrollarse y completar su formación. Al Dr. Óscar Duque Pérez, por ayudarme siempre que lo he necesitado, por todos los conocimientos que me ha transmitido, por su dedicación, su criterio, su disponibilidad y su paciencia. Gracias a los dos por haberos esforzado por ayudarme a llegar al punto en el que hoy me encuentro.

Me gustaría agradecer a la Escuela de Ingeniería de la Industria Forestal, Agronómica y de la Bioenergía (EIFAB) por haberme dado la oportunidad de desarrollar mi tesis en el departamento de Ingeniería Agrícola y Forestal y por haberme facilitado los medios necesarios, así como a la Universidad de Valladolid, que ha hecho posible la realización de esta tesis doctoral gracias a su apoyo de financiación predoctoral.

Además, quiero expresar mi más profundo agradecimiento a todos los compañeros de la EIFAB, de GDS OPTRONLAB, del CIEMAT, de SOLARIG y al resto de profesionales que han colaborado conmigo durante estos cuatro años, por toda la sabiduría que me han transmitido, por los buenos momentos compartidos, por sus consejos, por estar a mi disposición siempre y ante todo, por su gran valor como personas.

Por último, quiero dar las gracias a los incondicionales, a mis pilares. Me gustaría agradecer a mis amigos por sus largas horas de compañía, consejos y alegría, a Mario su cariño durante todos estos años y de una forma muy especial a mis padres, César y Milagros, y a mi hermana, Elena, su incondicional apoyo y el ejemplo de esfuerzo y honestidad que siempre han sido para mí. Me siento afortunada porque sé que esta tesis doctoral existe gracias a las personas que me rodean, así que a todas ellas mi más sincero agradecimiento.

A todos ellos gracias.

'If I have seen further it is by standing on the shoulders of Giants.'

Isaac Newton.

PROLOGUE / PREÁMBULO

De acuerdo con la normativa vigente de presentación y defensa de la tesis doctoral (RESOLUCIÓN de 8 de junio de 2016, del Rectorado de la Universidad de Valladolid, por la que se ordena la publicación del Acuerdo del Consejo de Gobierno de 3 de junio de 2016, por el que se aprueba la normativa para la presentación y defensa de la tesis doctoral en la Universidad de Valladolid), esta Tesis Doctoral se presenta como compendio de publicaciones.

A continuación se indican los artículos publicados incluidos dentro del compendio de publicaciones que ha dado lugar a la tesis, los cuales se adjuntan en el CAP. 2 Artículos publicados. Los artículos se han organizado siguiendo el orden conceptual que da forma y sentido a la tesis doctoral.

Artículo 1: Aceptado y publicado.

Título: **Quantitative failure rates and modes analysis in photovoltaic plants.**

Revista: Energy, volumen 183, pp. 825-836 (2019).

DOI: <https://doi.org/10.1016/j.energy.2019.06.185>.

Autores: **Sara Gallardo Saavedra**, Luis Hernández Callejo y Óscar Duque Pérez.

Web of Science (WoS): Journal Citation Reports (JCR)
<i>Factor de impacto:</i> 5.537 (2018)
<i>Categoría y Ranking:</i> Energy & Fuels, Q1 (15/103)
Scimago Journal & Country Rank (SJR)
<i>Factor de impacto:</i> 2.05 (2018)
<i>Categoría y Ranking:</i> Energy, Q1 (5/136)

Artículo 2: Aceptado y publicado.

Título: **Failure rate determination and Failure Mode, Effect and Criticality Analysis (FMECA) based on historical data for photovoltaic plants.**

Proceedings congreso: ISES Conference Proceedings of the ISES Solar World Conference 2017 and the IEA SHC Solar Heating and Cooling Conference for Buildings and Industry 2017, pp. 1232-1239.

DOI: <https://doi.org/10.18086%2Fswc.2017.20.04>

Autores: **Sara Gallardo Saavedra**, Javier Pérez Moreno, Luis Hernández Callejo y Óscar Duque Pérez.

Artículo 3: Aceptado y publicado.

Título: **A review of photovoltaic systems: Design, operation and maintenance.**

Revista: Solar Energy, 188, pp. 426-440 (2019)

DOI: <https://doi.org/10.1016/j.solener.2019.06.017>

Autores: Luis Hernández Callejo, **Sara Gallardo Saavedra** y Víctor Alonso Gómez.

Web of Science (WoS): Journal Citation Reports (JCR)
<i>Factor de impacto:</i> 4.674 (2018)
<i>Categoría y Ranking:</i> Energy & Fuels, Q1 (24/103)
Scimago Journal & Country Rank (SJR)
<i>Factor de impacto:</i> 1.59 (2018)
<i>Categoría y Ranking:</i> Renewable Energy, Sustainability and the Environment, Q1 (26/330)

Artículo 4: Aceptado y publicado.

Título: **Simulation, validation and analysis of shading effects on a PV system.**

Revista: Solar Energy, 170, pp. 828-839 (2018).

DOI: <https://doi.org/10.1016%2Fj.solener.2018.06.035>.

Autores: **Sara Gallardo Saavedra** y Björn Karlsson.

Web of Science (WoS): Journal Citation Reports (JCR)
<i>Factor de impacto:</i> 4.674 (2018)
<i>Categoría y Ranking:</i> Energy & Fuels, Q1 (24/103)
Scimago Journal & Country Rank (SJR)
<i>Factor de impacto:</i> 1.59 (2018)
<i>Categoría y Ranking:</i> Renewable Energy, Sustainability and the Environment, Q1 (26/330)

Artículo 5: Aceptado y publicado.

Título: **Influence of large periods of DC current injection in c-Si photovoltaic panels.**

Proceedings congreso: Proceedings of the 36th European Photovoltaic Solar Energy Conference and Exhibition, pp.1079-1080 (2019).

ISBN: 3-936338-60-4.

Autores: Ángel Moretón Fernández, **Sara Gallardo Saavedra**, Marta María Jiménez Martín, Víctor Alonso Gómez, Luis Hernández Callejo, José Ignacio Morales Aragonés, Óscar Martínez Sacristán, Miguel Ángel González Rebollo and Juan Jiménez López.

Artículo 6: Aceptado y publicado.

Título: **Failure diagnosis on photovoltaic modules using visual inspection, thermography, electroluminescence and I-V techniques.**

Proceedings congreso: Proceedings of the 36th European Photovoltaic Solar Energy Conference and Exhibition, pp.1171-1175 (2019).

ISBN: 3-936338-60-4.

Autores: **Sara Gallardo Saavedra**, Ángel Moretón Fernández, Marta María Jiménez Martín, Víctor Alonso Gómez, Luis Hernández Callejo, Óscar Martínez Sacristán, Miguel Ángel González Rebollo and José Ignacio Morales Aragonés.

Artículo 7: Aceptado y publicado.

Título: **Merged images for fault detection in photovoltaic panels.**

Proceedings congreso: Proceedings of the II Ibero-American Congress of Smart Cities (ICSC-CITIES 2019), pp. 167-178 (2019).

ISBN: 978-958-5583-78-8.

Autores: **Sara Gallardo Saavedra**, Luis Hernández Callejo, Ponciano Jorge Escamilla Ambrosio and Víctor Alonso Gómez.

Artículo 8: Aceptado.

Título: **Nondestructive characterization of solar PV cells defects by means of electroluminescence, infrared thermography, I-V curves and visual tests: experimental study and comparison.**

Revista: Energy.

Autores: **Sara Gallardo Saavedra**, Luis Hernández Callejo, María del Carmen Alonso García, José Domingo Santos, José Ignacio Morales Aragonés, Víctor Alonso Gómez, Ángel Moretón Fernández, Miguel Ángel González Rebollo and Oscar Martínez Sacristán.

Web of Science (WoS): Journal Citation Reports (JCR)

Factor de impacto: 5.537 (2018)

Categoría y Ranking: Energy & Fuels, Q1 (15/103)

Scimago Journal & Country Rank (SJR)

Factor de impacto: 2.05 (2018)

Categoría y Ranking: Energy, Q1 (5/136)

Artículo 9: Aceptado y publicado.

Título: **Analysis and characterization of PV module defects by thermographic inspection.**

Revista: Facultad de Ingeniería Universidad de Antioquía, no.93, pp. 92-104, Oct-Dec 2019.

DOI: <https://doi.org/10.17533/udea.redin.20190517>

Autores: **Sara Gallardo Saavedra**, Luis Hernández Callejo y Óscar Duque Pérez.

Scimago Journal & Country Rank (SJR)
<i>Factor de impacto:</i> 0.156 (2018)
<i>Categoría y Ranking:</i> Engineering, Q3 (358/771)

Artículo 10: Aceptado y publicado.

Título: **Technological review of the instrumentation used in aerial thermographic inspection of photovoltaic plants.**

Revista: Renewable and sustainable energy reviews, 93, pp. 566-579 (2018).

DOI: <https://doi.org/10.1016%2Fj.rser.2018.05.027>

Autores: **Sara Gallardo Saavedra**, Luis Hernández Callejo y Óscar Duque Pérez.

Web of Science (WoS): Journal Citation Reports (JCR)
<i>Factor de impacto:</i> 10.556 (2018)
<i>Categoría y Ranking:</i> Green & Sustainable Science & Technology, Q1 (1/35)
Scimago Journal & Country Rank (SJR)
<i>Factor de impacto:</i> 3.29 (2018)
<i>Categoría y Ranking:</i> Renewable Energy, Sustainability and the Environment, Q1 (8/330)

Artículo 11: Aceptado y publicado.

Título: **Aerial Thermographic Inspection of Photovoltaic Plants: Analysis and Selection of the Equipment.**

Proceedings congreso: ISES Conference Proceedings of the ISES Solar World Conference 2017 and the IEA SHC Solar Heating and Cooling Conference for Buildings and Industry 2017, pp. 1223-1231.

DOI: <https://doi.org/10.18086%2Fswc.2017.20.03>

Autores: **Sara Gallardo Saavedra**, Estefanía Alfaro Mejía, Luis Hernández Callejo, Óscar Duque Pérez, Humberto Loaiza Correa and Edinson Franco Mejía.

Artículo 12: Aceptado.

Título: **Low-cost infrared thermography in aid of photovoltaic panels degradation research.**

Revista: Facultad de Ingeniería Universidad de Antioquía.

Autores: Miguel Dávila Sacoto, Luis Hernández Callejo, Víctor Alonso Gómez, **Sara Gallardo Saavedra** and Luis González Morales.

Scimago Journal & Country Rank (SJR)
<i>Factor de impacto:</i> 0.156 (2018)
<i>Categoría y Ranking:</i> Engineering, Q3 (358/771)

Artículo 13: Aceptado y publicado.

Título: **Image Resolution Influence in Aerial Thermographic Inspections of Photovoltaic Plants.**

Revista: IEEE Transactions on Industrial Informatics, vol. 14, no. 12, pp. 5678-5686, december 2018.

DOI: <https://doi.org/10.1109%2Ftii.2018.2865403>.

Autores: **Sara Gallardo Saavedra**, Luis Hernández Callejo y Óscar Duque Pérez.

Web of Science (WoS): Journal Citation Reports (JCR)
<i>Factor de impacto:</i> 7.377 (2018)
<i>Categoría y Ranking:</i> Engineering, Industrial, Q1 (1/46)
Scimago Journal & Country Rank (SJR)
<i>Factor de impacto:</i> 1.68 (2018)
<i>Categoría y Ranking:</i> Control and Systems Engineering, Q1 (19/759)

Además de los artículos incluidos en el compendio de publicaciones, en el Anexo 1 (Additional publications), también se incluyen otros trabajos realizados en el marco de esta línea de investigación.

Por último, se hace constar que el presente documento adopta el formato de Tesis Doctoral como compendio de publicaciones y por lo tanto consiste en una síntesis de los conceptos teóricos que sustentan los trabajos de investigación publicados en lugar del formato tradicional de documento extenso autocontenido.

ABSTRACT

The recent growth in renewable power capacity has been led by solar photovoltaics (PV), with more than half of the renewable power installed in 2018 of solar PV. Being able to detect, to identify and to quantify the severity of defects that appear within PV modules is essential to constitute a reliable, efficient and safety system, avoiding energy losses, mismatches and safety issues. Therefore, the idea of advanced Operation and Maintenance (O&M) is very attractive for the PV exploitation sector, since it will guarantee certain levels of efficiency in their PV plants. Different techniques has been traditionally used to detect PV modules anomalies, as visual inspections, manual Infrared Thermography (IRT) or electrical tests as the Current-Voltage curves (I-V curves). Technological advances allow the existence of innovative low-cost techniques, superseding time-consuming traditional manual methods.

This doctoral thesis presents an analysis of the detection, characterization and classification of defects in PV modules through the use of IRT, EL, I-V curves and visual analysis, focusing on three main threads. Firstly, the state of the art of PV sites is analyzed, including the investigation on the failure rates and modes in PV plants and the design, operation and maintenance of PV sites, highlighting the importance of the research on PV modules failures. Secondly, it has been performed the detection, characterization and classification of defects in PV modules, by means of: analyzing and comparing the experimental results obtained with the different inspection techniques, the generation of merged images, the development of simulation circuits, the study of the effect of Electroluminescence (EL) tests in the modules service life, a quantitative analysis and characterization of manufacturing, soldering and breaking PV defects and a classification of PV defects attending to failure patterns. Thirdly, regarding the analysis of aerial IRT as a novel inspection technique the main contributions of the work are three: to review the available equipment focusing on their desirable characteristic for their application on aerial thermographic inspection of PV sites, to review the most important aspects in the tests that should be taken into account in order to obtain valid results and to study the influence of the resolution of IRT images.

It is important to note that the research performed and the contributions presented have arisen from real needs proposed by operators, manufacturers and owners dedicated to the PV field, not only from Spain but also from several countries, which underlines the importance of the practical application of the study developed.

El reciente crecimiento que han experimentado las energías renovables ha sido liderado por la energía solar fotovoltaica (FV), siendo FV más de la mitad de la energía renovable instalada en 2018. Poder detectar, identificar y cuantificar la gravedad de los defectos en módulos es esencial para constituir sistemas fiables, eficientes y seguros, evitando pérdidas de energía, desajustes y problemas de seguridad. Por lo tanto, la idea de Operación y Mantenimiento avanzado (O&M) es muy atractiva para el sector de explotación FV, ya que garantizará ciertos niveles de eficiencia en sus plantas. Tradicionalmente se han utilizado diferentes técnicas para detectar anomalías en módulos FV, como inspecciones visuales, termografía manual o pruebas eléctricas (curvas I-V). Los avances tecnológicos permiten el desarrollo de técnicas innovadoras de bajo costo, mejorando los laboriosos métodos manuales tradicionales.

Esta tesis doctoral presenta un análisis de la detección, caracterización y clasificación de defectos en módulos FV mediante el uso de termografía infrarroja (IRT), EL, curvas I-V y análisis visual, enfocándose en tres líneas principales. En primer lugar, se analiza el estado del arte de los sistemas fotovoltaicos, incluyendo la investigación sobre las tasas y modos de fallo en plantas FV y el diseño, operación y mantenimiento de las plantas. En segundo lugar, se realiza la detección, caracterización y clasificación de defectos en módulos FV, mediante los siguientes enfoques: el análisis y comparación de los resultados experimentales obtenidos con las diferentes técnicas de inspección, la generación de imágenes fusionadas, el desarrollo de circuitos de simulación, el estudio del efecto de las pruebas de electroluminiscencia (EL) en la vida útil de los módulos, el análisis cuantitativo y caracterización de defectos de fabricación, soldadura y roturas en células solares y la clasificación de defectos en función de sus patrones de fallo. En tercer lugar, en referencia al análisis de la termografía aérea como nueva técnica de inspección, las principales contribuciones del trabajo son tres: revisar el equipamiento disponible, enfocándose en las características deseables para su aplicación en inspecciones termográficas aéreas de plantas FV, la revisión de los aspectos más importantes que deben tenerse en cuenta en las pruebas para obtener resultados válidos y el estudio de la influencia de la resolución de las imágenes IRT.

Es importante señalar que la investigación realizada y las contribuciones presentadas han surgido de necesidades reales propuestas por operadores, fabricantes y propietarios de instalaciones FV, no solo de España sino también de diversos países, lo cual enfatiza la importancia de la aplicación práctica del estudio desarrollado.

INDEX

ACKNOWLEDGMENTS / AGRADECIMIENTOS	VII
PROLOGUE / PREÁMBULO	IX
ABSTRACT	XV
RESUMEN.....	XVII
CHAP. 1 INTRODUCTION	23
1.1. Conceptual framework.....	24
1.2. Justification	28
1.3. Hypothesis and objectives	30
1.4. Collaborations with other research groups.....	31
1.5. Project phases and methodology.....	32
1.5.1. Project inception and theoretical grounding phase.....	33
1.5.2. Analytical-dimensioning phase	33
1.5.3. Empirical research phase	36
1.5.4. Analytical-comparative phase.....	46
1.5.5. Results dissemination phase.....	50
1.6. Results and discussion	51
1.6.1. Study of the state of the art (Obj. 1)	52
1.6.2. Detection, characterization and classification of defects in PV modules through the use of different inspection techniques (Obj. 2)	56
1.6.2.1. Detection of PV defects.....	56
1.6.2.2. Characterization of PV defects.....	61
1.6.2.3. Classification of PV defects.....	71
1.6.3. Analysis of aerial IRT as a novel inspection technique (Obj. 3)	75
1.7. References	80
1.8. Abbreviations	91
1.9. Index of figures.....	92

1.10. Index of tables.....	95
CHAP. 2 PUBLISHED PAPERS	97
2.1. Study of the state of the art (Obj. 1)	98
2.1.1. Quantitative failure rates and modes analysis in PV plants.....	99
2.1.2. Failure rate determination and Failure Mode, Effect and Criticality Analysis (FMECA) based on historical data for photovoltaic plants	101
2.1.3. A review of photovoltaic systems: design, operation and maintenance	103
2.2. Detection, characterization and classification of defects in PV modules through the use of different inspection techniques (Obj. 2).....	105
2.2.1. Simulation, validation and analysis of shading effects on a PV system	106
2.2.2. Influence of large periods of DC current injection in c-Si photovoltaic panels	108
2.2.3. Failure diagnosis on photovoltaic modules using visual inspection, thermography, electroluminescence and I-V techniques.....	110
2.2.4. Merged images for fault detection in photovoltaic panels.....	112
2.2.5. Nondestructive characterization of solar PV cells defects by means of electroluminescence, infrared thermography, I-V curves and visual tests: experimental study and comparison.....	114
2.2.6. Analysis and characterization of PV module defects by thermographic inspection.	116
2.3. Analysis of aerial thermography as a novel inspection technique (Obj. 3)	118
2.3.1. Technological review of the instrumentation used in aerial thermographic inspection of photovoltaic plants	119
2.3.2. Aerial thermographic inspection of photovoltaic plants: analysis and selection of the equipment	121
2.3.3. Low-cost infrared thermography in aid of photovoltaic panels degradation research	123

2.3.4. Image Resolution Influence in Aerial Thermographic Inspections of Photovoltaic Plants.....	125
CHAP. 3 CONCLUSIONS AND FUTURE WORK	127
3.1. Conclusions and PhD contributions	128
3.2. Future work.....	132
ANNEX A ADDITIONAL PUBLICATIONS.....	135

Chapter 1

INTRODUCTION

'Nothing in life is to be feared, it is only to be understood. Now is the time to understand more, so that we may fear less.'

Marie Curie.

This doctoral thesis begins with an introduction that justifies the thematic relationship of the publications presented in the “compendium of publications” and the relevance of their joint contribution. To do this, the Introduction chapter starts explaining the conceptual framework, followed by the justification of the thesis. Thirdly, the global and partial objectives pursued by the investigation are described. The collaborations carried out with other research groups are detailed below, in the fourth section. This gives way to the phases of the project and the explanation of the methodology used, in section five, for ending in section six with the summary of the main results obtained and their discussion.

1.1. Conceptual framework

Renewable energy is now a fully mainstream element in the global electricity mix. Alongside energy efficiency, renewables are playing a critical role in reducing emissions in the energy sector and in end-use sectors. In many locations, new renewable energy is now the lowest-cost way to provide electricity services and can be brought online the fastest. Around the world, renewable electricity has spread thanks to both transferable and reliable technologies and effective policy frameworks. The recent growth in renewable power capacity has been led by solar photovoltaics (PV), with 100 GW of new solar PV capacity installed in 2018 of the more than 180 GW of renewable power installed this year, reaching a total installed PV solar capacity of 505 GW [1,2].

Low-power PV solar plants are proliferating in recent decades, sometimes due to the lack of electricity supply at one site, sometimes due to their geographical conditions (for instance in islands) and others due to the simple fact of reducing energy dependence on fossils fuels and approaching quasi sustainability [3–5]. But in the same way that low-power PV solar plants are being installed, it is more than likely that large-scale ones are installed much more [6–9], since the need for large-scale power generation is a need, together with the interest of maximizing the benefit of the installation [10,11]. High-power PV solar plants have a common feature, which is that they are formed by a large number of PV solar modules [12,13], and it is expected that in the future they will increase in size (in power and number of modules) [14,15].

It is well-known that the cost of purchasing PV solar modules has drastically fallen in recent decades, and especially in recent years [16–18], which makes the idea of installing PV solar plants even more attractive. Almost all the efforts of the PV exploitation

are focusing on carrying out inspections of their plants (maintenance) that allow them to maintain their efficiency (operation), with the clear objective of obtaining high productivity levels. Therefore, the idea of advanced Operation and Maintenance (O&M) is very attractive for the PV exploitation sector, since it will guarantee certain levels of efficiency in their PV plants [19,20].

PV cells are basically made up of a PN junction. When sunlight hits the cell, the photons are absorbed by the semiconductor atoms, freeing electrons from the negative layer. This free electron finds its path through an external circuit toward the positive layer resulting in an electric current from the positive layer to the negative one [21]. Crystalline silicon (c-Si) solar cells have dominated the PV market since the very beginning in the 1950's. Silicon is non-toxic and abundantly available in the earth crust, silicon PV modules have shown their long-term stability over decades in practice [22,23]. Three major families of PV cells are monocrystalline technology, polycrystalline technology and thin-film technologies. For this reason, this research has been performed using monocrystalline and polycrystalline PV cells, although in the market exist other crystalline semiconductor based PV cells in a minority, as Germanium (Ge), Gallium Arsenide (GaAs), Cadmium Telluride (CdTe), or even more complex formulas, like Indium-Gallium-Arsenide (InGaAs) [13].

Defects at the PV solar cells level are really important, since these are the ones that make up the defects at the PV modules, being responsible for the reduction of efficiency, as well as their durability and reliability. There has been extensive research on the types of failures [24–29], as it would be interesting to have them classified and even being able to estimate them. The failures in the plants are numerous and very heterogeneous, so their research is a challenge of interest to the scientific world [30–32]. Faults can appear in manufacturing, transportation, installation and operation. Many different failure modes can appear at the module level. In [33] four different groups of failures found in PV modules are defined. In the first group, it is described the common failures to all PV modules divided in the following failure modes: delamination, back sheet adhesion loss, junction box failure and frame breakage. The second group includes the following failures in silicon wafer-based PV modules: EVA discoloration, cell cracks, snail tracks, burn marks, Potential Induced Degradation (PID), disconnected cell and string interconnect ribbons, defect bypass diode. The thin-film failures described in the third group are: micro arcs at glued connectors and shunt hot spots. And finally, the fourth group describes the following failures found in CdTe thin-film modules: front glass breakage and back contact degradation. In reference [34] different aging mechanisms

that take place in PV modules and their cause-effect links are presented, as discoloration, delamination, bubbles, coating degradation, corrosion, crack in the cells, ribbon and solder bonds degradation and broken interconnect, dust and soiling, PID, junction box and bypass diodes effects, localized heating phenomena and detachment of the frame. Ideally, PV cells with defects are identified and replaced during the manufacturing process, using methods such as ultrasound, infrared thermography or Electroluminescence (EL) imaging [35]. However, new defects may appear during transportation, installation and operation due to shadows, cracks, interconnection of modules, degradation or other problems [36]. These defective cells create inequalities in current density that can lead to huge currents across small areas, causing very high temperatures (hot spots) responsible for module degradation or even irreparable damage.

Different techniques can be used to detect and quantify PV modules anomalies. Traditionally, faulty modules or cells within a PV plant have been located by applying visual inspections, electrical tests like the Current-Voltage (I-V) curve test or manual Infrared Thermography (IRT). Visual inspection is efficient, cheap and quick, but only reveals some of the failures. For example, typical failures found during visual inspections according to IEC 61215 [37] are bubbles, delamination, yellowing and browning in the front of the module, broken cells or discolored anti reflection, burned or oxidized cells metallization, failures in the frame, delamination, bubbles, scratches or burn in the back of the module, loose, oxidation or corrosion in the junction box and detachment or exposed electrical parts in wires or connectors. Comprehensive knowledge of the properties of defects requires electrical characterization techniques providing some information about the defect concentration, spatial distribution or physical origin [38]. I-V curve provides important information about the electrical performance of the system, and its main parameters, but it cannot be performed in common operation. In order to be able to compare results, since it is not always possible to measure the curve in the Standard Test Conditions (STC), it is necessary to apply a translation procedure, which can be used in a certain range from the measured conditions [39]. An accurate I-V curve interpretation gives relevant information about the module failures, revealing degradation, mismatched modules, cracked cells, improper resistance, shadings or bypass diodes malfunction [40]. However, although it allows the identification of abnormal underperformance situations, it gives vague information to recognize the exact reason and the location of the faulty module or cell. Technological advances allow the existence of non-destructive diagnosis and even without contact. These diagnoses are

more effective and reduce time and costs. The fastest and least expensive technique is thermographic inspection (IRT), which is a technique that detects heat distribution in an evaluated area. This technique has the great advantage that it is applied with the PV plant in operation, measuring the characteristics of radiative heat in order to set areas or points with higher or lower heat emissivity, areas that could indicate the presence of a fault. It can be carried out in both indoor (dark) and outdoor (illuminated) conditions. Possible thermographic defects detected in a PV module are: cell hotspot, overheated bypass circuit, junction box, connection or whole module [40].

The need for advanced and intelligent devices for their application to PV solar plants is a necessity. Traditionally, faulty modules or cells within a PV plant have been located by applying electrical tests to the modules like the I-V curve test and/or manual IRT described, which has been seen that is a costly and time-consuming technique. Furthermore, rapid growth of PV power capacity, and the trend of constructing bigger PV sites with a higher capacity, have motivated research into maintenance of PV plants as it is unproductive doing the inspection manually, walking all around the PV site. Additionally, there are some situations in which applying manual IRT is really difficult or even impossible, as in plants with trackers, since the modules are almost horizontal in the central time of the day, in which the ambient conditions are optimal to perform the IRT, since the irradiance should be relatively constant and more than 600 W/m^2 [41], or in countries in which the fixed modules are constructed with a small inclination angle to optimize the land area, as in some Asian countries. All these things have been responsible of the development of innovative alternatives, such as the aerial IRT [40] using Unmanned Aerial Vehicles (UAVs), to enable or optimize maintenance activities. Several researchers have shown its real feasibility for detection of faults in PV modules [42,43,52–59,44–51] and, in relation to this issue, time reduction with regard to manual thermographic inspections, with an approximate inspection time of 5-8 minutes for a 1,000 kWp site using UAVs [45]. There is an intense research effort to automate data capture and post-processing steps in aerial IRT, which suggests a trend towards a fully automatic system [60–62].

A fourth method to analyze the system condition is EL, which can be used in the manufacturing process, shipped to a lab after unmounting the modules from the site or on the field, with a structure or specific tripod or also by means of EL cameras mounted on UAVs. In this case, by means of this non-invasive technique, the radiative recombination of charge carriers causes light emission in the solar cells, which is captured by an EL camera and the emission intensity serves as an indicator of the

Detection, classification and characterization of defects in photovoltaic modules through the use of thermography, electroluminescence, I-V curves and visual analysis

healthiness of the solar cell [63]. The high resolution of the EL images enables resolving some defects more precisely than in IR images [64]. According to [65], IRT and EL imaging are efficient and powerful methods for the characterization of PV panels. As it has been seen, each of these techniques has some advantages and disadvantages, and based on them, PV plant operators usually apply only one or two of these techniques within the O&M activities.

Something that seems to fit in the advances in O&M is the use of techniques based on Artificial Intelligence (AI), to be able to guarantee the early detection of failures, or the increase of the energy efficiency of PV solar plants [66–70]. However, to be able to automatically detect the faults, it is prior necessary to analyze the patterns of the different defects.

1.2. Justification

As previously explained the maintenance of PV plants is one of the highest investment costs that this kind of systems present. In addition, the rapid growth of the PV power capacity installed worldwide and the trend of constructing bigger PV sites during the last years makes its maintenance a fundamental factor to obtain reliable and safe energy, preventing their energy losses. In utility scale PV plants, typically the monitoring system trails the string series current of multiple modules connected, or even the inverter current, which is the sum of the parallel string current, and does not track the performance of the individual PV modules, which is the key element on a PV system as it converts the incident irradiance into electric power and their operation will affect the overall plant performance. Therefore, PV module alarms are not frequently automatically generated being especially complicated the detection of failures at this level and even more difficult the recognition of the failure cause and mode. PV module's cost is commonly upon 50% of the total PV installations cost [71]. All these facts support the need to investigate this type of defects, which justifies the doctoral research presented in this document.

In this context, it is needed research on maintenance techniques that minimize costs and human labor. Likewise, it has been illustrated the worldwide trend towards the production of alternative energies. Especially, and due to the advantages it presents, PV energy leads this trend. Therefore, it is essential to obtain this energy safely and efficiently.

This doctoral thesis focuses on the detection, characterization and classification of PV defects by means of different inspection techniques: IRT, EL, I-V curves and visual analysis. The aim is to study the failures in solar PV cells and modules, detecting them with different inspection techniques, and the analysis and comparison between the results obtained, finding synergies, in order to facilitate the identification and classification of the different anomalies, quantifying their severity and characterizing different defects. The analysis of patterns of each of the different defects, studying location within the module, size, shape and temperature statistical results as well as their characterization and classification, can be useful as a base to develop the patterns of the different kind of defects in a software to automatically detect if a module has an anomaly and its classification, substantially reducing the image processing costs. Additionally, the research efforts are focused on the analysis of aerial IRT inspections as a novel technique for PV defects detection, which minimize costs and human labor respect the traditional techniques used.

The doctoral thesis has been mainly accomplished in the Department of Agricultural and Forestry Engineering of the School of Forestry, Agronomic and Bioenergy Industry Engineering (EIFAB) at the Campus Duques de Soria of the University of Valladolid (UVa). Although scientists of the department had no extensive experience in this field before the beginning of the research because of its novelty, in the framework of this thesis numerous advances have been made, obtaining financing through several differentiated projects and taking advantage of synergies with other departments and centers. Specifically, a research group has been formed with the Optronlab GdS of the Department of Physics of Condensed Matter of the Uva, a Consolidated Research Unit of Castilla y León (No. UIC051), specialized in the microscopic analysis of various semiconductors, devices (LEDs, laser diodes, etc.), and semiconductor nanostructures. The group has extensive experience in semiconductors of group IV (Si, Ge and its SiGe alloy), group III-V (GaAs, InP, InGaP, etc.) and group II-VI (CdTe, CdS, etc.), using optical techniques. In recent years the group has also focused on the characterization of PV wafers and solar cells of various materials, for which it has been equipped with a wide range of complementary, optical and electrical characterization techniques, adapted to this type of studies. The members of the research group have extensive experience in regional, national, and international projects, having also participated as researchers in various European Projects, as well as projects with different companies. Together with Optronlab GdS, the following projects have been achieved in the last years: ENE2017-89561-C4-R-3 and RTC-2017-6712-3 of the Spanish Ministry of Science, Innovation and Universities.

Continuing with this research line, the natural next step, which is planned to be proposed for the postdoctoral period, is to address the needs of future PV solar plants, for which automated fault detection processes will be designed, which will be based on the classic inspection techniques analyzed in this thesis (IRT, EL, I-V curves and visual images) complemented with AI, using UAVs and other advanced smart devices.

1.3. Hypothesis and objectives

The thesis is based on the **hypothesis** that it is possible to avoid the on-site tasks focused on the diagnosis of PV modules of the maintenance personnel of PV plants, or to minimize it to a great extent, with the consequent reduction of maintenance costs. Additionally, it is also hypothesized that it is possible to produce reliable and safe energy and increase the performance of the installation if the defects at the PV module and cell levels are correctly identified, characterized and quantified and the appropriated measures are taken.

To contribute with this goal, the **main objective** of this doctoral thesis is the detection, classification and characterization of defects in PV modules through the use of IRT, EL, I-V curves and visual analysis. To achieve this general objective, the fulfillment of **three partial objectives** is required:

1. **Objective 1 (Obj. 1)** Study of the state of the art, including the analysis of failure rates and modes in PV plants and a review of PV systems attending their design, operation and maintenance. This allows the understanding of the level of development of PV sites and of the use of different techniques at present, determining the key points to be analyzed and highlighting the importance of the research.
2. **Objective 2 (Obj. 2)** Detection, characterization and classification of defects in PV modules through the use of different inspection techniques. This objective comprises the use of IRT, EL, I-V curves and visual analysis for defects detection, the comparison between different techniques and the characterization of solar PV cells defects. Once the failures have been detected, it is proposed to give a more thorough diagnosis of the causes of failure and their severity classifying the defects. For this, a broad database based on experimental thermographic measurements at field level on modules with hot spots has been developed, in order to identify the different failure modes that the modules can develop and the

patterns of each of the modes of failure. This database will greatly minimize the need for field checks of each of the modules with hot spots, significantly reducing maintenance costs of PV plants. To facilitate the understanding of the different failure mechanisms and their effects on the performance of the PV module, simulations of the electrical model of a module have been carried out using LTSpice program.

- 3. Objective 3 (Obj. 3)** Analysis of aerial IRT as a novel inspection technique. The huge size of newer PV plants makes development of innovative techniques necessary, such as the aerial IRT, to enable or to optimize maintenance activities. This partial objective includes the review of the instrumentation used in aerial thermographic inspections and the analysis of the best flight conditions taking into account several factors, such as the height of flight, air speed, image resolution, the position of the camera with respect to the module surface, image angle and its dependence on weather conditions, or drone positioning in the plant, among others.

The papers and contributions done throughout this doctoral thesis that cover the objectives detailed are presented in Chapter 2, Published papers. It has been structured in three subchapters, corresponding each of them with the publications related to each of the three partial objectives established.

1.4. Collaborations with other research groups

As it has been detailed, the doctoral thesis has been mainly accomplished in the Department of Agricultural and Forestry Engineering EIFAB at the Campus Duques de Soria of the Uva. However, it has been given importance to the search for synergies with other research centers or groups whose collaboration would enrich the research results. Therefore, there have been different collaborations with other organizations and stays in other institutions, which are detailed in this section.

During the first year of the doctoral thesis, there has been a collaboration with the Department of Building, Energy and Environmental Engineering of the Faculty of Engineering and Sustainable Development at the University of Gävle, in Sweden, based on the simulation of the electrical model of a module to analyze the influence of defects and shading on the power of a PV string.

Detection, classification and characterization of defects in photovoltaic modules through the use of thermography, electroluminescence, I-V curves and visual analysis

Additionally, for the analysis of the equipment used in aerial thermographic inspections, the first year of the thesis there has also been a collaboration with the School of Electrical and Electronic Engineering of the Valle University in Colombia.

From the second year of the doctoral period, the PhD labor has been focused as part of the working group for the research projects ENE2017-89561-C4-R-3 and RTC-2017-6712-3 of the Spanish Ministry of Science, Innovation and Universities, in collaboration with GdS-Optronlab group.

During the third year, it has been cooperation with the National Polytechnic Institute of Mexico for the processing of EL and thermographic merged images and with the Department of Electrical Engineering of the Faculty of Engineering of the University of Cuenca, in Ecuador, for the low-cost IRT application.

Throughout the fourth year of the doctoral thesis, a three-month stay in the Photovoltaic Solar Energy Unit at the Energy department of the Center for Energy, Environmental and Technological Research (CIEMAT) in Madrid has been accomplished. There, all the specialized PV equipment of the center has been accessible for the defects characterization and for the inspection techniques comparison.

The renewable energies investigation group at the EIFAB has a research collaboration agreement with Solarig, a worldwide operating company with more than 4,000 MW distributed in twenty countries in four continents, that has contributed during the entire doctoral thesis with access to some sites to perform on-site measurements, documentation and experimental data of the operation of its PV plants.

1.5. Project phases and methodology

This section explains the methodology followed in the development of the doctoral thesis divided into the five different phases of the project. This section starts with the first phase, the project inception and theoretical grounding, followed by the analytical-dimensioning phase. These two phases allow the understanding of the level of development of PV sites and of the use of different techniques at present, determining the key points to be analyzed and highlighting the importance of the research. The third phase is the empirical research, which comprises the empirical objective and field work. In this phase, the design, development and validation of the different campaigns of measures necessary to carry out the research project are carried out. The fourth phase,

the analytical comparative phase, is focused on extracting results and drawing conclusions from the empirical data. Finally, the last phase details the dissemination of the results of the research performed.

1.5.1. Project inception and theoretical grounding phase

The research work has a first theoretical-analytical phase. The collection of theoretical information is based primarily on peer-reviewed articles published in scientific journals, prioritizing those with high impact factor, as well as books and other sources of information such as conference or congress articles. The library from the UVa (both physically and through the website) has made most of these means accessible. Additionally, it is also remarkable the countless equipment manufacturers, resellers and professional operators who have contributed to the state-of-the-art review, showing the latest trends and key points for the specific cases studied.

In this theoretical phase, it has been reviewed, analyzed and synthesized the following information (in parentheses it is indicated the thesis objective related with each theoretical study):

- Failure rates and modes in PV systems (Obj. 1).
- Design, operation and maintenance of PV plants (Obj. 1).
- Typology and relevance of defects at the module level (Obj. 1 and Obj. 2).
- State of the art of PV module inspection techniques (Obj. 2 and Obj. 3).
- Modelling of solar cells (Obj. 2).
- Aerial thermographic inspection of PV plant related work (Obj. 3).
- Instrumentation requirements to carry out aerial inspections, including the study of the most suitable characteristics for this application (Obj. 3).
- Analysis of the best flight conditions and influencing factors (Obj. 3).

This phase has been mainly completed in the Department of Agricultural and Forestry Engineering of the EIFAB.

1.5.2. Analytical-dimensioning phase

Within the study of the state of the art (Obj. 1), it is included the analysis of the failures rates and modes in PV plants for the dimensioning of the problem studied. To complete this phase, the alarms in a PV portfolio have been analyzed, corresponding to the ones generated during five years (2012-2016) in sixty-three different PV sites distributed along Italy and Spain, from the smallest of 200 kW to the highest of 10,000 kW. The data has been obtained through the PV plants monitoring systems and the

Detection, classification and characterization of defects in photovoltaic modules through the use of thermography, electroluminescence, I-V curves and visual analysis

feedback of the field technicians, which feed the Computerized Maintenance Management Systems (CMMS) of the operator. With this information, it has been performed a quantitative analysis of failure rates and modes in PV plants and a Failure Rate, Effect and Criticality Analysis (FMECA) based on PV plants historical data.

For the quantitative analysis of failure rates and modes, the PV portfolio has been divided into five different groups depending on their Power (p): $p \leq 750$ kW, $750 < p \leq 995$ kW, $995 < p \leq 1,300$ kW, $1,300 < p \leq 2,300$ kW and $1,300 < p \leq 10,000$ kW. The main information that can be obtained from the CMMS of each of the alarms is listed right after: state, ID alarm number, type, name, PV plant, country, element affected, element affected code, activation time, repercussion, priority, deactivation time, technician, cause, description, actions performed and report state. In order to process the data, the PV system has been simplified considering the main groups of elements that compose a PV site: PV generator, inverter, Medium Voltage (MV) transformer station, metering elements, security system, communication system, monitoring system, grid and civil works. Along the paper, different statistical indicators are used, as the mean, the typical deviation and the Mean Time Between Failures (MTBF). The latter can be defined as the mean exposure time between consecutive failures of a component. It can be estimated by dividing the exposure time by the number of failures in that period, provided that enough failures have occurred in that period [72]. It has been calculated using the following (Eq. 1). Further information about this study methodology can be found in the paper presented in subsection 2.1.1.

$$MTBF = \frac{\text{Power [kW]}}{\frac{\text{Number of failures [#failures]}}{\text{Period [year]}}} \quad \text{(Eq. 1)}$$

Additionally, for the FMECA, the failure rates, the MTBF and the subjective evaluations of solar experts with more than a decade experience are used to define three ranking criterions: Severity, Detection and Occurrence. The Occurrence based on the failure rates calculated is classified following this criterion: 1 for unlikely failures, 2 for remote probability, 3 for occasional probability, 4 for moderate probability and 5 for high probability. Each ranking follows a scale from 1 to 5, in which 1 denotes the best situation while 5 denotes the worst. As a result, the Risk Priority Number (RPN) goes from 1 to 125, where a highest value of RPN indicates a most risky situation. Finally, thermographic tests have been applied at a module level to complete the FMECA of the whole PV Plant. Further information about this study methodology can be found in the paper presented in subsection 2.1.2.

Table 1: Severity ranking intervals calculated from the fixing price and the loss of profit that a failure produces

		Loss of Profit (LOP)				
		57.000 €	13.300 €	950 €	190 €	- €
Fixing Price (Spares and Workforce)	60.000 €	117,000 €	73,300 €	60,950 €	60,190 €	60,000 €
	15.000 €	72,000 €	28,300 €	15,950 €	15,190 €	15,000 €
	1.000 €	58,000 €	14,300 €	1,950 €	1,190 €	1,000 €
	500 €	57,500 €	13,800 €	1,450 €	690 €	500 €
	- €	57,000 €	13,300 €	950 €	190 €	0 €

Table 2: Severity ranking criteria

Rank	X (Fixing Cost + LOP)	Description
1	$X < 690 \text{ €}$	Minor failure with almost no influence in the performance of the plant and insignificant parts deterioration
2	$1,950 \text{ €} < X < 690 \text{ €}$	Failure with low influence in the performance of the plant and parts deterioration
3	$28,300 \text{ €} < X < 1,950 \text{ €}$	Failure with quite important influence in the performance of the plant and parts deterioration
4	$60,950 \text{ €} < X < 28,300 \text{ €}$	Failure with important influence in the performance of the plant and parts deterioration
5	$X > 60,950 \text{ €}$	Major failure with extreme influence in the performance of the plant and parts deterioration

Table 3: Detection ranking criteria following [73].

Rank	Description
1	Almost certain that the problem will be detected (chance 81–100%)
2	High probability that the problem will be detected (chance 61–80%)
3	Moderate probability that the problem will be detected (chance 41–60%)
4	Low probability that the problem will be detected (chance 21–40%)
5	None/minimal probability that the problem will be detected (chance 0–20%)

This phase has also been mainly completed in the Department of Agricultural and Forestry Engineering of the EIFAB in collaboration with Solarig.

1.5.3. Empirical research phase

Subsequent stages comprise the empirical objective, including the fieldwork and the analysis and treatment of the data and images obtained. This subsection expounds the methodology used in this phase, and it has been divided considering the facilities, instrumentation and experimental techniques and the modules tested.

- **Facilities, instrumentation and experimental techniques**

To facilitate the understanding of different failure mechanisms and their effects on the performance of the PV module, simulation, validation and analysis of the electrical model of faulty and shaded modules have been carried out. This research has been performed in collaboration with the Department of Building, Energy and Environmental Engineering of the Faculty of Engineering and Sustainable Development at the University of Gävle, in Sweden. There, two different kinds of tests have been done to validate the simulation results: to a string of six modules and to an individual module at Högskolan i Gävle (HIG) laboratory. In each group, seven different configurations have been studied. These cases start from the reference case, in which any cell is defective or any shading has been induced in the module. After that, an opaque tape is added to generate the shading or simulate the cells defects. The string of modules can be seen in the upper left part of Figure 9 and one of the seven shading configurations studied is presented in Figure 10. For all the shading configurations tested, the benefits of installing optimizers in each module will be considered and detailed in the discussion. The DC-DC optimizers installed at HIG laboratory are dual maximizers model MM-2ES 50 of Tigo Energy manufacturer. Further information about this study methodology can be found in the paper presented in subsection 2.2.1.

An important part of the experimental investigations for failure diagnosis on PV modules using visual inspection, IRT, EL and I-V techniques have been performed in the EIFAB facilities, at the Campus Duques de Soria of the Uva. There, indoor and outdoor tests have been conducted. Between the indoor tests, EL has been performed in controlled ambient conditions simultaneously than IRT in the fourth quadrant. For these tests, the University has a temperature and humidity controlled chamber, which is shown in Figure 1. In this chamber, each module is continuously fed with its short circuit current, using a laboratory source, during 72 hours. EL images are captured with a PCO 1300 camera each 30 minutes with an exposure of 5,000 ms. Thermal images have been captured with a Flir C2 system and a Workswell Wiris Pro camera. This capturing system

is presented in Figure 2, in which can be seen the EL camera, the IR camera and the PC which control the acquisition.



Figure 1: Temperature and humidity controlled chamber at the EIFAB in Soria, Spain

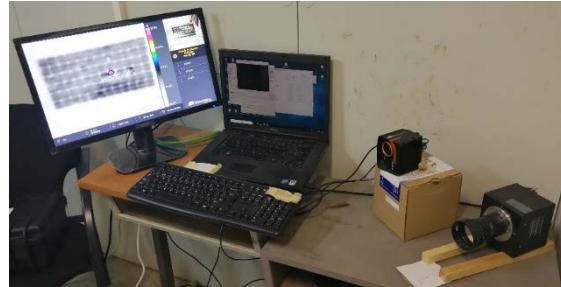


Figure 2: EL and IR imaging capturing system used in the temperature and humidity controlled chamber

Outdoor tests include I-V curves, IRT and Red, Green Blue (RGB) images in the PV field of the Campus Duques de Soria, which can be seen in Figure 3. The thermal camera used outdoor is a Workswell Wiris Pro camera, with a 640x512 pixels resolution, a thermal sensitivity of 0.05°C and an accuracy of $\pm 2\%$ o $\pm 2^\circ\text{C}$. Additionally, the camera has a frame rate of 30Hz, is calibrated to be used with two different lenses, 32° y 69°, and includes a Full HD RGB sensor with a resolution of 1920x1080 pixels and x10 zoom. The I-V curves have been traced using an IV HT 1500V Solar I-V tracer.



Figure 3: PV field of the Campus Duques de Soria, University of Valladolid.

The results obtained throughout these empirical assessments have been used to feed the studies performed on the influence of large periods of Direct Current (DC) injection in c-Si PV panels (subsection 2.2.2), failure diagnosis on PV modules using

Detection, classification and characterization of defects in photovoltaic modules through the use of thermography, electroluminescence, I-V curves and visual analysis

visual inspection, IRT, EL and I-V techniques (subsection 2.2.3) and merging EL and thermographic images (subsection 2.2.4).

The nondestructive characterization of solar PV cells defects by means of EL, IRT, I-V curves and visual tests has been performed in the Photovoltaic Solar Energy Unit at the Energy department of CIEMAT, in Madrid. Firstly, the indoor measurements have been performed in the Solar Simulator Pasan SunSim 3CM, class A, flash type. Starting with the I-V curves acquisition at two different irradiance levels, $1,000 \text{ W/m}^2$ and 100 W/m^2 , with temperature controlled conditions of $25 \pm 0.5^\circ\text{C}$. The second irradiation level has been chosen to characterize the defects behavior in low irradiation conditions. With the objective of better characterizing the defects behavior, EL tests to individual cells have been performed to identify the light emission caused by radiative recombination of carriers in each case. During this EL test, the temperature of the different cells has been measured with IRT. In this case, the module is fed with a power source and the EL and IR images are captured with a PCO 1300 and a FLIR SC 640 camera, respectively. EL tests to individual defective cells have been performed at the Isc injected current, 8.9 A, a focal distance of 4 cm and exposure time of 40 s. EL tests to the whole module have been performed at two injected current levels, 8.9 A and 0.89 A, with a focal distance of 4 cm and exposure time 50 s and 15 min, respectively. This image acquisition is presented in Figure 4. RGB images of the module have been taken with a Nikon D80 camera and images in detail of defects in the PV laboratory at the CIEMAT in Madrid with a Nikon SMZ 800 microscope. Finally, IRT has also been performed outdoor using the same IR camera, as presented in Figure 5.



Figure 4: Set up of the EL and IRT cameras for the indoor tests at the Photovoltaic Solar Energy Unit of the CIEMAT, in Madrid.



Figure 5: Outdoor IRT testing bench at the Photovoltaic Solar Energy Unit of the CIEMAT, in Madrid.

These images have been taken in the lower current step of the I-V curve at 7.3A-24 V and in the middle current step of the I-V curve at 7.8 A-15 V at 933 W/m². Further information about this study methodology can be found in the paper presented in subsection 2.2.5.

Within the objectives, once the different techniques have been used and analyzed, it is proposed to give a more thorough diagnosis of the causes of failure and their severity. For this, a broad database based on experimental thermographic measurements at field level on modules with hot spots has been developed, in order to identify the different failure modes that the modules can develop and the patterns of each of the modes of failure. This research has been performed in a 3 MW capacity PV site (17,142 modules), located in Spain, in Castilla y León region, in collaboration with Solarig. The thermographic inspection has been performed using the traditional manual IRT method, walking all around the PV site inspecting each module with the thermographic camera. The manual camera used was a Testo 870-2. The manual camera used captures visual RGB images simultaneously to thermographic images, allowing certifying the detected failures during the post-processing steps and avoiding false positives. However, the presence of false positives is less significant in case of manual inspection, as specialists performing inspections on site can check the presence of shadows or dirt in modules during the inspection. Every single failure detected during the inspection regardless of its temperature, was registered, identified and reported. The time needed to complete this inspection has been 34 working days; and to post-process and to analyze the results, 26 working days. More information about this analysis and characterization of PV module defects by thermographic inspection is presented in subsection 2.2.6.

The experimental tests for the analysis of the image resolution influence in aerial thermographic inspections of PV plants have been performed in the same 3 MW PV site than the previous analysis. Three different tests have been performed on the entire site to study the influence of the resolution on aerial thermographic inspections.

- Traditional manual IRT method, walking all around the PV site inspecting each module with the thermographic camera (it has been used the information from the inspection detailed above for the thermographic failures characterization and classification).
- The second and third thermographic inspections were carried out on the 4th of August of 2017 using aerial thermographic inspection. This technique consists of a UAV transporting a thermographic camera specially designed to

be integrated into aerial vehicles. These aerial inspections were performed at 30 m and 80 m from the ground level respectively. These heights have been selected with the objective of obtaining results that clearly show the impact of Spatial Resolution. With this aim, and considering that the available manual images already have a high resolution, it has been selected 30 m of elevation that provides a pixel size of 3.9 cm x 3.9 cm, which is within the acceptable range for this application (considering an acceptable pixel of 3 cm to 5 cm) and 80 m, that results in a pixel of 10.4 cm x 10.4 cm, out of this acceptable range. Both inspections were performed in 3 hours, considering all the time needed on-site to prepare and mount the equipment, prepare the inspection based on the previously prepared flight plan, taking off and landing, changing the batteries and downloading the images. The UAV used to deliver the FLIR TAU 2 thermographic sensor and the black edition go pro +3 RGB camera during the inspections is presented in Figure 6. It is a hexacopter model DJI S900, prepared to fly with the RGB and the thermographic cameras at the same time, in addition to other telemetry sensors. A hexacopter was chosen since they are more powerful than quadcopters, allowing the transportation of heavier payloads and being safer.



Figure 6: Equipment used in the aerial inspections to the 3 MW PV site, composed by a thermographic camera FLIR TAU 2 640 on board of a hexacopter DJI S900. At the back the STREAM monocrystalline modules with two portrait distribution.

Additionally, a fourth test was accomplished to six faulty modules, which were selected in detail from the results obtained in the previous tests, in order to clarify the results obtained. It consists on capturing manual images of six different failures at twelve different distances with the Testo 870-2 thermographic camera. More than 250 images were taken in this fourth test in order to study the distribution of temperatures within a PV cell hotspot and to compare the temperature obtained for different hotspots the same

day, with the same environmental conditions at twelve different distances, revealing how the resolution affects the results. Further information about this study methodology can be found in the paper presented in subsection 2.3.4.

The low-cost IRT application has been studied in cooperation with the Department of Electrical Engineering of the Faculty of Engineering of the University of Cuenca, in Ecuador, in which thermographic analysis with different cameras and I-V curves have been captured. University of Cuenca's solar farm has 35 kWp installed, with a total of 160 modules, and it has been under production since 2016. After manual inspection of all these modules, only two were found with hot spots. These anomalies have been further studied with a Flir One Pro, a Cat S60 and a Flir TG167 cameras, obtaining temperature tables, image reconstruction intensity graphs, X-Y dispersion of the thermal images, three-dimensional mesh, contours of the three-dimensional mesh of the thermal image and standard grayscale static images. Results have been validated using a Solmetric PVA-600 IV tracer [74] and DS18B20 temperature sensors (Figure 7).



Figure 7: Temperature sensor matrix validation (a) Setup (b) Sensors deployed.

Additionally, the Cat S60 camera has been mounted onboard a DJI Mavic Pro drone and used as proof of concept in order to verify if this camera can show the hot spot on the faulty panel (Figure 8). Further information about this study methodology can be found in the paper presented in subsection 2.3.3.

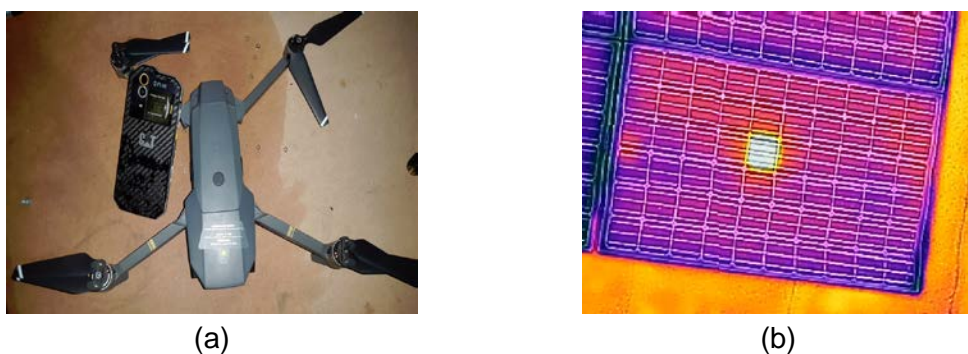


Figure 8: Solar panel IRT with drone (a) Cat S60 thermal camera and DJI Mavic Pro drone (b) captured image.

- **Tested modules**

The PV installations at Höskolan i Gävle (HIG) laboratory, in Sweden, are presented below in Figure 9 and Figure 10. The string of six modules is monocrystalline EOPLLY 125MF / 72 200W and the individual module is a monocrystalline Windon 265W.

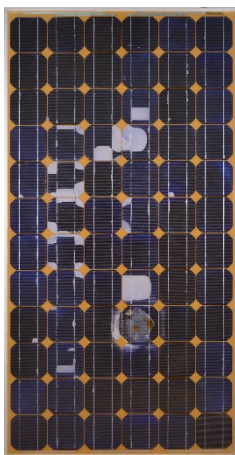


Figure 9: String of six modules with bypass diodes at HIG laboratory.

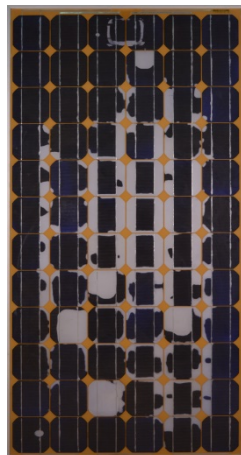


Figure 10: One of the shading cases studied (37% of a row shaded in three modules).

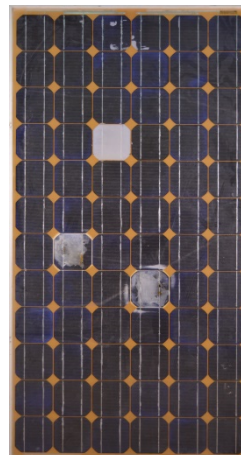
The modules tested in the EIFAB facilities, presented in Figure 11, present different kinds of defects and they are mono and poly crystalline modules from different manufacturers.



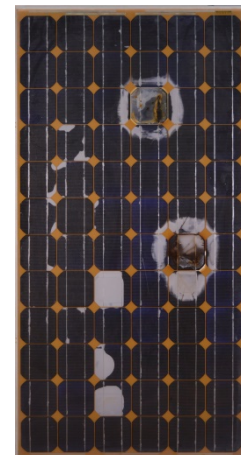
(a) E-3



(b) E-8



(c) S-E2



(d) S-E3

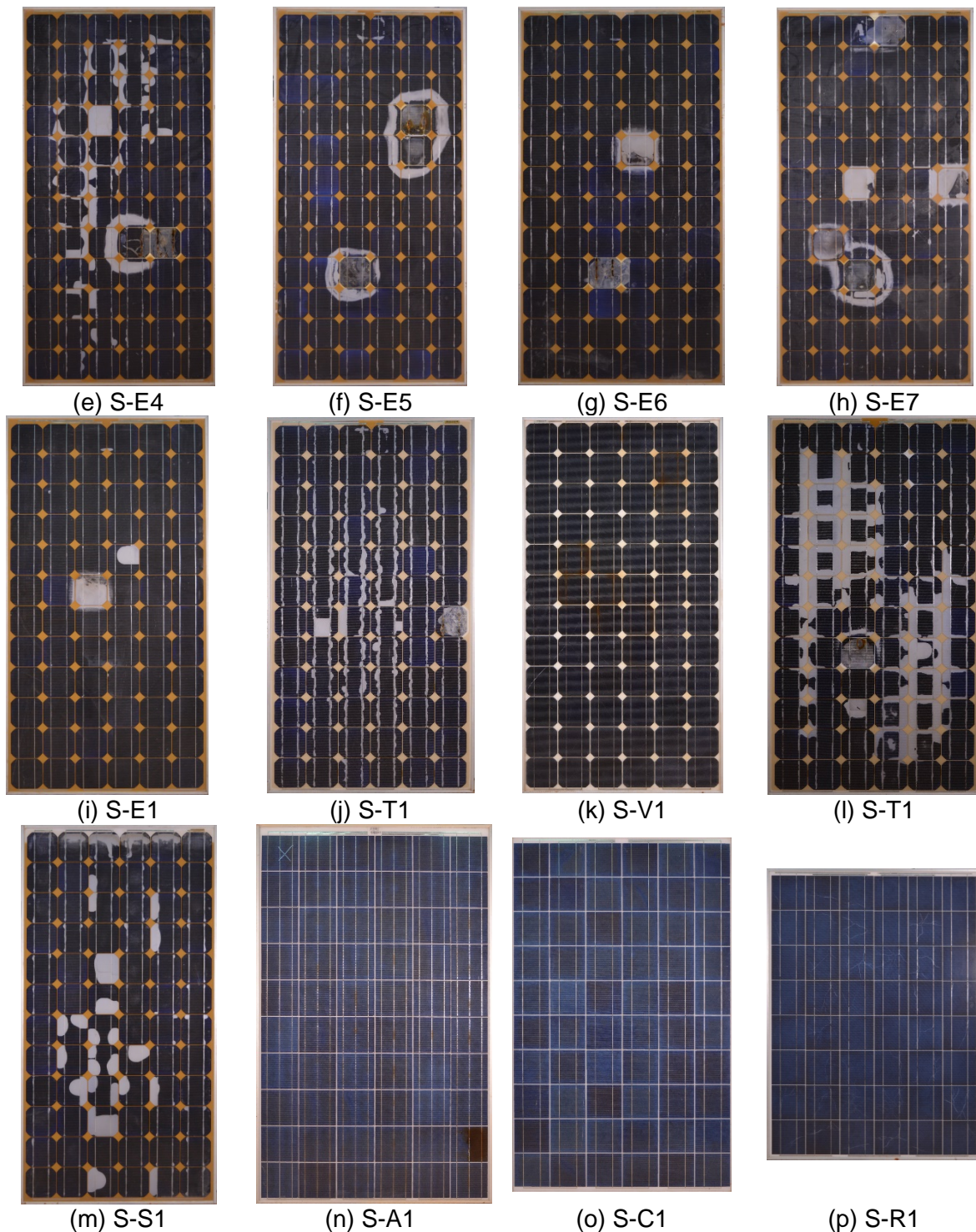


Figure 11: (a) to (m) Monocrystalline and (n) to (p) Polycrystalline modules tested in the research, presenting different kinds of defects.

For the characterization performed in the CIEMAT, a singular polycrystalline module composed of different defective and non-defective cells has been specifically designed. The module has been ad-hoc manufactured by ATERSA with cells of three buses. The front and back views of the module are presented in Figure 12 a) and b), respectively. In order to be able to analyze the module in detail, all cells are accessible

from the back side of the module. Similar kinds of defects have been integrated in the same string as seen in Figure 12 c). In this way, the string corresponding to columns A and B (string AB) contains manufacturing defects, the string CD contains soldering faults and the string EF contains breaking deficiencies. The defects of the three module strings are summarized in Table 4. The low efficiency defects (defect E-L, cells A2 and A5) are due to manufacturing problems, but they do not correspond with breaking or short-circuited cells. Short-circuit cell (defect E-SC, cell A7) has been generated by extending the cell connection tabs beyond the ordinary placement, short-circuiting the cell. In order to simulate the bad soldering defects, buses from the back of some cells have been left without soldering, either one bus (defect S-A, cell C3) or two buses (defect S-B, cell D5). Three buses have not been left without soldering in any case as it would had meant that this cell would not be series connected to the rest. The cell with only 1cm welded (defect S-C, cell C8) simulates a bad soldering, in which only 1 cm of the bus is welded instead of the typical 15 cm welded. When a piece of broken cell is placed on top of another cell (defect B-3, cells E10, F9 and F10), what it really generates is a partial shading. It could simulate an important permanent bird crap. These types of defects are analyzed as they ordinarily appear in commercial modules in operation, either in manufacturing, transport or operation. However, commercial modules are not accessible at the cell level. That is why an ad hoc module has been manufactured for the defects characterization.

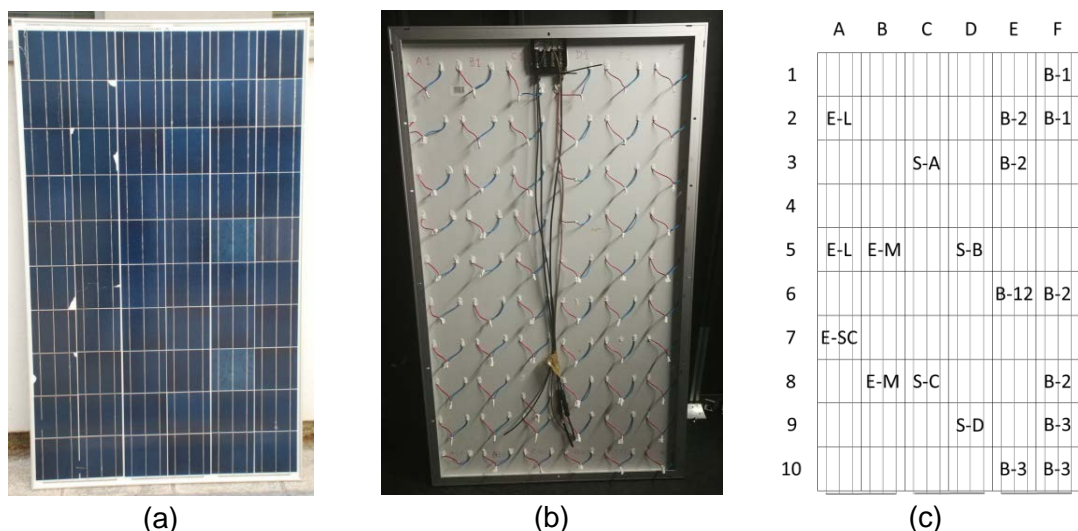


Figure 12: (a) Front view of the tested module. (b) Back view of the tested module. (c) Defective cells distribution showed in the back view of the tested module.

Table 4: Cells defects types and codes per string.

	Defect code	Defect type	Cell affected
String AB – Manufacturing defects (E)	E-L	Low efficiency cell (9%)	A2, A5
	E-M	Medium efficiency cell (16.4%)	B5, B8
	E-SC	Short-circuited cell	A7
String CD – Soldering defects (S)	S-A	One bus without soldering	C3
	S-B	Two buses without soldering	D5
	S-C	Only 1cm of each bus welded	C8
	S-D	All tabs loose (without soldering)	D9
String EF – Breaking defects (B)	B-1	Split cell (without cell area decrease)	F1, F2
	B-2	Cracked cell (with cell area decrease)	E2, E3, F6, F8
	B-12	Defects B-1 and B-2 in the same cell	E6
	B-3	Piece of other broken cell over the cell surface	E10, F9, F10

More details of the manufacturing process at ATERSA facilities are given below. The cells were welded with an automatic tabbing or by hand the special cells if necessary. A laminate was made with a standard PV lamination process using high transmissivity and tempered glass, then one sheet of EVA, the cells welded, another sheet of EVA, the backsheet and introduced into the laminator. The lamination process consists of a machine that makes the vacuum and at the same time heats the pre-laminate, to melt the EVA. At any given time, pressure is applied to eliminate the volatile components and to imbibe all the materials with the EVA as well as to achieve a good adhesion between the materials. It is subsequently cooled to room temperature. Before framing, some windows were opened just in the areas of the tabs. This was made with a high-temperature knife, removing a square of about 4X4mm of backsheet and EVA, until reaching the tab. Subsequently, cables were soldered in the tabs, which were to allow electrical measurements to be made at the cell level at four points in the research. To protect this solder it was covered with silicone for solar use. Finally, to give rigidity to the set, the laminate was framed with an extruded aluminum profile.

The PV site in which the thermographic analysis for the thermal defects classification (2.2.6) and the image resolution analysis (2.3.4) have been performed is located in Spain, in Castilla y León region, it has a capacity of 3 MW, with 17,142 monocrystalline modules, model STREAM 175 W, and was commissioned in 2008. Each PV structure is composed of thirty-two modules, divided electrically in two arrays of

Detection, classification and characterization of defects in photovoltaic modules through the use of thermography, electroluminescence, I-V curves and visual analysis

sixteen modules, which are connected in parallel in the combiner box. PV structures have a fixed 30° tilt structure and a general view of them can be seen in Figure 13. Each module has 72 cells (12x6).



Figure 13: General view of the PV structures of the 3 MW PV plant analyzed.

University of Cuenca's solar farm, in which the low-cost infrared cameras analysis has been carried out, has 35 kWp installed, with 80 polycrystalline and 80 monocrystalline PV panels, (a total of 160 modules), and it has been under production since 2016 (Figure 14). PV panels found with hot spots are monocrystalline ATERSA A-250P of 250 Wp.



Figure 14: General view of the PV modules of the 35kWp at the University of Cuenca.

1.5.4. Analytical-comparative phase

This fourth phase is focused on extracting results and drawing conclusions from the empirical data. It has been done in parallel with the third phase (empirical research), throughout the entire duration of the thesis. This subsection details the software used for the images treatment, simulations and data processing along the doctoral thesis.

- **2/3 Diode Fit** [75]: it has been used to calculate the main parameters of the single-diode model of a solar cell equivalent circuit for the PV cells characterization (subsection 2.2.5). A screenshot of the program is shown in Figure 15.

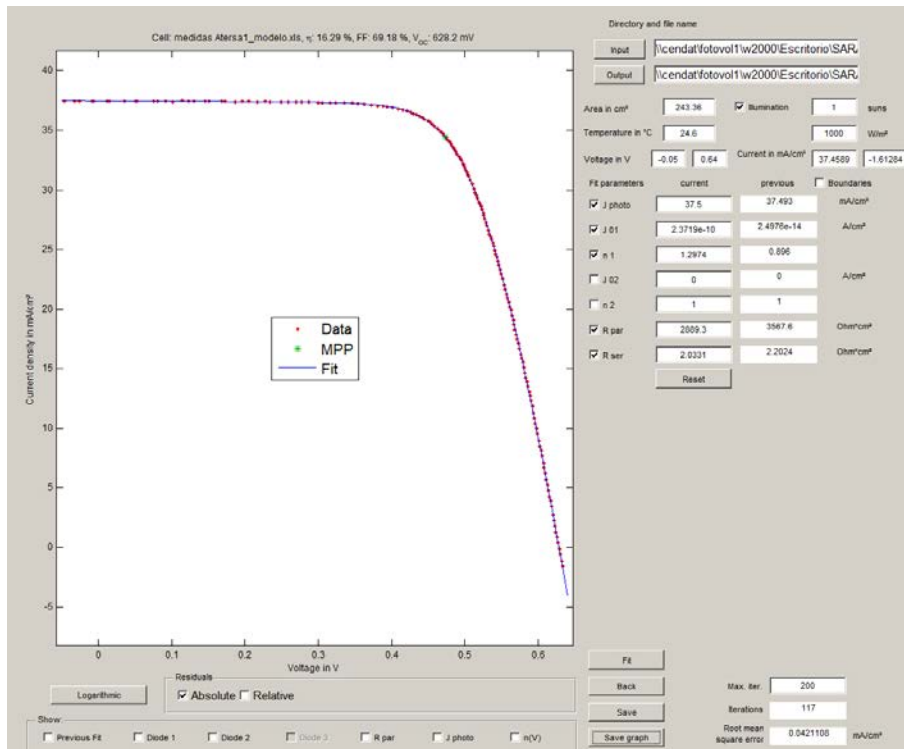


Figure 15: 2/3 Diode Fit program screenshot while obtaining the single-diode model of a solar cell equivalent circuit.

- **ImajeJ** [76]: for the image processing, obtaining statistical information from images and stack of images analytics. For instance, in the nondestructive characterization of solar PV cells, individual histograms of the light emission in defective cells have been obtained (subsection 2.2.5). In the study of the influence of large periods of DC current injection in c-Si PV panels (subsection 2.2.2) the evolution of the IRT and EL mean value intensities with the current injection in the module has been obtained using ImajeJ software.
- **LTSpice** [77]: simulation, validation and analysis of the electrical model of faulty and shaded cells have been carried out using LTSpice program. To obtain an accurate model, the I-V curve obtained experimentally has to be used to adjust the ideality factor, n , and the parallel resistance, R_p . Later on, the cell model has been used to create the desired PV module, as it can be seen in Figure 16 and PV array, connecting the desired number of PV modules in series. The model selected to do the simulations is the real single-diode model of a solar cell (1M5P), which is presented in Figure 17. Further information about this study methodology can be found in the paper presented in subsection 2.2.1.

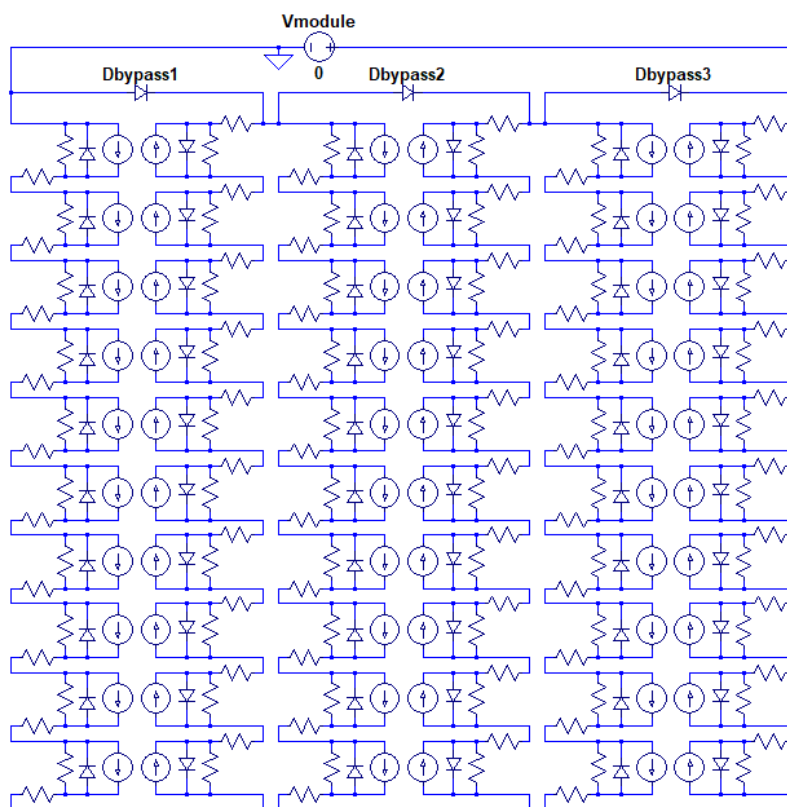


Figure 16: Module Windon 265W Mono-crystalline simulated in Ltspice IV with the real single-diode model cells presented in Figure 17.

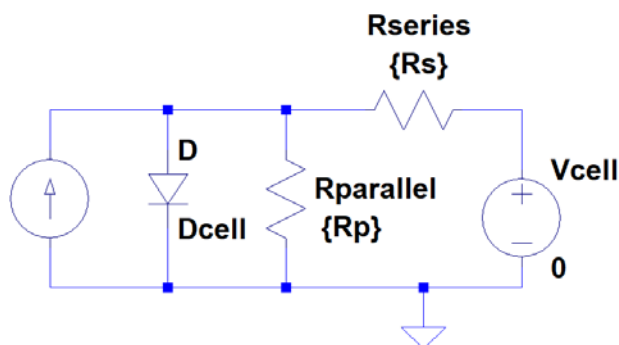


Figure 17: Real single-diode model of a solar cell simulated in Ltspice IV.

- **Matlab 9.3** [78]: this software has been used for merging EL and thermographic images (subsection 2.2.5). In general terms, image fusion is the process of combining different information from several images (sensors) taken from the same scene to obtain a composite image, which will contain the best information coming from the original images [79]. In that sense, it is expected that the fused image will have better quality (or more information) than any of the original images. In this work, a pixel-level fusion or image signal level is adopted, which

is the lowest-level type of fusion and involves the combination of raw source images into a single composite image. In order to be able to fuse images at this level, it is essential that the images are adequately aligned prior to being fused. This process is known as image registration, which is the process of overlaying two or more images of the same scene taken at different times, from different viewpoints, and/or by different sensors. In general terms, it geometrically aligns two images, which are usually referred to as the reference image and the sensed image [80]. Image registration helps to correct problems such as image rotation, scale and inclination, which are common when overlaying images. The initial available images in their original format are presented in Figure 18. Note that in EL image, the panel is placed vertically and in the thermographic image horizontally, in addition to being in different formats, EL and thermal image. Hence, image registration of these images is needed. Firstly, for the image alignment process to be performed in a better and automatic way, cropping followed by a rotation of both images was performed manually. Once this is performed, it was observed that the two images to be merged are of different sizes. Therefore, the images were resized to have the same size, in this case the thermal image is resized to the size of the EL image. Also, both images were transformed to grey scale. The resized and transformed images are presented side by side in Figure 19. The registration process was then performed using the Matlab function `imregister()`. Thereafter, nine different fusing image algorithms were performed, as `diff`, `blend`, `fpde`, `ifm`, `gff`. Further information about this study methodology can be found in the paper presented in subsection 2.2.4.

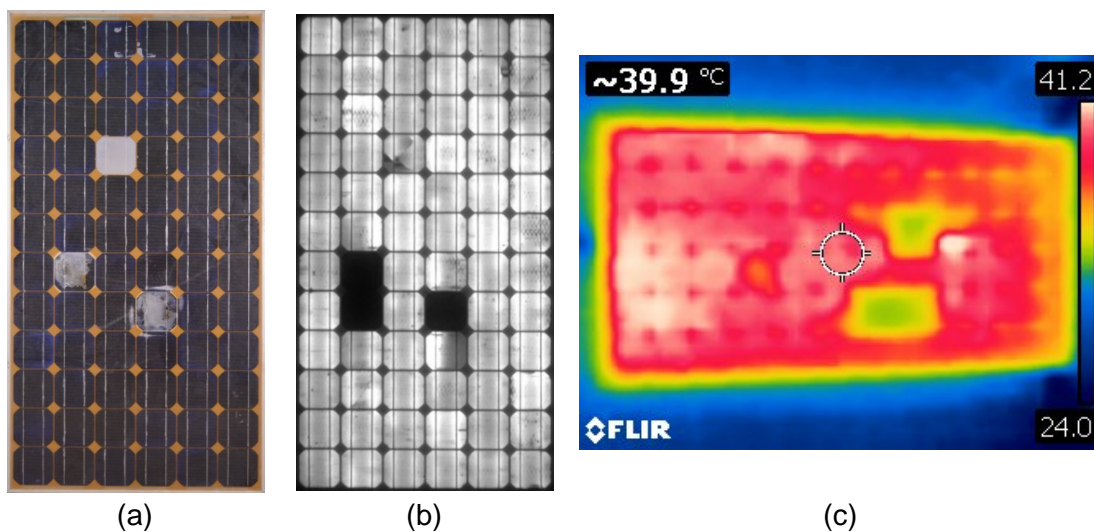


Figure 18: (a) RGB of the module under analysis (SE-2). Initial available (b) EL and (c) thermographic images in their original format for the fusion.

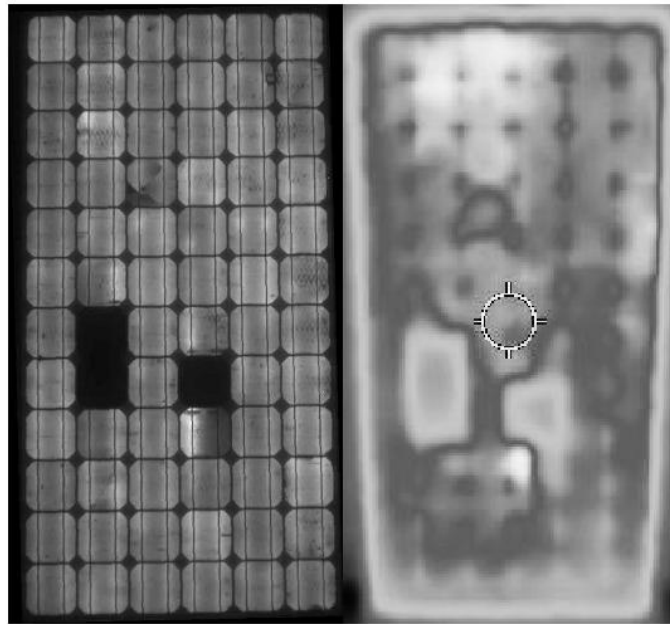


Figure 19: EL and thermographic images resized and in grey scale, placed side by side.

- **Flir Tools** [81], **Workswell CorePlayer** [82] and **IRSoft** [83]: Cell defects detected in thermographic inspections have been analyzed using the thermographic cameras software. It has been used to import, to edit, to process and to analyze thermographic images, obtaining the relative temperature of the defect, the mean temperature of the healthy area and the difference between them, which indicates the overheat of the fault. Flir Tools has been used for images captured with Flir cameras (FLIR SC 640 camera in subsection 2.2.5, Flir C2 in subsections 2.2.2, 2.2.3 and 2.2.4 and TAU 2 in subsection 2.3.4), CorePlayer for Workswell cameras (Wiris Pro in subsections 2.2.2, 2.2.3 and 2.2.4) and IRSoft for Testo cameras (Testo 870-2 in subsections 2.2.6 and 2.3.4).
- **Microsoft Office 365** [84]: It has been the program used for most of the storage, analysis, organization and exposure of data, including the use of Excel, Word, OneDrive and PowerPoint.

1.5.5. Results dissemination phase

It is also necessary to foster active dissemination of the results of research. It has been done once finished the empirical data acquisition (third phase) and its analysis and comparison for extracting results and drawing conclusions (fourth phase) for each

research performed throughout the entire duration of the thesis. This phase also includes the writing of the doctoral thesis document.

Below is a list of the conferences in which the doctoral student has participated and the scientific journals in which the results obtained have been published. More information about papers published is detailed in the Prologue and in Chapter 2 (Published papers).

- **Conferences:**

- EUROSUN 2016: International Conference on Solar Energy for Buildings and Industry (11th Oct – 14th Oct 2016).
- ISES SWC 2017: Solar World Congress & IEA Solar Heating and Cooling Conference (29th Oct – 02nd Nov 2017).
- ICSC-CITIES 2018: Congreso Iberoamericano de Ciudades Inteligentes (26th Oct – 27th Oct 2018).
- PVSEC 2019: 36th European Photovoltaic Solar Energy Conference and Exhibition (09th Oct – 13th Oct 2019).
- ICSC-CITIES 2019: Congreso Iberoamericano de Ciudades Inteligentes (07th Oct – 09th Oct 2019).

- **Scientific journals and books:**

- Energy, 2019 (Q1).
- Solar Energy, 2019 (Q1).
- Solar Energy, 2018 (Q1).
- Revista Facultad de Ingeniería Universidad de Antioquía, 2019 (Q3).
- Energy, 2020 (Q1).
- Renewable and Sustainable Energy Reviews, 2018 (Q1).
- Revista Facultad de Ingeniería Universidad de Antioquía, 2020 (Q3).
- IEEE Transactions on Industrial Informatics, 2018 (Q1).

1.6. Results and discussion

This section presents a summary of the most relevant empirical findings of the doctoral thesis and a brief explanation and interpretation of the results. It has been structured in three subsections, coinciding with the three partial objectives of the doctoral thesis.

1.6.1. Study of the state of the art (Obj. 1)

Like any other technology, PV production is never faultless. It is essential for main players involved in PV plants, as investors, operators and equipment manufacturers, to identify the failure modes and rates that the main equipment experiences to reduce investment risk, to focus their maintenance efforts on preventing those failures and to improve longevity and performance of PV plants. It can be considered as a relatively new technology that has evolved a lot in recent years and there are many manufacturers with very variable qualities. Moreover, from the point of view of the installation, O&M, due to the inherent characteristics of this technology, PV fields are highly atomized, so there is also great diversity in terms of procedures. Besides, PV systems consist of many different vulnerable components and their operation is highly dependent on temperature, power losses, and ambient environments. In addition, the input power is variable and uncontrollable what may cause electrical stress in the panels [15].

The greater challenge that researchers address and indicate while investigating about PV system failures is the lack of accessible reliable real quantitative data, since most operators are private and do not disclose the figures or either they do not have enough capabilities to record this data [85]. Different authors have contributed to the advance of this research with their accessible information [28,86–92]. Through the implementation of advanced PV plant monitoring systems [93], the application of Computerized Maintenance Management Systems (CMMS) and the feedback of the field technicians it is possible to have an experimental database to assess the failure rate analysis of the PV plants [73]. This fact is one of the greater strengths of the research performed, in which the information from the historical data of the sixty-three PV plants portfolio in Italy and Spain has been accessible. Important results have been obtained in this research, which are summarized in this subsection and are further analyzed in the paper presented in subsection 2.1.1. The absolute number of failures per year in the portfolio analyzed is 19,325.

Firstly, an analysis of the average number of failures per PV site has been performed, considering defects in all elements, showing that although PV plants are getting older each year, proper maintenance can be responsible for keeping the defects ratio or even reducing it. Additionally, properly performed predictive, preventive and corrective maintenance include improvements in PV plants, which reduces the failure ratio in the long term. An important conclusion from the five years data analyzed in this study is the amount of alarms or failures registered in a PV plant per year, resulting in an

average ratio of 321 failures/year/plant. Lately, a similar study has been performed, calculating the number of failures per kW instead of per PV site, revealing an average ratio of 0.23 failures/year/kW.

After that, the plants have been divided in five groups considering their power. Logically, bigger plants present a higher number of defects per plant, as they have more components and it is just a probabilistic fact, presenting a deviation of -72.6%, +191% from the average previously calculated if the sites capacity is not considered. Therefore, the extension of this study per power unit instead of per site has been done, with the objective of obtaining more accurate failure ratios. It has been seen how there are defects that do not depend on the plant size or the plant number of elements or components; therefore, the failure number per power unit is higher in smaller plants (Figure 20). For instance, regarding the grid, there is usually just a connection point in the plant, regardless of its size and it can generate failures as a consequence of overvoltage, overcurrent or disconnections among other causes. Other example of this fact are the alarms due to failures in the wired ethernet, wireless Wi-Fi or fiber optic of the communication system, which can be independent of the size of the plants in many cases. Three different important annual ratios are obtained; 0.45 failures/year/kW for plants with a capacity under 750 kW, 0.18 failures/year/kW for plants with a capacity beyond 750 kW and 0.23 failures/year/kW without any plant capacity consideration.

All these alarms are distributed among the different elements that compose the PV sites as presented in Figure 21. The existence of failures in different components can lead to the detection of failures in the monitoring or communication system, which explains the large amount of failures attributed to them, adding more than 50% of the alarms. For instance, a failure in the auxiliary services transformer can be responsible of an interruption of communications, as it feeds the communication system. In this case, the presence of a failure in the auxiliary services transformer would also generate a communications alarm. Further information about the results of this research can be found in the paper presented in subsection 2.1.1.

However, having a higher failure rate does not mean they are the most relevant alarms of the plant, as shown in Figure 22. In a FMECA, the results present the failure modes and the severity of the consequences with relatively high probability, obtaining the RPN that multiplies severity, detection and occurrence based on a ranking criteria. Further information about the results of this research can be found in the paper presented in subsection 2.1.2.

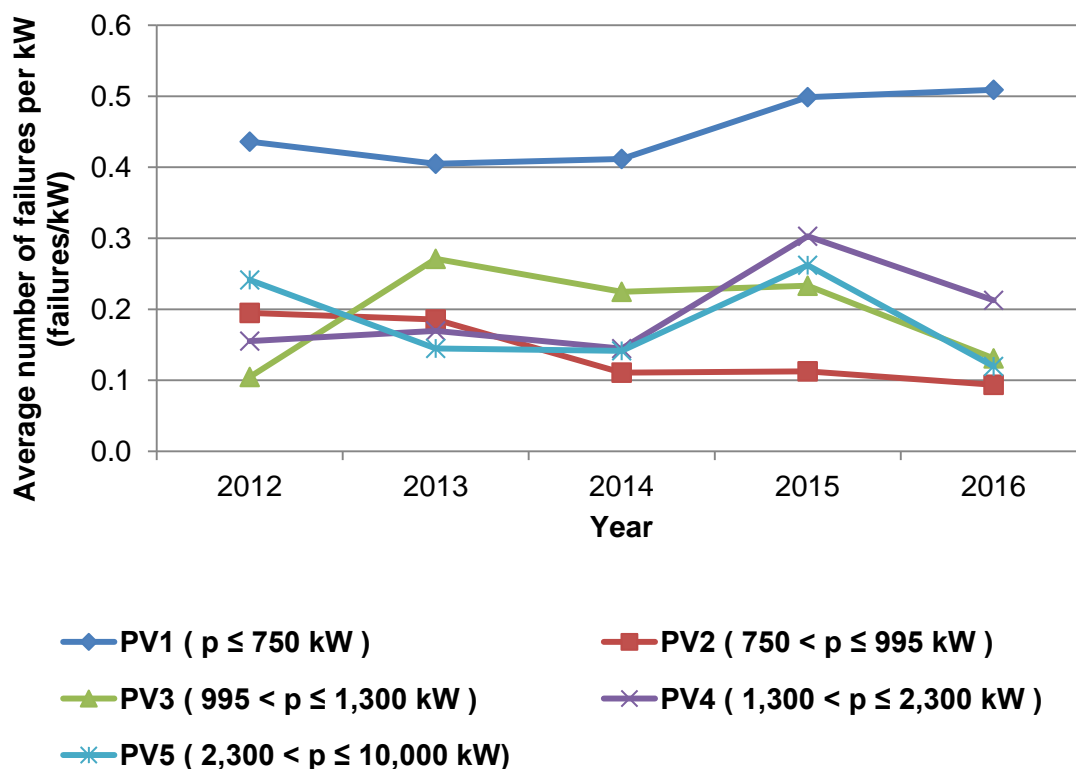


Figure 20: Average number of failures per kW for the different defined groups (from PV1 to PV5) from 2012 to 2016.

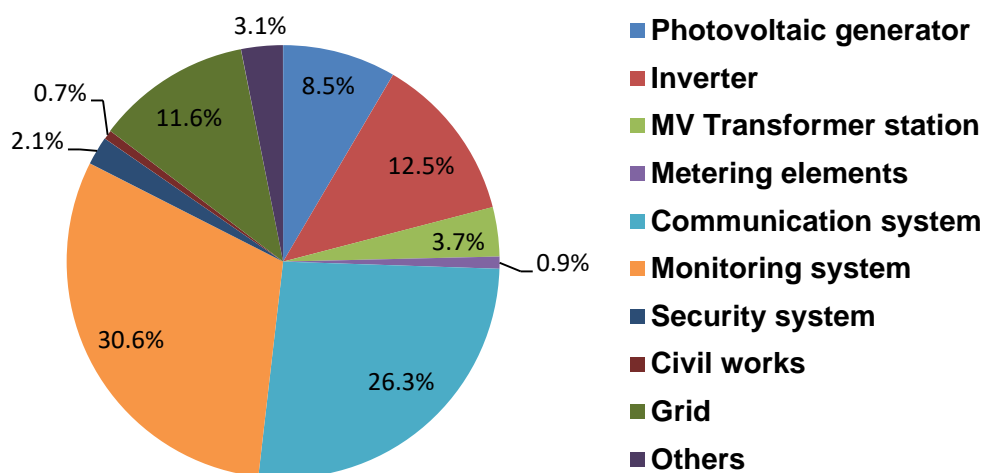


Figure 21: Distribution of the registered failures in each of the PV plants monitored elements, considering data from 2012 to 2016.

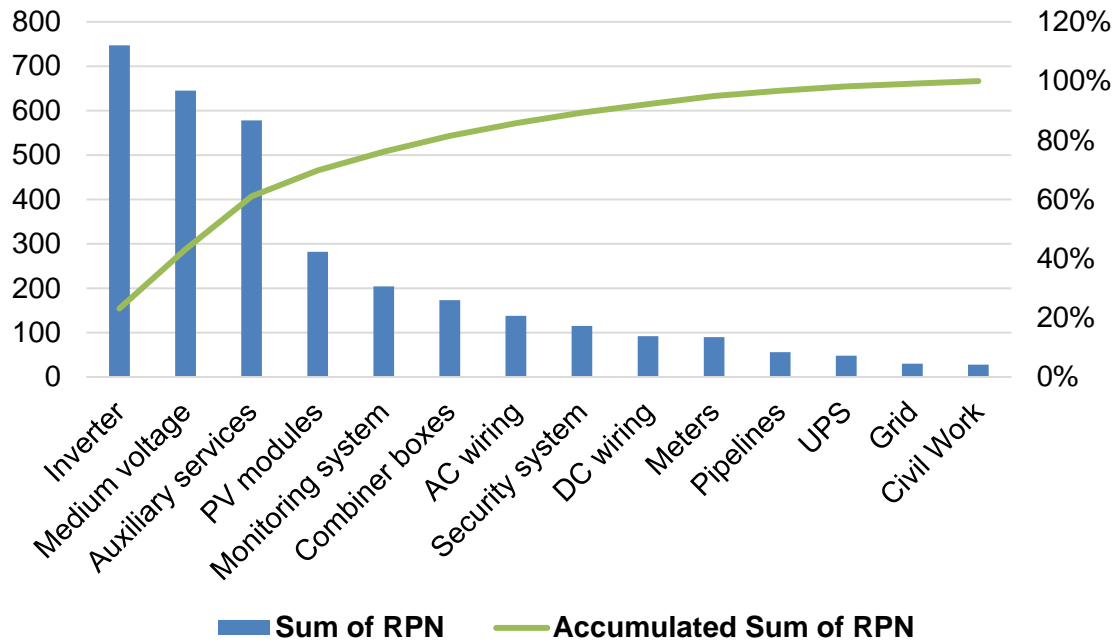


Figure 22: Sum of the RPN for each of the groups of elements under study and the accumulated RPN sum

Accordingly, each defect involves each own repairing time to fix a defect, and excluding the elements that usually require the presence of the manufacturer or outsourcing for their reparation and have a higher reparation time, the PV generator is the element with the higher fixing time value, with 8.15 hours/failure. Additionally, as it has been introduced, in utility scale PV plants, typically the monitoring system trails the string series current of multiple modules connected, or even the inverter current, which is the sum of the parallel string current, and does not track the performance of the individual PV modules, which is the key element on a PV system as it converts the incident irradiance into electric power and their operation will affect the overall plant performance. Therefore, PV module alarms are not frequently automatically generated being specially complicated the detection of failures at this level and even more difficult the recognition of the failure cause and mode. PV module's cost is the highest cost of PV installations, having reached its price up to 50% of the price of the installation in the last decade, according to reference [71] of 2012. All these facts support the need to investigate this type of defects. Further information about PV systems, including design, O&M, module failures and inspection techniques can be found in the paper presented in subsection 2.1.3.

As it has been seen, the module is the key element on a PV system, but, even so, it has limited access to local monitoring alarms, which are not frequently automatically

Detection, classification and characterization of defects in photovoltaic modules through the use of thermography, electroluminescence, I-V curves and visual analysis

generated. From the study of the state of the art, it is highlighted the importance of the research on PV modules failures detection, classification and characterization in order to produce reliable, efficient and safety energy. This justifies the research on this investigation line, summarized in the following subsection 1.6.2., and with the complete related published papers in section 2.2. The use of the different inspection techniques has been reviewed, emphasizing aerial IRT as a novel and promising inspection technique in this field, so it has been further studied, presenting the results obtained in subsection 1.6.3 and the related published papers in section 2.3.

1.6.2. Detection, characterization and classification of defects in PV modules through the use of different inspection techniques (Obj. 2)

PV modules experience thermo-mechanical loads during manufacturing and subsequent life stages leading to the origination of the appearance of different defects [94], which are responsible for the reduction of their efficiency, as well as their durability and reliability. These defects can result in power loss and module degradation [65]. Consequently, defect finding in PV modules has had substantial attention of researchers during the last years. This subsection summarizes the results of the doctoral thesis on this regard included in section 2.2, and it has been structured in three parts. In the first, it is presented the detection of PV defects using different techniques and the comparison of the information obtained with each of them, the second includes the characterization of different PV defects and the third, the classification of PV defects attending to failure patterns.

1.6.2.1. Detection of PV defects

As it has been seen, different techniques can be used to detect and quantify PV modules anomalies, as visual inspections, electrical tests like the I-V curve test, IRT or EL. PV plants operators usually apply only one or two of them within the O&M activities. Additionally, researchers usually studied them separately. However, these methods provide complementary results, glimpsing interesting information about the PV site state.

Throughout this doctoral research, all these inspection techniques have been simultaneously applied and analyzed, studying the correlation between them.

Regarding the I-V curves, several electrical circuits that model a PV system have been simulated using Ltspice and validated with experimental measurements carried out

in the laboratory of the University of Gävle (Sweden). The results of this research are summarized in the paper included in subsection 2.2.1. The simulations show remarkable agreement with the experimental data, which means that the designed model supposes a very useful tool that can be used to study the performance of shaded or defective PV systems, allowing the simulation of numerous faults. The novelty introduced in this research is not related to the electrical model of the PV cell, as it has been used a well-known model to do the simulations, the real single-diode model. This research aims to perform a detailed analysis on how shadowing and other defects, as cell breaks that cause isolation of part of the cell, affect the PV production of the modules in different situations, specifying the way that PV modules work when they are affected by these faults.

In relation with EL tests, operators agree that there is a generalized concern about how the current injection needed in EL measurements can affect the PV modules service life, and how these periodical inspections can affect the long term life of the modules. In order to give a practical answer to this problem, a series of tests consisting of long periods of current injection on several monocrystalline silicon modules has been carried out, and it is included in the paper presented in subsection 2.2.2. The modules tested had already fulfilled their useful life and present multiple defects. In order to analyze how the current injection affects the state of the module, images of IRT and EL were acquired during the current injection period (during 96 hours). Figure 23 shows the EL images of the module taken before and after 96 h of I_{sc} current injection.

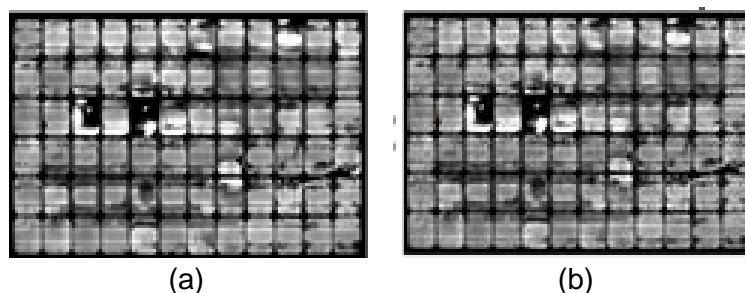
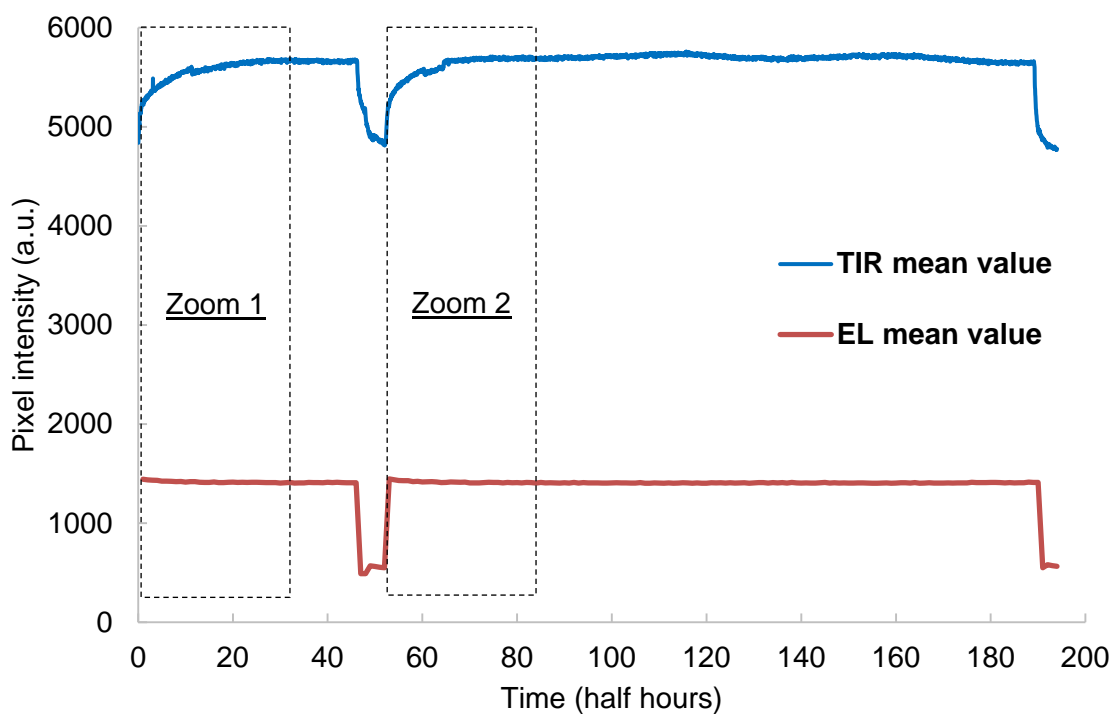


Figure 23: EL images taken before (a) and after 96 h of I_{sc} current injection of a Tynsolar 175W monocrystalline module (b).

The mean values of the EL and IRT intensity over the full images were calculated, Figure 24. For a better understanding of the results and to analyze how EL could affect the modules efficiency, the current injection was switched off after 24 h to check the module behavior in a second EL test after completing a first injection cycle. In this way, the module was cooled during 24 h, after which the current injection was reestablished for a total time of 96 h.



(a)

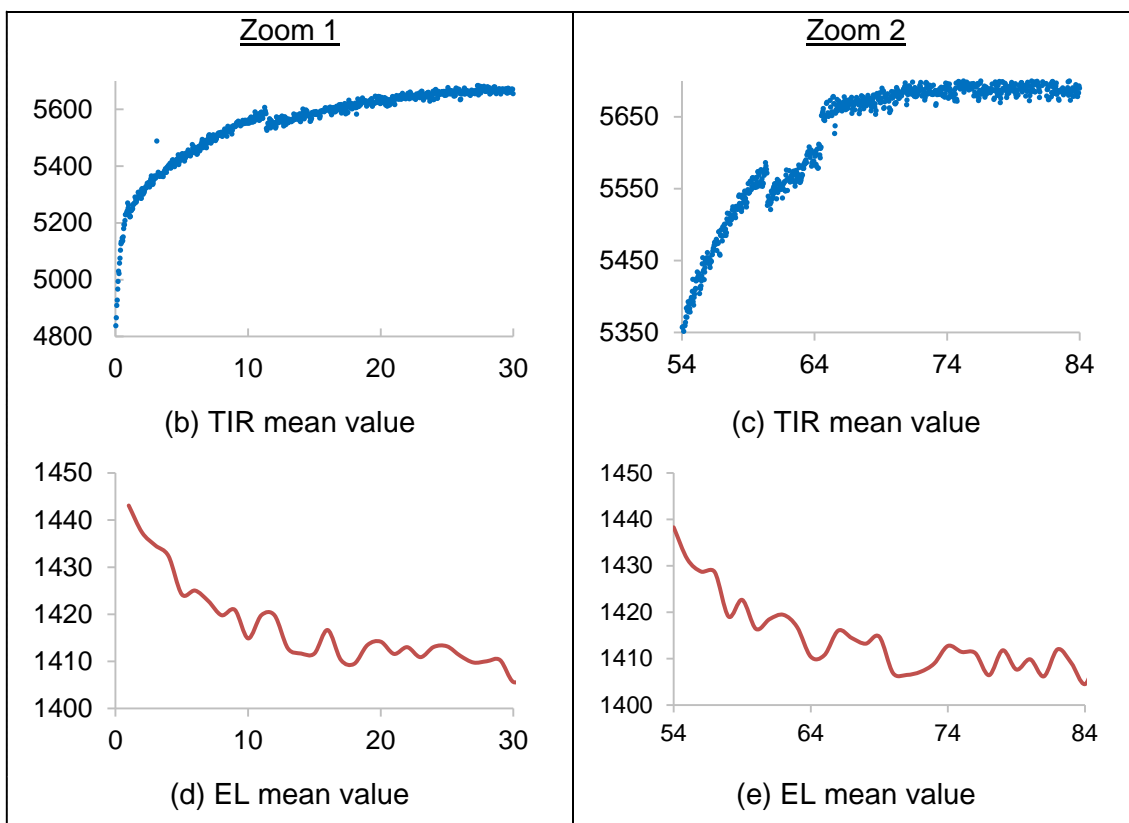


Figure 24: Evolution of the IRT and EL mean value intensities with the current injection in the module (a). Detailed evolution after the initial current injection in two periods are depicted in (b-e).

In the tests carried out in this work, it is not appreciated that the current injection in EL measurements has any negative effect on the performance of damaged modules. However, it has been observed a small effect during the heating period in the EL intensity results at the beginning of each test, presenting a direct relationship between the heating of the module and the decrease of the EL signal. But that decrement is very small ($\leq 3.5\%$) and stops when the PV module temperature is stabilized, not affecting the module performance.

For each of the defective modules presented in Figure 11, it has been performed its I-V curve before and after the EL, EL images each 30 min during 72 hours, thermal images of the fourth quadrant each minute during the EL process and thermal images of the second quadrant during the modules operation in the PV field of the Campus Duques de Soria. Additionally, RGB images have been captured before and after each test. All these tests have allowed the detection of their defects. As an example, the resultant RGB, IR and EL images of S-E1 module are presented in Figure 25, and further information of these results can be found in subsection 2.2.3.

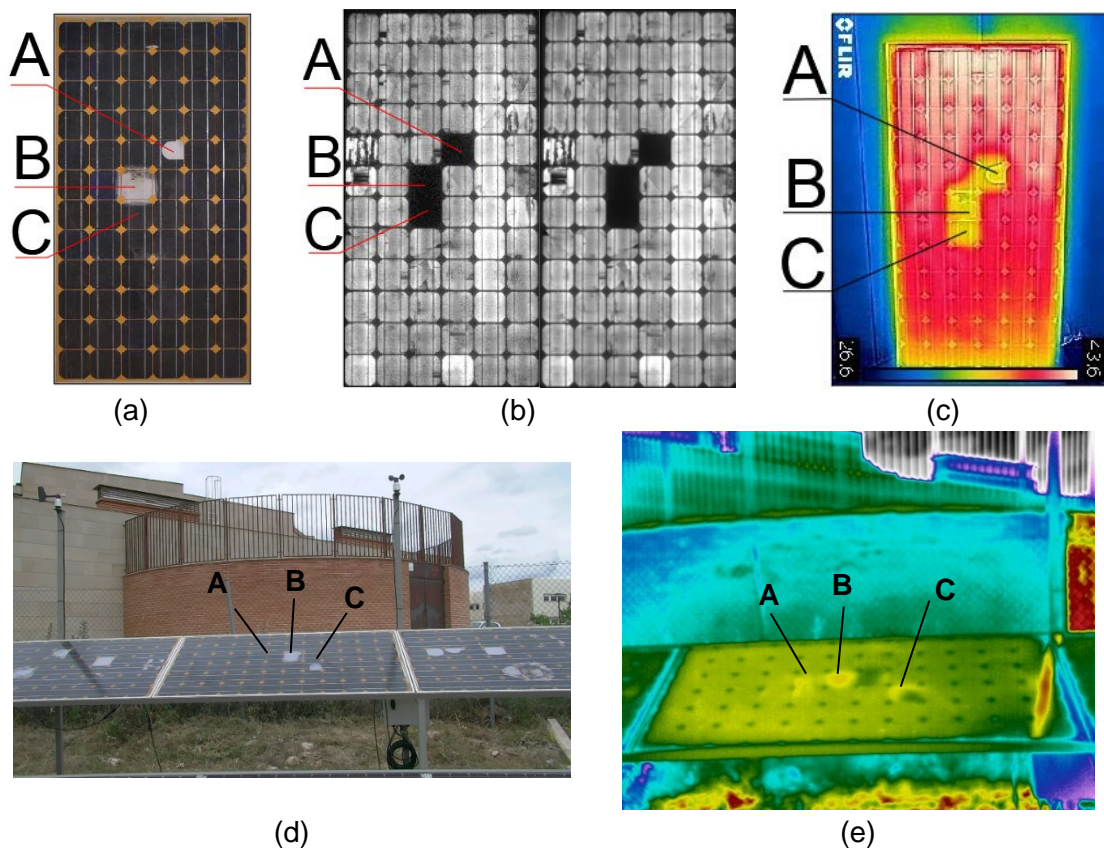


Figure 25: S-E1 PV module: RGB appearance (a), first and last EL images (b), IR image in the fourth quadrant during the EL test (c), visual (d) and IR (e) outdoor images in ordinary module operation.

Results confirm that EL and IRT under current injection on modules are closely correlated, while IRT under normal operation (sun exposure) reveals complementary information not detected in EL but existing in the visible spectrum.

The following paragraphs present a concluding remark on the inspection techniques analyzed. IRT is a non-destructive measurement technique, which provides fast, real-time, and two-dimensional distributions of characteristic features of PV modules. IRT can be performed in illuminated or dark conditions.

In the former instance, the illuminated IRT or IRT under common operating conditions of the PV system, is similar to luminescence, where the current flowing through cells increases PV module temperature. In this case, it is used as a contact less method for diagnosing some thermal and electrical defects in PV modules, as one module warmer than others, one bypass diode string warmer than others in the same module, single cells warmer than others without following any pattern or in the lower parts or closer to the frame, a part of a cell warmer, a pointed heating or a bypass diode string part remarkably hotter than others when equally shaded [33]. However, results reveal complementary information between IRT and EL techniques, adding value to individual findings. Performed IRT measurements proved that on the one hand not all identified defects lead to an increase in temperature and on the other hand cells or modules with unremarkable EL images sometimes supply IRT images with hot areas, which are caused by high power losses [95]. It has been experimentally observed how using EL is especially interesting to detect cell cracks in PV modules, appearing as dark lines on the solar cell in the EL image as well as interrupted contacts or a number of process failures (e.g. shunts or defects in the antireflection layer) [95]. Irregular areas indicate the presence of cracks in the silicon wafers while regular rectangular dark areas can be due to broken front grid fingers. In this case, outdoor IRT can complement EL locating the most restrictive cell within a string [96], although IRT will not provide details of the defect patterns in this case, as not all identified defects lead to an increase in temperature. Therefore, sometimes the high resolution of the EL images enables resolving some defects more precisely than in IRT images. Hence, a combination of both techniques is advisable in order to identify as many defects as possible.

In the latter instance, IRT in dark conditions shares some similarities with EL technique, being the module subjected to a forward voltage. In the EL test, modules operate under forward bias like a light emitting diode (LED), and therefore have to be power supplied. Excitation current can be lower or equal to I_{sc} [97]. Therefore, dark-IRT

can be performed simultaneously to EL test, while injecting current to the modules. It has been observed from visual inspection of EL and IR images in the fourth quadrant that most of the defects detected in dark IRT images under forward bias condition can also be identified in the EL images while not all the defects detected in the EL images can be detected with dark-IRT, as some broken cells or soldering defects over one or more buses [96]. Therefore, it can be advisable using different techniques to characterize the actual state of the module and to explain its I-V curve.

Finally, it has been studied the possibility to use different algorithms to generate merged images of frames captured by means of EL and IRT in the fourth quadrant, with the objective of exploring how using image processing techniques to align multiple scenes in a single integrated image simplifies the analysis and reporting of results of inspections of PV plants. It has been shown that merging images for determining the PV modules impact is a very interesting and promising field, as it helps in the fault detection. EL and IRT in the fourth quadrant have been analyzed in this merging images research as they can be both performed simultaneously in the temperature and humidity controlled chamber. This study could also be extended with other images, as IRT in the second quadrant (revealing hot spot under ordinary operation of the system) or visual images. Some examples of the treated final merged images are presented in Figure 26. Further information about this research can be seen in the paper included in subsection 2.2.4.

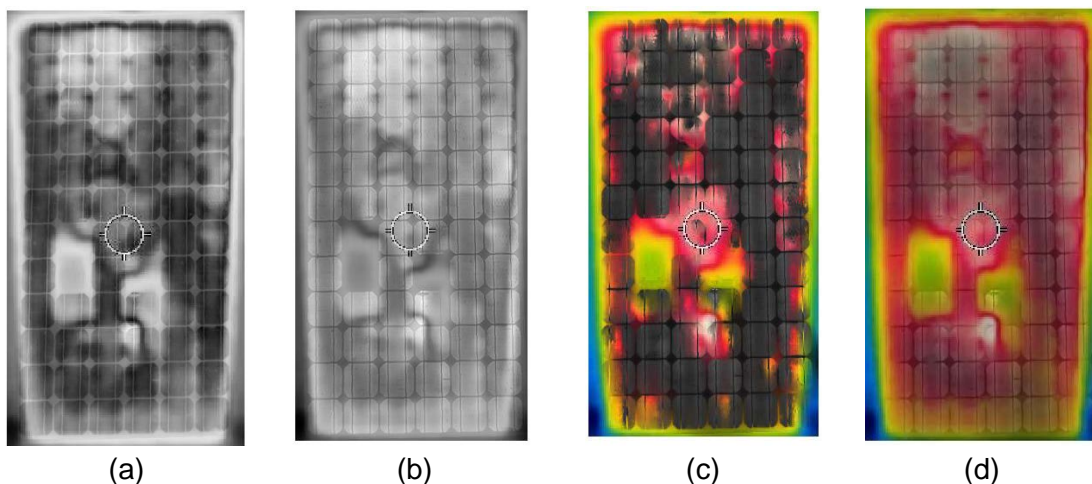


Figure 26: Merged images using (a) 'diff', (b) "fpde_fusion", (c) "ifm_fusion", and (d) "gff_fusion" algorithms.

1.6.2.2. Characterization of PV defects

As it has been introduced, PV modules are exposed to different loads and other degradation factors which can produce a large range of defects. In order to be able to characterize three of these possible defects, a singular polycrystalline module composed

of different defective and non-defective cells has been specifically designed, as described in the methodology (subsection 1.5.3). The three kinds of defects analyzed and characterized have been: manufacturing, soldering and breaking PV defects, by a combination of EL, IRT, I-V curves and visual tests. This has been performed to control, to mitigate or to eliminate their influence, and being able to do a quality assessment of a whole PV module. Results of this research are summarized in the following paragraphs, and can be further analyzed in subsection 2.2.5.

Three different kinds of manufacturing defects have been studied: low efficiency, medium efficiency and short circuited cells. I-V curves of the manufacturing defective cells studied at 1,000 W/m² and 100 W/m² are presented in Figure 27 and Figure 28, respectively. As it can be seen, manufacturing defects are much more evident at higher irradiance levels, having a greater impact. The module has been properly cleaned before each test to avoid any soiling influence.

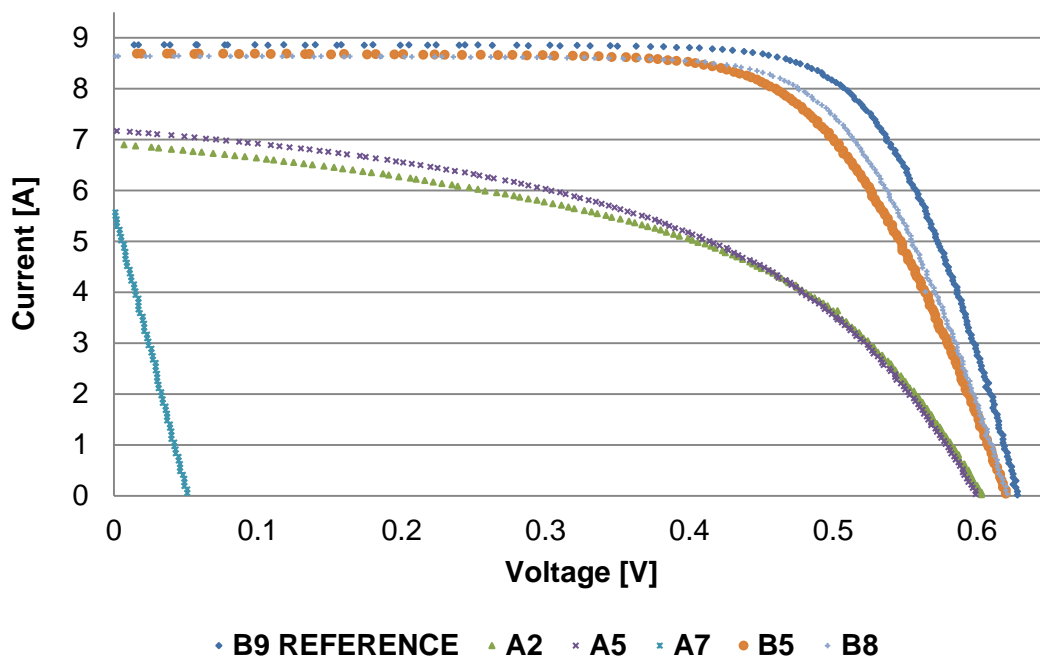


Figure 27: I-V Curves of the manufacturing defective cells of the first string (string AB) at 1,000 W/m², using B9 as the healthy reference cell of the string for comparison.

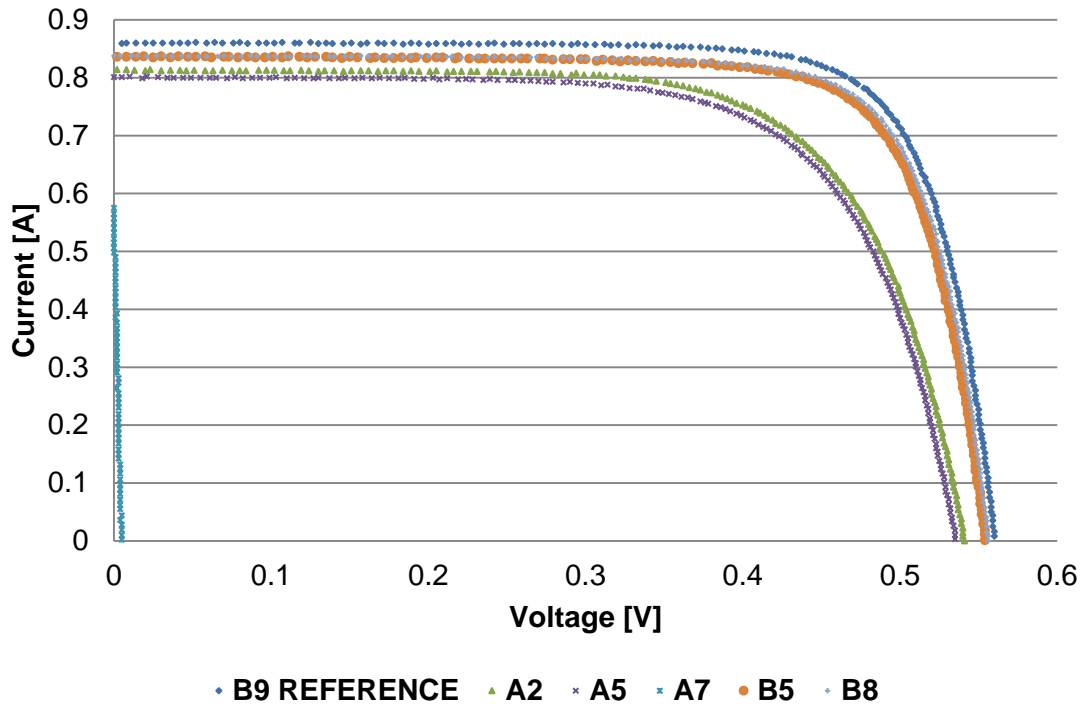
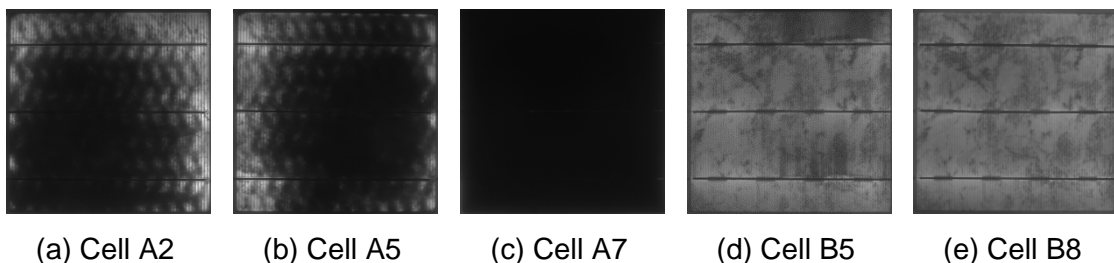


Figure 28: I-V Curves of the manufacturing defective cells of the first string (string AB) at 100 W/m^2 , using B9 as the healthy reference cell of the string for comparison.

Additionally, it has been seen that there is a tendency to decrease the light emission during EL tests with the efficiency drop, as seen in Figure 29. Short-circuited cell does not emit any light during EL and it is seen colder than the rest in IRT, which authors propose to denominate as *cold spot*, defining it as cell or group of cells at abnormal low temperature in a PV system. Figure 30 shows the temperature of these defective cells during EL tests. Low-efficiency defects are seen as a tire imprint in the cell EL images and can be originated due to inhomogeneity during the firing process or in the transportation belt in the cell production and they can experiment almost a 50% power loss.



(a) Cell A2

(b) Cell A5

(c) Cell A7

(d) Cell B5

(e) Cell B8

Figure 29: EL images of the manufacturing defective cells of the first string (string AB) with an injected current of 8.9 A. Images taken with PCO 1300 camera, with a focal distance of 4 cm and exposure time 40 s.

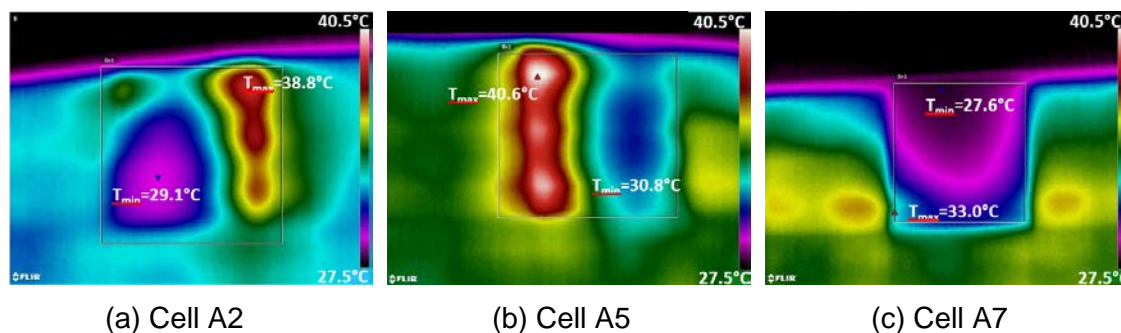


Figure 30: Indoor IRT images of the low efficiency (a and b) and the short-circuited I defective cells of the first string (string AB) during EL tests, injecting a current of 8.9A. Images taken with FLIR SC 640 IR camera. Their maximum and minimum temperatures in these conditions are: a) $T_{max}=38.8^{\circ}\text{C}$ and $T_{min}=29.1^{\circ}\text{C}$. b) $T_{max}=40.6^{\circ}\text{C}$ and $T_{min}=30.8^{\circ}\text{C}$ and c) $T_{max}=33.0^{\circ}\text{C}$ and $T_{min}=27.6^{\circ}\text{C}$.

The second characterized failure has been the soldering defects. The soldering of the wires to the solar cells results in generating significant thermomechanical stresses in different layers due to the diversity of thermal expansion of different components, which can lead to small cracks in the solar cells [98,99]. Soldering defective cells present smaller parameter deviations than the rest of the defects studied. Additionally, it has been seen that there are more losses when there is a local soldering defect in just a part of the bus, as the series resistance is considerably increased. Conversely, having all (or some) tabs loose does not interrupt the electrical contact despite not being welded, and its influence is not disastrous. However, this could be altered after some years of operation of the module in which the encapsulation is exposed to thermal cycles.

Soldering defects studied are not visible in EL. It could be because the faults are made on the back side of the module. An additional analysis has been performed to check if these defects are visible with IRT performed from the back side of the module in short circuit current injection conditions. The IRT image of the back side of the whole module can be seen in a). In these conditions, the only defect which certainly experiments an overheating is cell C8, corresponding the heating area with the centimeter of the three buses welded.

The greatest danger of bad welds is usually the electric arcs, since that bad contact causes the tab to warm up and it can come out to disconnect it. At that moment there is a relevant tension difference between two points very close and micro arcs can be generated. That ends up burning the back sheet behind, or if they are generated in broken cells, the edges of the cell are usually burned and also depending on the

composition of the paste together with the permeability of the back sheet, the humidity causes the fingers to blacken, being easily identifiable the cell breakages, which is commonly known as snail trails.

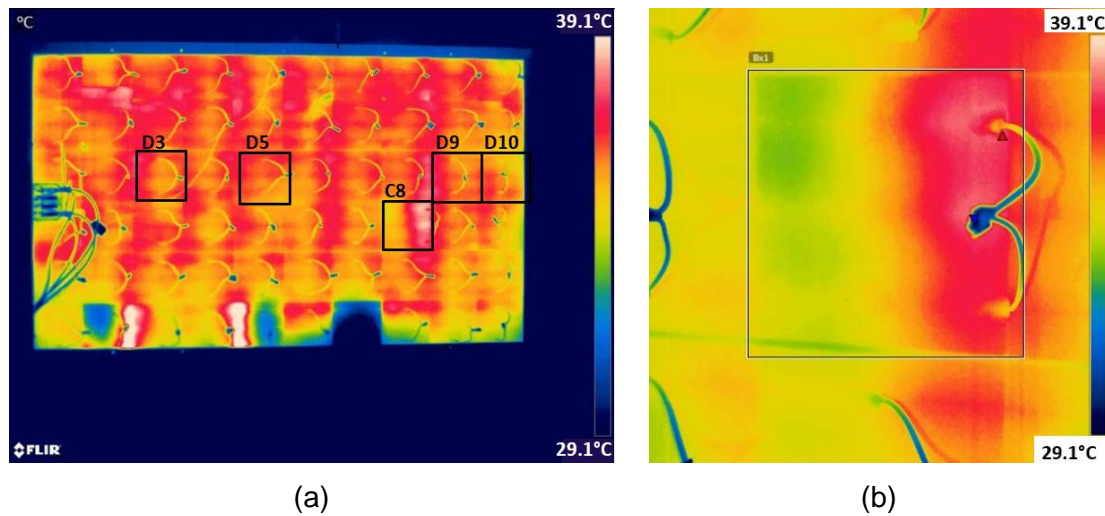
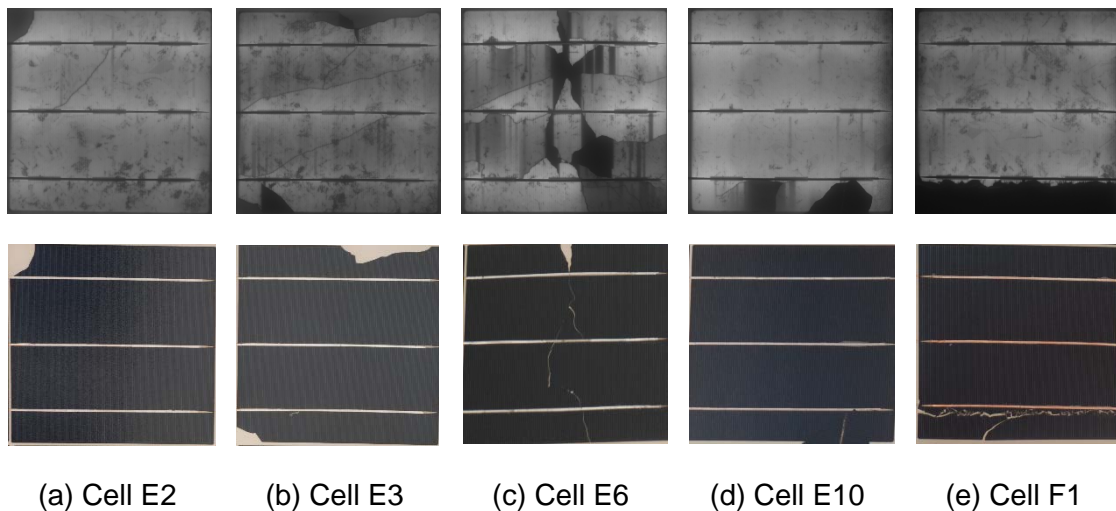


Figure 31: Indoor IRT images of the back side of the module (a) and of the C8 cell (b) during EL tests, injecting current of 8.9A. Images taken with FLIR SC 640 IR camera. The maximum and minimum temperatures in C8 cell in these conditions are: $T_{max}=38.2^{\circ}\text{C}$ and $T_{min}=29.6^{\circ}\text{C}$.

Concerning broken cells, it has been analyzed how the shape of the I-V curves of the affected cells is very similar to the one of the nominal equivalent cell but decreasing the current proportionally, as in the case of shading [100,101]. The EL images of defective cells, complemented in this case by their corresponding RGB images that allow seeing the breaking patterns, are shown in Figure 32. It has been seen that if a piece of one cell is placed on another cell it generates a parallel electrical path which is responsible of a small R_{sh} in the cell, turning the I-V curve into a straight line.



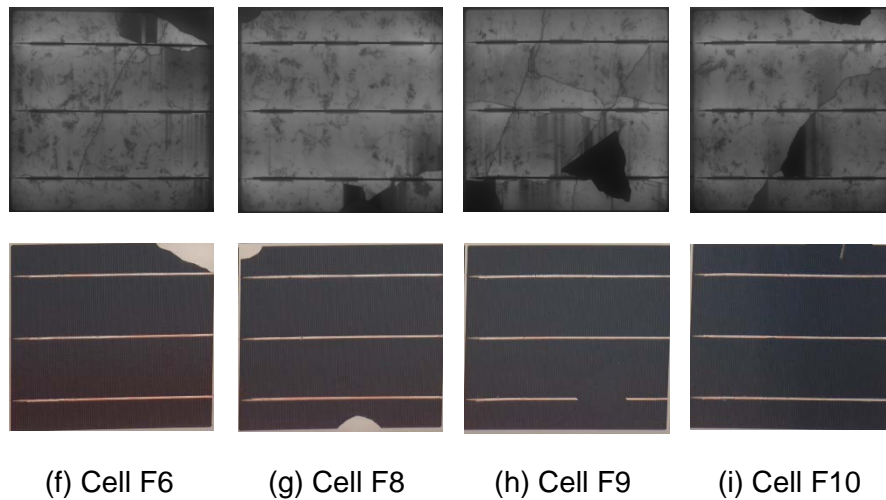


Figure 32: EL and RGB images of the broken defective cells of the third string (string EF) with an injected current of 8.9A. EL images taken with PCO 1300 camera, with a focal distance of 4 cm and exposure time 40s.

Failures like cell cracks, solder corrosion, and broken cell interconnects have no limits in power loss and the PV module may become unusable [33]. Two distinct types of dark areas are observable in the EL images (Figure 32), irregularly shaped regions and regular rectangular shaped areas. The irregular areas indicate the presence of cracks in the silicon wafers. However, the presence of regular rectangular dark areas can be due to broken front grid fingers, which are broken at the busbar [102,103]. Finally, an optical microscope has been used for imaging a crack in cell F9 solar cell, which displayed a dark irregular area in the crack zone in the EL measurement. It proves how a small crack, not visible for the human eye, can isolate a part of the cell Figure 33.

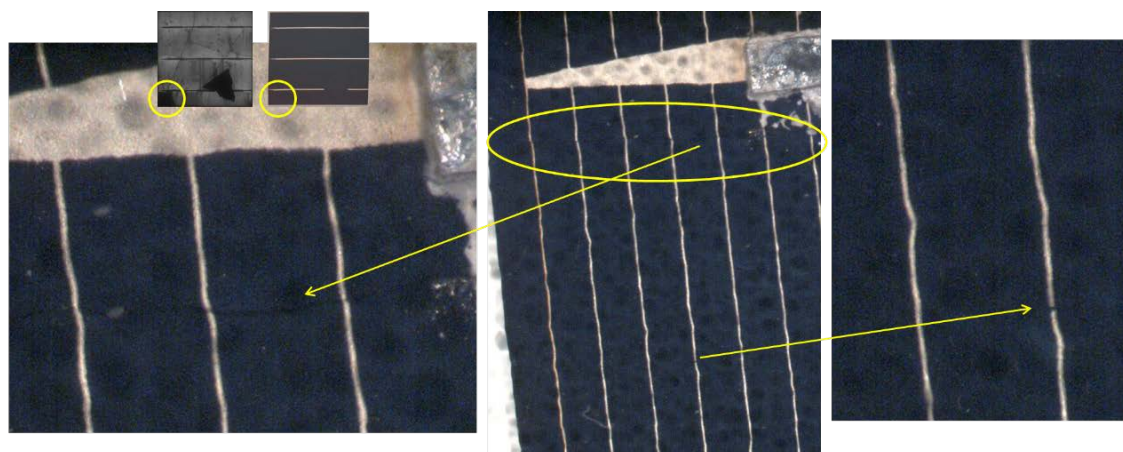


Figure 33: Optical micrographs of a crack in F9 solar cell which displayed a dark irregular area in the crack zone in the EL. Images captured with a Nikon SMZ 800 microscope.

Regarding the three kinds of defects combination or mix within a module, it has been seen how when the cells are series connected, the cell which delivers the lowest current will limit the current of the string. In this module, there is a total of three bypass diodes, one every 20 cells. As it has been seen, each bypass string contains different defects (of manufacturing, soldering and breaking cells) and each of them is able to produce a different current. Therefore, the electrical characteristic curve of the whole module, which is composed by the three bypass circuits in series, will contain three steps, each at the I_{sc} of each bypass circuit, as seen in Figure 34.

It has also been concluded that for soldering defects, in which the series resistance has an important influence, having more buses connecting the cells could increase the whole module performance. The effect of a shunt resistance is particularly severe at low light levels, since there will be less light-generated current. There is a clear tendency to increase the shunt resistance on lower irradiance levels in illumination tests [104], as seen in the following Figure 35, in which this effect is extremely evident in cell E10.

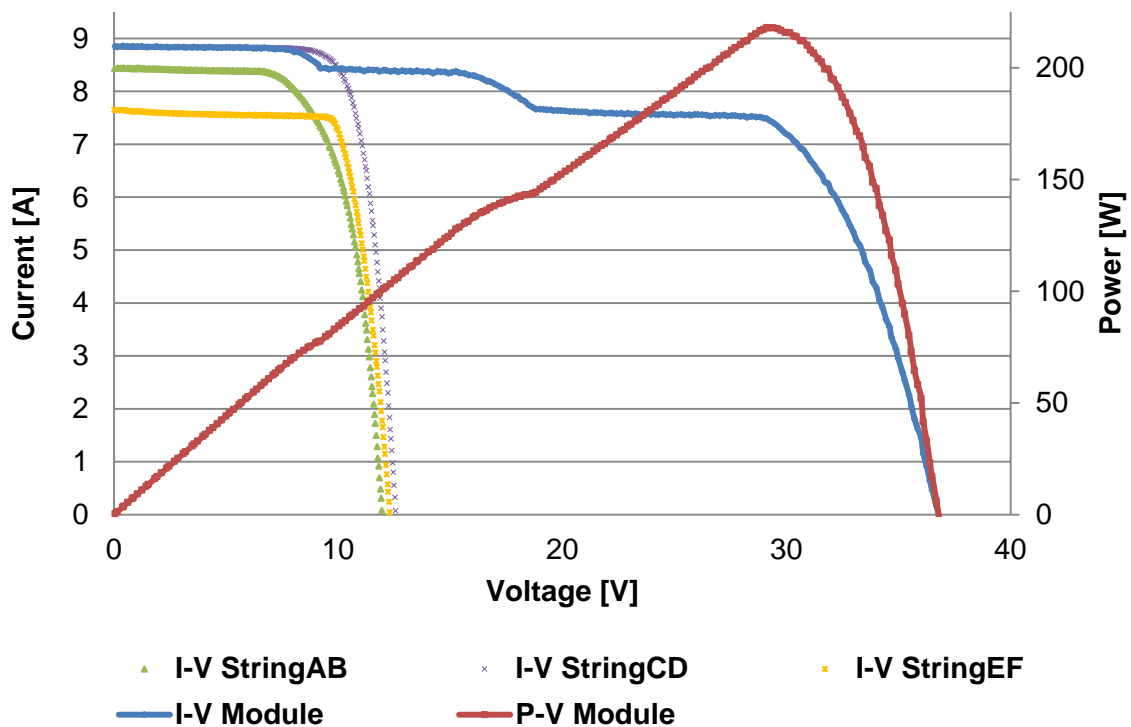


Figure 34: I-V Curves of the complete module and separate strings at 1,000 W/m². The secondary axis presents the P-V curves of the module at this irradiance.

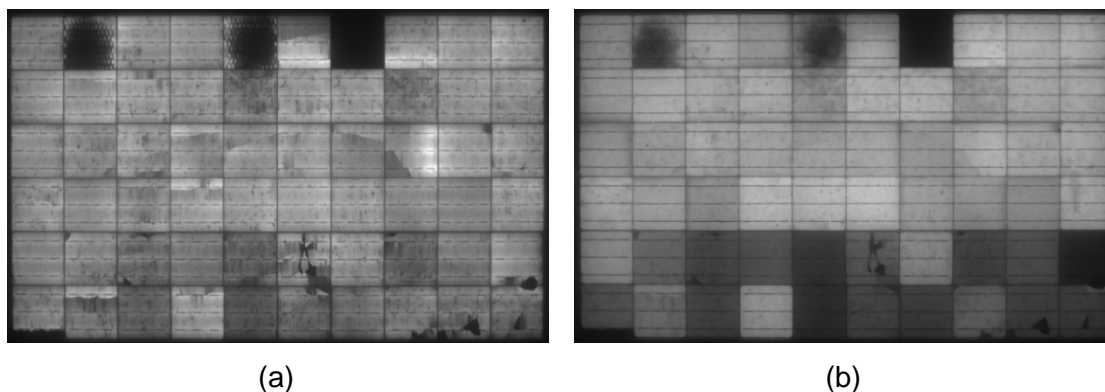


Figure 35: EL images of the tested module with an injected current of 8.9 A (a) and 0.89 A (b). EL images taken with PCO 1300 camera, with a focal distance of 4 cm and exposure time 50 s (a) and 15 min (b).

In the outdoor IRT, the most restrictive cell is detected as a severe hotspot. It can be seen in Figure 36.

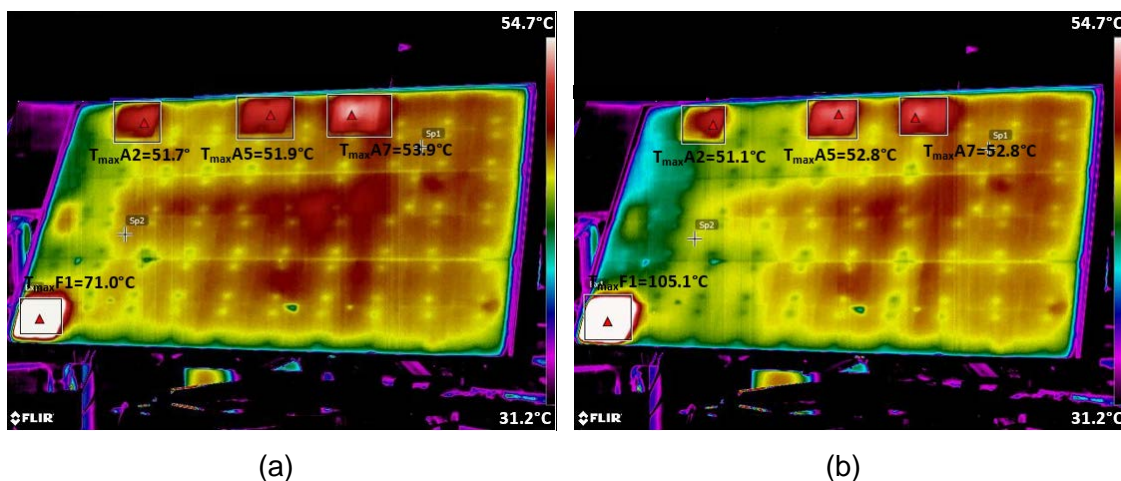


Figure 36: Outdoor IRT images of the module in the lower current step of the I-V curve at 7.3 A-24 V (a) and in the middle current step of the I-V curve at 7.8 A-15 V (b) at 933 W/m². Images taken with FLIR SC 640 IR camera. The maximum temperature values of the different hot spots are indicated in the figures.

At the low current step (Figure 36 a), the diodes are not operating. However, in the second current step (Figure 36 b), at 7.8 A, the temperature in F1 increases a lot, as string EF has the most restrictive current in the module and throughout the bypass diode of this string has to circulate the current that the string is not able to do. In the short-circuited cell (cell A7), all the external energy received from the sun is not used to generate electricity. The absorbed photons generate pairs of electrons in the cell

material, that are recombined by other mechanisms not useful for the electricity generation and therefore, the material becomes hotter.

From this study it has been possible to obtain a concluding remark on each inspection method and defect type, to highlight the information provided by each surveying technique considering the defect type, with the aim of not missing any information during the examination. It has been seen that authors and main players involved in PV systems mainly work with the different inspection techniques separately. The remarks presented in this section will determine the validity of the different alternatives and their complementarity.

In relation with manufacturing defects, it has been checked that the different inspection techniques show:

- I-V characterization: low-efficiency and medium-efficiency defects are clearly evidenced at STC conditions, as well as the short-circuited cells. Their FF is reduced while increased the irradiance levels and therefore their maximum power output. The efficiency defects present high values of R_s , which is shown as an increment in the curve slope at V_{oc} . Severe defects are also revealed with a slope increment at I_{sc} because of their reduced R_{sh} . Power loss can almost achieve 50% in low efficiency cells, as seen in the research.
- EL and indoor IRT characterization: low efficiency cells can be seen as a tire imprint in the EL images and they experiment a local overheating in the emitting area. Medium efficiency cells do not present any special pattern in EL neither indoor IRT, although it has been observed a tendency to decrease the light emission during EL tests with the efficiency drop. Short-circuited cells do not emit any light during EL and its whole area is seen colder in thermography, which has been denominated as cold spot.
- Outdoor IRT characterization: low efficiency cells as well as short-circuited cells are revealed as minor hot spots in normal outdoor operation, with a ΔT of around 5°C . Medium efficiency defects are not evidenced in outdoor IRT examination.

Therefore, the most complete inspection technique for efficiency defects is the I-V characterization, in which all the manufacturing defects types analyzed are evidenced. In low efficiency cells, EL complements the I-V curves checking the EL defects patters. Regarding the outdoor IRT, it should be very exhaustive in order to be valid, as these defects present low ΔT . In relation with short-circuited cells, EL and indoor IRT would be

Detection, classification and characterization of defects in photovoltaic modules through the use of thermography, electroluminescence, I-V curves and visual analysis

the most effective inspections, presenting this kind of defect the clear patterns detailed in these conditions.

In relation with soldering defects, it has been checked that the different inspection techniques show:

- I-V characterization: local soldering defects, in just a part of the bus, considerably increase the R_s , presenting an I-V curve affected near the V_{oc} , incrementing the curve slope. Additionally, having one, two or all the three tabs not welded reduces the V_{oc} .
- EL and indoor IRT characterization: soldering defects analyzed are not visible in EL. Only local soldering defects experiment an overheating during current injection. Therefore, defects with one or more buses not welded in the backside of the cell are apparently neither detectable using indoor IRT.
- Outdoor IRT characterization: soldering defects analyzed are not detectable in outdoor IRT.

It has been seen that soldering defects performed in the backside of the module present small parameter deviations than the rest of failures studied, being the I-V characterization the most effective to detect them, which can be complemented with indoor IRT in case of local soldering defects.

Finally, in relation with broken cells defects, it has been checked that the different inspection techniques show:

- I-V characterization: the shape of the I-V curve of the affected cell is very similar to the nominal equivalent cell but decreasing the current proportionally to the disconnected area. The V_{oc} is also slightly decreased. Parallel electrical paths distort the I-V curve, turning it into a straight line due to small R_{sh} .
- EL, visual and indoor IRT characterization: EL clearly evidences disconnected areas and breaks with dark regions. Irregular areas indicate the presence of cracks in the silicon wafers while regular rectangular dark areas can be due to broken front grid fingers. Not the totality of dark regions in EL corresponds with disconnected cell areas, as the case in which a piece of other cell is over placed in the front part of another cell. Broken cells defects analyzed have not been detected in indoor IRT.
- Outdoor IRT characterization: Disconnected areas restring the current through the cell, and this can generate a hot spot, which can reach high temperatures.

The hotspot temperature will depend on the disconnected area. In the broken cell analyzed (F1), the ΔT is 23.6°C in normal operation.

Therefore, in the case of breaks in cells, the most interesting information is probably provided by the EL tests, clearly showing the breaks and disconnected areas, while outdoor IRT can complement EL locating the most restrictive cell within a string. It has been seen in the hot spot examined that it present high ΔT , so regarding the outdoor IRT, it should not be such exhaustive as in other defects analyzed in order to be valid.

1.6.2.3. Classification of PV defects

Once the detection and characterization of different defects have been studied, a classification of thermographic defects has been performed to complete objective 2. An onsite study of 17,142 monocrystalline modules has been carried out with the aim of detecting every single existing defect, classifying them in different groups, studying the variance of the same kind of defect in different modules and the patterns of each group of thermographic defects. This analysis can be reviewed in the paper presented in subsection 2.2.6. In this case, the thermographic analysis for the identification of defects in this research is performed manually, as the spatial resolution of the thermographic images is higher than using UAVs. However, this study is complemented with the results of the aerial thermographic inspections explained in subsection 1.6.3. A 3 MW PV plant, commissioned in 2008, has been chosen with the aim of gathering larger amount of data and different cases in comparison with the information which would be available in a small installation in the rooftop of a building. However, the results are perfectly extended for their subsequent application in aerial thermographic inspections and in small scale installations in roofs or façades of buildings, as same defects have to be identified in all PV inspections.

From the 17,142 modules thermographically inspected, the number of detected modules with some failure has been 1,140, which corresponds to 6.65%. According to some recent research, it is predicted that 2% of the PV modules do not meet the manufacturer's warranty after 11-12 years of operation [105]. The percentage of failures detected is over this rate because every single anomaly has been reported in this study, independently of the temperature difference between the overheated area and the healthy part. However, according to [64], due to normal tolerances in cell sorting and module production, thermal abnormalities of less than 10 % of the recorded modules do not indicate a special quality issue regarding the used modules.

Attending the results obtained, all these faults detected have been classified in five different thermographic defects modes: hotspot in a cell or in a group of cells, bypass circuit overheated, hotspot in the junction box, hotspot in the connection of the busbar to the junction box and whole module overheated. The distribution of defects among these five groups can be observed in Table 4. As it can be seen, more than three quarters of the affected modules correspond to cell hotspots, presenting one or more cells overheated. This prevailing number of hotspot failures in cells with respect to the rest of failures types is not an isolated case. Statistically, there are a greater amount of cells, 72 cells per module in this case, than of the rest of components, three bypass circuits, one junction box, four bus ribbons and one module. Additionally, there are a large number of causes responsible for the occurrence of cell hotspots, as cell cracks, snail trails, potential induced degradation (PID) or delamination [105]. Although some of the defects are slightly visible to the human eye, as snail trails, most of them are undetectable without the use of a thermographic camera [64]. Additionally, other defects within the PV module can be the result of a cell failure. For instance, a diode fault can be caused by a hotspot in a string of cells that forces the continuous operation of the diode, overheating it. Therefore, a correct characterization of this kind of failures is essential for a proper automatic detection of cell hotspot supported by software, as it represents more than three quarters of the defects.

Table 5: Thermographic defects detected classified by the module affected component

Affected component	Number of defects detected	Percentage
Hotspot	859	75.35%
Bypass circuit	123	10.79%
Junction box	79	6.93%
Connection	78	6.84%
Module	1	0.09%

Commonly, the severity of defects is given, based on the difference of temperature between overheated and healthy areas, ΔT , within a module. The absolute temperature of the defect is not used to determine the severity as it is strongly dependent on different weather conditions, as the ambient temperature, the irradiance or the wind speed. This ΔT varies significantly between different kinds of defects, as it can be observed in Figure 37, which presents a box chart showing the difference of temperature for each of the 1,140 defective modules detected, grouped by defect type.

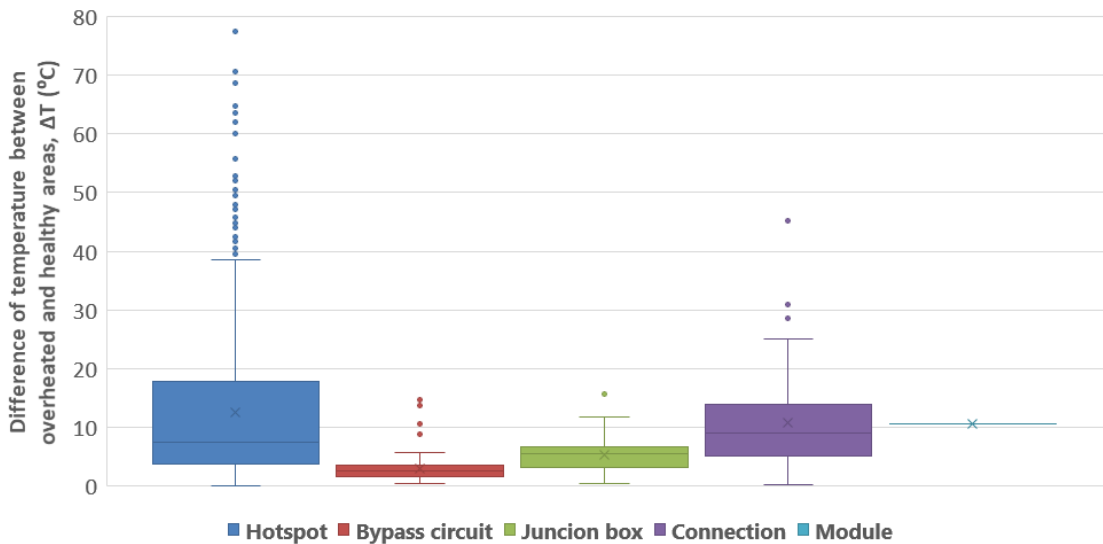


Figure 37: Box chart showing the delta temperature between overheated and healthy areas, ΔT , grouped by defect type for each of the 1,140 defective modules detected

Three different common ranges of temperature for all defects types have been defined attending the severity of the anomalies for manual thermal inspection proposed in [61]. Differences higher than 30°C are considered as severe failures, from 10°C to 30°C are considered as medium severity failures, and lower than 10°C as minor failures. According to [64], temperature gradients lower than 10°C are normally considered as unproblematic and do not have to be listed separately. Temperature gradients from 10°C to 20°C are unproblematic in the current stage [64], although they have to be reported and observed in subsequent regular thermal inspections as they can increase during the operation of the PV power plant. Differences in temperature above 20°C are expected to cause degradations of panel output and eventually, the material compound may even degrade, resulting in a safety issue [64]. Table 5 summarizes the severity of all defects detected, grouped by defect type or affected component.

Table 6: All defects detected classified by the affected component and in three temperature groups

Affected component	$\Delta T \geq 30^{\circ}\text{C}$		$10 \leq \Delta T < 30^{\circ}\text{C}$		$\Delta T < 10^{\circ}\text{C}$		Total
	Count	Percentage	Count	Percentage	Count	Percentage	
Hotspot	89	10.36%	262	30.50%	508	59.14%	859
Bypass circuit	0	0%	4	3.25%	119	96.75%	123
Junction box	0	0%	4	5.06%	75	94.94%	79
Connection	2	2.56%	32	41.03%	44	56.41%	78
Module	0	0%	1	100%	0	0%	1

Based on the results obtained in the tests performed, hotspot is the defect type that shows higher temperature differences, achieving up to 77.4°C between the overheated hotspot and the healthy area in one of the tested modules. The second type of defect that presents higher ΔT is the connection, reaching 45.1°C. These two kinds of defects have some similarities. The defect area and consequently the overheated area are small, so the heat is concentrated in a smaller area. Hotspots typically appear in just one cell and the connection defects in a small busbar point. Additionally, these two kinds of defects are revealed in the front part of the module, so the thermographic camera captures directly this temperature during a regular inspection, in which the front temperature of PV modules is revised.

Reviewing all cells hotspot defects, it has been concluded that the pattern of this fault is an overheated cell, of approximate 15 x 15 cm² depending on the module manufacturer, located in any cell along the module. The analysis performed does not reveal any preference of appearance of the overheated cell in any of the three strings circuits. Revising all bypass circuit defects it has been concluded that the pattern of this fault is two mainly homogeneous overheated columns of cells, with total approximately dimensions of 180 cm x 30 cm for 72 cells modules and 150 cm x 30 cm for 60 cells modules, depending on the module manufacturer. The overheated area can be located in any of the three strings of the module. The analysis performed does not reveal any preference of appearance of the overheated string in any of the three strings circuits. Regarding the junction box failures, it has been shown that they are revealed as an overheated point in the middle part of the shorter side in which the box is located. This overheated point habitually appears in the middle of two different cells. In relation to connection defects, it has been concluded that the pattern of this fault is an overheated point, generally smaller than a cell, located next to the frame in the same side in which the junction box is placed. Finally, it has been noticed that differences in temperature between a module and the rest of modules of the same row or string could be due to an erroneous connection between them, mismatching or to internal defects of the module affecting all the bypass circuits. This kind of defect can be automatically detected as a difference in the mean temperature of one module with respect to the rest of the modules of the same PV structure. This study results can be useful as a base to develop the patterns of the different kind of defects in a software to automatically detect if a module has an anomaly and its classification.

1.6.3. Analysis of aerial IRT as a novel inspection technique (Obj. 3)

Photogrammetric studies performed with UAV have recently become more popular as they present an interesting low-cost alternative. A novel application of IRT with UAVs has been validated during the last years: aerial IRT for inspection of PV plants as a useful diagnostic technique to assess the performance of PV modules, superseding time-consuming traditional manual methods. As it has been introduced, PV energy is one of the most promising markets in the field of the generation of renewable and sustainable energy. Traditional techniques to detect faulty modules or cells within a PV plant, as the I-V curve test and/or manual IRT, are costly and time-consuming techniques, which are not viable in the current massive PV sites. All these facts have motivated research into innovative O&M techniques, such as the aerial IRT, to enable or optimize maintenance activities.

In order to invest in the required equipment to perform aerial IRT, it is absolutely necessary to know the equipment that it is going to be used and its characteristics perfectly, with the aim of obtaining accurate and usable results. Image quality will have a great impact on the accuracy of the photogrammetric end product [106,107]. Although there are several researchers developing this novel technique, there are no clear guidelines for the selection of involved instrumentation meeting the needs of PV inspections. This makes it necessary to investigate needs and aspects involved in this issue, regarding key characteristics of sensors and platforms and current instrumentation technologies available on the market, which has been analyzed throughout this doctoral research and can be reviewed in the papers presented in subsections 2.3.1, 2.3.2 and 2.3.3. In summary, it could be said that the most important characteristics in a thermographic camera for its usage with an UAV are: the resolution of the detector (up to 640x512 pixels), the thermal sensitivity or Noise-Equivalent Temperature Difference (NETD) (below than 50 mK), the accuracy (leading brands offer accuracies of $\pm 2\%$), camera weight (1-400 g), batteries, lens (according to the pixel resolution, the Field of View (FOV), Instantaneous Field of View (IFOV) and flying altitude), radiometric camera, RGB sensor, camera software, frame rate (advisable from 30 to 50 Hz as the camera is in motion) and temperature range (typical values are between -20°C and $+500^{\circ}\text{C}$).

Regarding the UAVs, the most appropriate ones to perform PV thermographic inspections are multicopter or multirotor systems, as they are the most stable ones. Before planning any flights, it is essential to study the applicable regulatory framework governing use of UAVs in public areas in the country concerned. For example, in Spain,

Detection, classification and characterization of defects in photovoltaic modules through the use of thermography, electroluminescence, I-V curves and visual analysis

UAVs are not allowed to fly over populated areas, in controlled air space or less than 8 km from an airport or airfield. Additionally, in Spain, licenses required to pilot UAVs, compulsory aviation liability insurance and accreditation by the State Aviation Safety Agency are a legal requirement [108,109]. Multicopters are usually classified by the number of motors they have such as tricopter, quadcopter, hexacopter and octocopter with three, four, six and eight motors, respectively. Deciding the kind of multicopter in terms of the number of rotors will influence in the payload that the UAV is able to deliver, the flight height, safety of landing and stability during flight. For this application, hexacopters are safer than quadcopters, allowing a safe landing even in the event of a damaged or dead motor (and octocopters allow a safe landing even if they lose two or three rotors), increasing the stability of the aircraft and having less influence from wind and rain.

Nevertheless, although the usefulness of aerial thermographic inspection has been proved, a review of the most important aspects in the tests that should be taken into account in order to make them valid has been performed, presented in section 2.3.4. Firstly, it has to be assured that the measurement is done under steady state conditions of the PV module. IRT measurements should be performed on a sunny, clear, cloudless day, with at least 600 W/m^2 irradiation at the module array [41]. Ideally, the ambient temperature as well as the wind speed should be low, with the aim of no influencing the hotspot or the module temperature, especially in the corner of the PV tables, where the cooling effect is most important. Radiometric measurements only report the surface temperature that can be very sensitive to strong winds. Infrared imaging should be done with a maximum wind speed of 4 bft (from 20 km/h to 28 km/h), which is already a significant wind speed that can affect the absolute measured temperatures. Additionally, in aerial IRT the UAV shall be capable of maintaining the working height and heading even in case of wind, so the manufacturer recommendations relative to maximum wind speed of each UAV should be met. It is important to consider the moving speed of the thermographic camera, with a maximum target value of 3 m/s according to the IEC standard [110]. UAVs are affected by wind, turbulence, sudden input by the operator and also by the flight movement of the aircraft itself as well as vibrations of the engines [111]. In the same way, it is essential to use the UAV automated flying features to avoid taking blurring images, as waypoints navigation, automatic landing and take-off, altitude and position hold, GPS, position save, coming home, boat mode and others. The modules should be clean to obtain accurate results. A prior cleaning of soiling, bird drops or other dirt is recommended previous to the inspection. The angle of view should be set as close

as possible to 90° but not less than 60° to the module glass plane, being the UAV operator aware of avoiding reflections [112]. The Operation and Maintenance personnel that will perform the inspections must be properly informed and trained. The level 1 certification according to the standard proves the qualification and knowledge needed [113]. For correct temperature measurement, the camera must be set to the correct reflected temperature and the emissivity values for the inspected surface, which is one of the main causes of measurement error. Typical emissivity values are 0.85 for the glass and 0.95 for the polymer back sheet, respectively, if the angle of view is within $90^\circ - 60^\circ$ (glass) and $90^\circ - 45^\circ$ (polymer) [33]. Other important parameter to consider while performing outdoor thermographic images is the atmospheric transmission influence, especially at large distances from the inspected object. The earth's atmosphere interferes with the thermal image by absorbing and emitting infrared radiation based on the air density, relative humidity, and distance between the object surface and the camera, attenuating the thermal radiance. It is also essential to correctly select the temperature range in the thermographic camera, defined as maximum and minimum temperature values that the camera can measure, as cameras present different measurement accuracies depending on temperature range. Finally, the thermographic camera should be properly calibrated [114,115].

One of the most relevant aspects to consider in aerial thermographic planning is the resolution of the thermographic images. Therefore, through this doctoral thesis it has been analyzed the influence of the height of the flight and the resolution of the image in the detection of faults in PV modules, which is explained in subsection 2.3.4. Data from numerous tests on a 3 MW real PV plant, performed manually and with an UAV flying at 30 and 80 m, have been evaluated for performing this investigation, as detailed in the methodology. The number of anomalies identified in each of the three inspections to the entire site is shown in Table 6 and the difference of temperature captured for each of the failures in the three inspections is represented in Figure 38.

Table 7: Anomalies identified, classified by their temperature.

Anomalies Detected	Manual Inspection	Aerial Inspection 30 m	Aerial Inspection 80 m
$\Delta T \geq 30^\circ\text{C}$	92	9	0
$10 \leq \Delta T < 30^\circ\text{C}$	305	231	73
$\Delta T < 10^\circ\text{C}$	738	181	202
<i>Total</i>	1,132	421	275

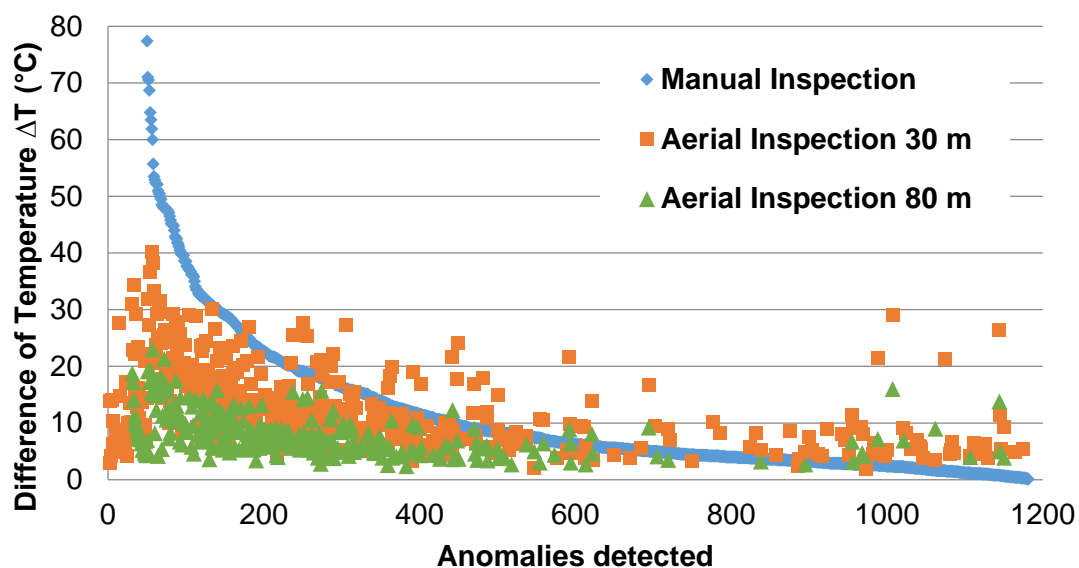


Figure 38: Temperature difference between the hotspot and the healthy area of the faulty modules detected in the manual inspection (blue), aerial inspection at 30 m (red) and aerial inspection at 80 m (green).

The differences in the results are mainly attributed to the resolution of the thermographic images. Although the thermal camera used in the aerial thermographic inspections has a higher resolution than the manual camera, the distance to the modules is higher, so the final resolution of the images decreases. The Spatial Resolution should be approximately from $3 \times 3 \text{ cm}^2$ to $5 \times 5 \text{ cm}^2$ to obtain accurate results if the distribution of temperatures within a faulty cell were constant, however it has been proved that the maximum temperature area in a hotspot strongly depends on the defect. In the manual and aerial inspections at 30 and 80 m performed the Spatial Resolutions are $1.8 \times 1.8 \text{ cm}^2$, $3.9 \times 3.9 \text{ cm}^2$ and $10.4 \times 10.4 \text{ cm}^2$, respectively.

Therefore, although an optimal resolution was not reached, it is essential to understand how it affects the results and how to interpret them depending on the images resolution. The six different hotspots thermographically analyzed at twelve different distances from each module are shown in Figure 39. This study has been done in order to define how temperature decreases with the distance, which can be seen in Figure 40. As it can be seen, there is a clear tendency to decrease the temperature with the increase of the distance to the failure, that is, with the increase of the pixel size. A regression analysis has been performed to obtain a more clear view of the dependency of the registered temperature in a cell hotspot on the distance to the module and on the real hotspot temperature. A first order polynomial has been chosen, (Eq. 2), obtaining an R-

squared value of 0.689, which explains most part of the existing variance. Although regression equations of higher order lead to better predictions, it has been preferred a physically interpretable solution. It could be completed considering other factors, as irradiation level or the ambient and module temperatures.

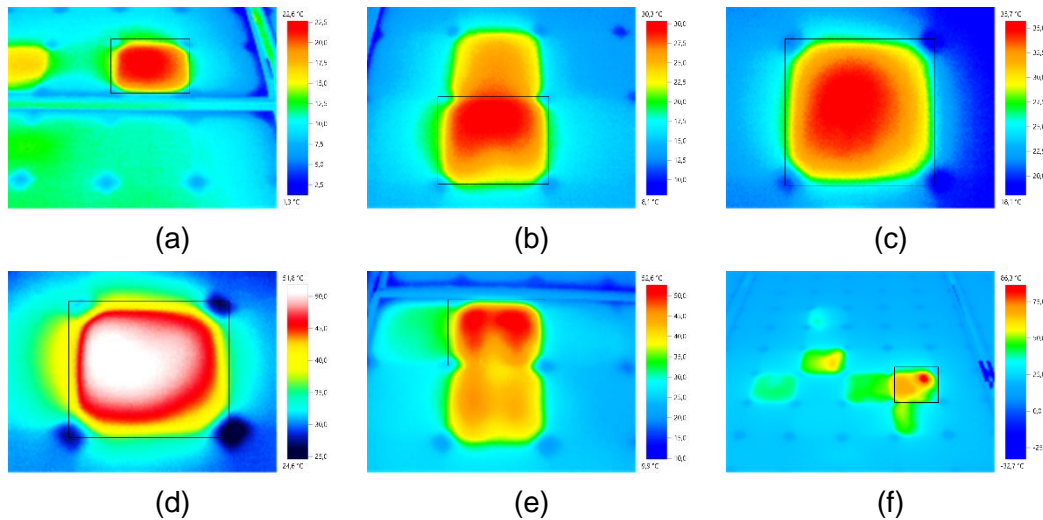


Figure 39: Thermographic images of defects 1 (a) to 6 (f). The temperature range in each of the six thermographic images is: (a) 1.3-22.6°C, (b) 8.1-30.3°C, (c) 18.1-35.7°C, (d) 24.6-51.8°C, (e) 9.9-52.6°C, (f) -32.7-86.3°C.

$$\Delta T^{\text{estimated}} = 2.21 - 0.41 \cdot \text{Distance} + 0.39 T_{\text{hotspot}} \quad (\text{Eq. 2})$$

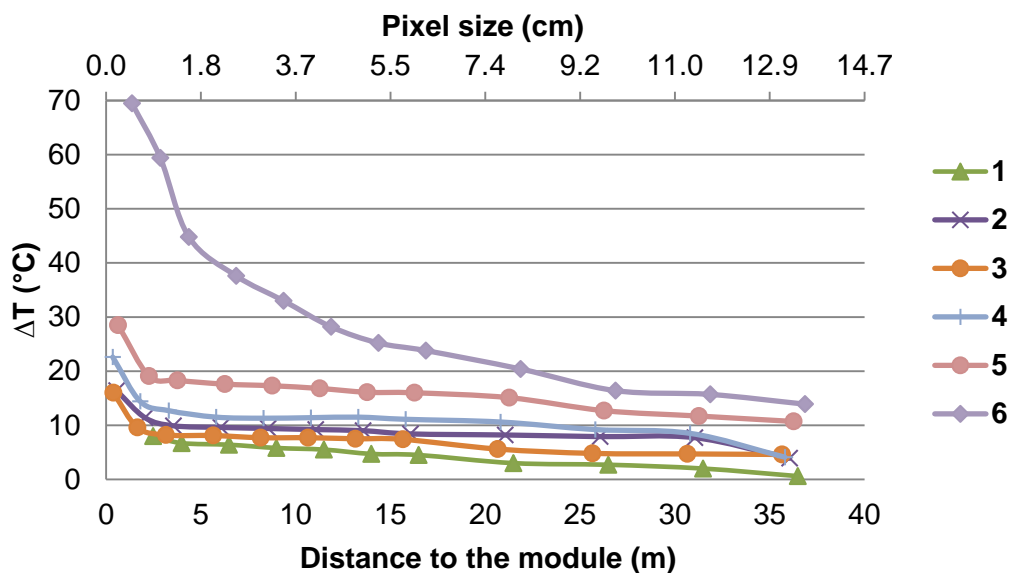


Figure 40: Difference of temperature between the hotspot and the healthy area of the six defects captured at twelve different distances. The secondary horizontal axis shows the pixel size at each distance. The images have been captured manually with the camera Testo 870-2.

It has been proved that the same failure will be registered as a different temperature depending on the distance from the thermographic camera to the faulty cell. Therefore, it is necessary to determine the severity range criteria to classify the failures detected as a function of the flight height, as it cannot be the same as the criteria used previously in the manual inspections. For the inspections performed, this criteria should change from the manual (1) to the aerial inspections at 30 m (2) and 80 m (3) as follows: severe failures, temperature difference higher than 30°C (1), 17.8°C (2) and 9.0°C (3); medium severity failures, from 10°C to 30°C (1), from 4.4°C to 17.8°C (1), from 0°C to 9°C (1) ; and minor failures, lower than 10°C (1), lower than 4.4°C (2) and not detectable (3).

1.7. References

- [1] REN21. REN21 - 2019 Global Status Report. 2019.
- [2] Sampaio PGV, González MOA. Photovoltaic solar energy: Conceptual framework. *Renew Sustain Energy Rev* 2017;74:590–601. <https://doi.org/10.1016/j.rser.2017.02.081>.
- [3] Herold D, Horstmann V, Neskakis A, Plettner-Marliani J, Piernavieja G, Calero R. Small scale photovoltaic desalination for rural water supply - demonstration plant in Gran Canaria. *Renew Energy* 1998;14:293–8. [https://doi.org/10.1016/S0960-1481\(98\)00080-9](https://doi.org/10.1016/S0960-1481(98)00080-9).
- [4] Bakos GC. Distributed power generation: A case study of small scale PV power plant in Greece. *Appl Energy* 2009;86:1757–66. <https://doi.org/10.1016/J.APENERGY.2008.12.021>.
- [5] Bouzardoum M, Mellit A, Massi Pavan A. A hybrid model (SARIMA–SVM) for short-term power forecasting of a small-scale grid-connected photovoltaic plant. *Sol Energy* 2013;98:226–35. <https://doi.org/10.1016/J.SOLENER.2013.10.002>.
- [6] Araneo R, Lammens S, Grossi M, Bertone S. EMC Issues in High-Power Grid-Connected Photovoltaic Plants. *IEEE Trans Electromagn Compat* 2009;51:639–48. <https://doi.org/10.1109/TEMC.2009.2026055>.
- [7] Moradi-Shahrbabak Z, Tabesh A, Yousefi GZ. Economical Design of Utility-Scale Photovoltaic Power Plants With Optimum Availability. *IEEE Trans Ind Electron* 2014;61:3399–406. <https://doi.org/10.1109/TIE.2013.2278525>.

-
- [8] Institution of Engineering and Technology. R, Mithulananthan N, Lee KY, Bansal RC. Wide-area measurement signal-based stabiliser for large-scale photovoltaic plants with high variability and uncertainty. vol. 7. Institution of Engineering and Technology; 2007.
- [9] Cabrera-Tobar A, Bullich-Massagué E, Aragüés-Peñalba M, Gomis-Bellmunt O. Topologies for large scale photovoltaic power plants. *Renew Sustain Energy Rev* 2016;59:309–19. <https://doi.org/10.1016/J.RSER.2015.12.362>.
- [10] Akinyele DO, Rayudu RK, Nair NKC. Development of photovoltaic power plant for remote residential applications: The socio-technical and economic perspectives. *Appl Energy* 2015;155:131–49. <https://doi.org/10.1016/J.APENERGY.2015.05.091>.
- [11] Oliver M, Jackson T. Energy and economic evaluation of building-integrated photovoltaics. *Energy* 2001;26:431–9. [https://doi.org/10.1016/S0360-5442\(01\)00009-3](https://doi.org/10.1016/S0360-5442(01)00009-3).
- [12] Simola A, Kosonen A, Ahonen T, Ahola J, Korhonen M, Hannula T. Optimal dimensioning of a solar PV plant with measured electrical load curves in Finland. *Sol Energy* 2018;170:113–23. <https://doi.org/10.1016/J.SOLENER.2018.05.058>.
- [13] Hernández-Callejo L, Gallardo-Saavedra S, Alonso-Gómez V. A review of photovoltaic systems: Design, operation and maintenance. *Sol Energy* 2019;188:426–40. <https://doi.org/10.1016/j.solener.2019.06.017>.
- [14] Braun M, Stetz T, Bründlinger R, Mayr C, Ogimoto K, Hattta H, et al. Is the distribution grid ready to accept large-scale photovoltaic deployment? State of the art, progress, and future prospects. *Prog Photovoltaics Res Appl* 2012;20:681–97. <https://doi.org/10.1002/pip.1204>.
- [15] Zhang P, Li W, Li S, Wang Y, Xiao W. Reliability assessment of photovoltaic power systems: Review of current status and future perspectives. *Appl Energy* 2013;104:822–33. <https://doi.org/10.1016/j.apenergy.2012.12.010>.
- [16] Harder E, Gibson JM. The costs and benefits of large-scale solar photovoltaic power production in Abu Dhabi, United Arab Emirates. *Renew Energy* 2011;36:789–96. <https://doi.org/10.1016/J.RENENE.2010.08.006>.
- [17] de La Tour A, Glachant M, Ménière Y. Predicting the costs of photovoltaic solar modules in 2020 using experience curve models. *Energy* 2013;62:341–8. <https://doi.org/10.1016/J.ENERGY.2013.09.037>.
-

- [18] Raugei M, Frankl P. Life cycle impacts and costs of photovoltaic systems: Current state of the art and future outlooks. *Energy* 2009;34:392–9. <https://doi.org/10.1016/J.ENERGY.2009.01.001>.
- [19] Spertino F, Corona F. Monitoring and checking of performance in photovoltaic plants: A tool for design, installation and maintenance of grid-connected systems. *Renew Energy* 2013;60:722–32. <https://doi.org/10.1016/J.RENENE.2013.06.011>.
- [20] Moore LM, Post HN. Five years of operating experience at a large, utility-scale photovoltaic generating plant. *Prog Photovoltaics Res Appl* 2008;16:249–59. <https://doi.org/10.1002/pip.800>.
- [21] Salmi T, Bouzguenda M, Gastli A, Masmoudi A. MATLAB/Simulink Based Modelling of Solar Photovoltaic Cell. *Int J Renew Energy Res* 2012;2:213–8.
- [22] Glunz SW, Preu R, Biro D. Crystalline silicon solar cells. State-of-the-art and future developments. *Compr. Renew. Energy*, vol. 1, 2012, p. 353–87. <https://doi.org/10.1016/B978-0-08-087872-0.00117-7>.
- [23] Green MA. Crystalline and thin-film silicon solar cells: State of the art and future potential. *Sol Energy* 2003;74:181–92. [https://doi.org/10.1016/S0038-092X\(03\)00187-7](https://doi.org/10.1016/S0038-092X(03)00187-7).
- [24] Schneller EJ, Brooker RP, Shiradkar NS, Rodgers MP, Dhere NG, Davis KO, et al. Manufacturing metrology for c-Si module reliability and durability Part III: Module manufacturing. *Renew Sustain Energy Rev* 2016;59:992–1016. <https://doi.org/10.1016/J.RSER.2015.12.215>.
- [25] Boix PP, Garcia-Belmonte G, Muñecas U, Neophytou M, Waldauf C, Pacios R. Determination of gap defect states in organic bulk heterojunction solar cells from capacitance measurements. *Appl Phys Lett* 2009;95:233302. <https://doi.org/10.1063/1.3270105>.
- [26] Chen S, Gong XG, Walsh A, Wei SH. Defect physics of the kesterite thin-film solar cell absorber $\text{Cu}_2\text{ZnSnS}_4$. *Appl Phys Lett* 2010;96:021902. <https://doi.org/10.1063/1.3275796>.
- [27] Gallardo-Saavedra S, Hernández-Callejo L, Duque-Pérez O. Quantitative failure rates and modes analysis in photovoltaic plants. *Energy* 2019;183:825–36. <https://doi.org/10.1016/j.energy.2019.06.185>.
- [28] Gallardo-Saavedra S, Hernández-Callejo L, Duque-Perez O. Analysis and
-

-
- characterization of PV module defects by thermographic inspection. *Rev Fac Ing Univ Antioquia* 2019;92–104. <https://doi.org/10.17533/udea.redin.20190517>.
- [29] Soutanis NL, Papathanasiou SA, Hatziaargyriou ND. A Stability Algorithm for the Dynamic Analysis of Inverter Dominated Unbalanced LV Microgrids. *IEEE Trans Power Syst* 2007;22:294–304. <https://doi.org/10.1109/TPWRS.2006.887961>.
- [30] Ji D, Zhang C, Lv M, Ma Y, Guan N. Photovoltaic Array Fault Detection by Automatic Reconfiguration. *Energies* 2017;10:699. <https://doi.org/10.3390/en10050699>.
- [31] Silvestre S, Silva MAD, Chouder A, Guasch D, Karatepe E. New procedure for fault detection in grid connected PV systems based on the evaluation of current and voltage indicators. *Energy Convers Manag* 2014;86:241–9. <https://doi.org/10.1016/j.enconman.2014.05.008>.
- [32] Chine W, Mellit A, Pavan AM, Kalogirou SA. Fault detection method for grid-connected photovoltaic plants. *Renew Energy* 2014;66:99–110. <https://doi.org/10.1016/j.renene.2013.11.073>.
- [33] Köntges M, Kurtz S, Packard C, Jahn U, Berger KA, Kato K, et al. Review on Failures of Photovoltaic Modules, Report IEA-PVPS T13-01:2013. 2013.
- [34] Manganiello P, Balato M, Vitelli M. A Survey on Mismatching and Aging of PV Modules : The Closed Loop. *IEEE Trans Ind Electron* 2015;62:7276–86.
- [35] Paper C, Energy TA, Co AE. Quantifying the Impact of Hot Spots on the Performance of Photovoltaic Modules by Infrared Thermography and a Simulation Model. 2nd Int. Exergy, Life Cycle Assessment, Sustain. Work. Symp., NISYROS - GREECE: 2011, p. 1–8. <https://doi.org/10.13140/2.1.3955.7125>.
- [36] Molenbroek E, Waddington DW, Emery KA. Hot spot susceptibility and testing of PV modules. *Conf. Rec. IEEE Photovolt. Spec. Conf.*, vol. 1, 1992, p. 547–52. <https://doi.org/10.1109/pvsc.1991.169273>.
- [37] UNE-EN 61215-1:2017 Terrestrial photovoltaic (PV) modules - Design qualification and type approval, 2017.
- [38] Dueñas S, Pérez E, Castán H, García H, Bailón L. The role of defects in solar cells: Control and detection defects in solar cells. 2013 Spanish Conf. Electron Devices, Valladolid, Spain: 2013. <https://doi.org/10.1109/CDE.2013.6481402>.
- [39] Bühler AJ, Perin Gasparin F, Krenzinger A. Post-processing data of measured I–V curves of photovoltaic devices. *Renew Energy* 2014;68:602–10.
-

<https://doi.org/10.1016/J.RENENE.2014.02.048>.

- [40] Deviations IT. Solar I-V Curves Interpreting I-V 2014.
- [41] IEC 62446 Grid connected photovoltaic systems -Minimum requirements for system documentation, commissioning tests and inspection, 2019.
- [42] Quater PB, Grimaccia F, Leva S, Mussetta M, Aghaei M. Light Unmanned Aerial Vehicles (UAVs) for cooperative inspection of PV plants. *IEEE J Photovolt* 2014;4:1107–13. <https://doi.org/10.1109/JPHOTOV.2014.2323714>.
- [43] Grimaccia F, Aghaei M, Mussetta M, Leva S, Quater PB. Planning for PV plant performance monitoring by means of unmanned aerial systems (UAS). *Int J Energy Env Eng* 2015;6:47–54. <https://doi.org/10.1007/s40095-014-0149-6>.
- [44] Denio H. Aerial solar Thermography and condition monitoring of photovoltaic systems. 38th IEEE Photovolt. Spec. Conf., Austin, TX, USA: IEEE; 2012, p. 613–8. <https://doi.org/10.1109/PVSC.2012.6317686>.
- [45] Buerhop C, Weißmann R, Scheuerpflug H, Auer R, Brabec C. Quality Control of PV-Modules in the Field Using a Remote-Controlled Drone with an Infrared Camera. 27th Eur. Photovolt. Sol. Energy Conf. Exhib., Frankfurt, Germany: 2012, p. 3370–3.
- [46] Aghaei M, Bellezza Quater P, Grimaccia F, Leva S, Ogliari E, Mussetta M. PV Plant Planning and Performance Monitoring by means of Unmanned Aerial Systems (UAS). VIII Congr. Naz. AIGE Reggio Emilia, Reggio Emilia, Italy: 2014, p. 55–60.
- [47] Aghaei M, Quater PB, Grimaccia F, Leva S, Mussetta M. Unmanned Aerial Vehicles in Photovoltaic Systems Monitoring Applications. 29th Eur. Photovolt. Sol. Energy Conf. Exhib. (EU PVSEC 2014), Amsterdam: 2014, p. 2734–9. <https://doi.org/10.1017/CBO9781107415324.004>.
- [48] Kauppinen T, Panouillot P-E, Siikanen S, Athanasakou E, Baltas P, Nikopoulos B. About infrared scanning of photovoltaic solar plant. In: Hsieh, SJ and Zalameda J, editor. *THERMOSENSE Therm. INFRARED Appl.* XXXVII, vol. 9485, 1000 20TH ST, PO BOX 10, BELLINGHAM, WA 98227-0010 USA: SPIE-INT SOC OPTICAL ENGINEERING; 2015, p. 948517 1-14. <https://doi.org/10.1117/12.2180165>.
- [49] Muntwyler U, Schüpbach E, Lanz M. Infrared (IR) Drone for Quick and Cheap PV

-
- Inspection. 31st Eur. Photovolt. Sol. Energy Conf. Exhib., Hamburg, Germany: WIP; 2015, p. 1804–6. <https://doi.org/10.4229/EUPVSEC20152015-5CO.15.6>.
- [50] Aghaei M, Grimaccia F, Gonano CA, Leva S. Innovative Automated Control System for PV Fields Inspection and Remote Control. *IEEE Trans Ind Electron* 2015;62:7287–96. <https://doi.org/10.1109/TIE.2015.2475235>.
- [51] Aghaei M, Gandelli A, Grimaccia F, Leva S, Zich RE. IR real-time analyses for PV system monitoring by digital image processing techniques. 2015 Int. Conf. Event-based Control. Commun. Signal Process., IEEE; 2015, p. 1–6. <https://doi.org/10.1109/EBCCSP.2015.7300708>.
- [52] Aghaei M, Leva S, Grimaccia F. PV power plant inspection by image mosaicing techniques for IR real-time images. 2016 IEEE 43rd Photovolt. Spec. Conf., IEEE; 2016, p. 3100–5. <https://doi.org/10.1109/PVSC.2016.7750236>.
- [53] Dotenco S, Dalsass M, Winkler L, Wurznner T, Brabec C, Maier A, et al. Automatic detection and analysis of photovoltaic modules in aerial infrared imagery. 2016 IEEE Winter Conf. Appl. Comput. Vis., Lake Placid, NY, USA: 2016, p. 1–9. <https://doi.org/10.1109/WACV.2016.7477658>.
- [54] Aghaei M, Dolara A, Leva S, Grimaccia F. Image resolution and defects detection in PV inspection by unmanned technologies. 2016 IEEE Power Energy Soc. Gen. Meet., IEEE; 2016, p. 1–5. <https://doi.org/10.1109/PESGM.2016.7741605>.
- [55] Grimaccia F, Leva S, Dolara A, Aghaei M. Survey on PV Modules' Common Faults After an O&M Flight Extensive Campaign Over Different Plants in Italy. *IEEE J Photovoltaics* 2017;7:810–6. <https://doi.org/10.1109/JPHOTOV.2017.2674977>.
- [56] Dalsass M, Scheuerpflug H, Fecher FW, Buerhop-Lutz C, Camus C, Brabec CJ. Correlation between the generated string powers of a photovoltaic power plant and module defects detected by aerial thermography. 2017 IEEE 44th Photovolt Spec Conf PVSC 2017 2018:1–6. <https://doi.org/10.1109/PVSC.2017.8366737>.
- [57] Tsanakas JA, Vannier G, Plissonnier A, Ha DL, Barruel F. Fault diagnosis and classification of large-scale photovoltaic plants through aerial orthophoto thermal mapping. 31st Eur. Photovolt. Sol. Energy Conf. Exhib. EU PVSEC 2015, Hamburg, Germany: 2015, p. 1783–8.
- [58] Addabbo P, Angrisano A, Bernardi ML, Gagliarde G, Mennella A, Nisi M, et al. A UAV infrared measurement approach for defect detection in photovoltaic plants. 2017 IEEE Int. Work. Metrol. Aerosp., IEEE; 2017, p. 345–50.
-

<https://doi.org/10.1109/MetroAeroSpace.2017.7999594>.

- [59] Abdin Jaffery Z, Kumar Dubey A, Haque A. Scheme for predictive fault diagnosis in photovoltaic modules using thermal imaging. *Infrared Phys Technol* 2017;83:182–7. <https://doi.org/10.1016/j.infrared.2017.04.015>.
- [60] Gallardo-Saavedra S, Hernández-Callejo L, Duque-Pérez O. Analysis and Characterization of Thermographic Defects at the PV Module Level. *Commun. Comput. Inf. Sci.* 1st Ibero-American Congr. Smart Cities, ICSC-CITIES 2018; Soria; Spain; 26 Sept. 2018 through 27 Sept. 2018, Soria (Spain): Communications in Computer and Information Science; 2019, p. 80–93. https://doi.org/10.1007/978-3-030-12804-3_7.
- [61] Gallardo-Saavedra S, Hernandez-Callejo L, Duque-Perez O. Image Resolution Influence in Aerial Thermographic Inspections of Photovoltaic Plants. *IEEE Trans Ind Informatics* 2018;14:5678–86. <https://doi.org/10.1109/TII.2018.2865403>.
- [62] Gallardo-Saavedra S, Alfaro-Mejia E, Hernández-Callejo L, Duque-Pérez Ó, Loaiza-Correa H, Franco-Mejia E. Aerial thermographic inspection of photovoltaic plants: analysis and selection of the equipment n.d. <https://doi.org/10.18086/swc.2017.20.03>.
- [63] Hallam B, Hamer P, Kim M, Nampalli N, Gorman N, Chen D, et al. Field Inspection of PV Modules: Quantitative Determination of Performance Loss due to Cell Cracks using EL Images. 2017 IEEE 44th Photovolt. Spec. Conf. PVSC 2017, 2017, p. 1858–62. <https://doi.org/10.1109/PVSC.2017.8366560>.
- [64] Jahn U, Herz M, Köntges M, Parlevliet D, Paggi M, Tsanakas I, et al. Review on Infrared and Electroluminescence Imaging for PV Field Applications. 2018.
- [65] Tsanakas JA, Ha L, Buerhop C. Faults and infrared thermographic diagnosis in operating c-Si photovoltaic modules: A review of research and future challenges. *Renew Sustain Energy Rev* 2016;62:695–709. <https://doi.org/10.1016/j.rser.2016.04.079>.
- [66] Youssef A, El-Telbany M, Zekry A. The role of artificial intelligence in photo-voltaic systems design and control: A review. *Renew Sustain Energy Rev* 2017;78:72–9. <https://doi.org/10.1016/j.rser.2017.04.046>.
- [67] Platon R, Martel J, Woodruff N, Chau TY. Online Fault Detection in PV Systems. *IEEE Trans Sustain Energy* 2015;6:1200–7.
-

-
- <https://doi.org/10.1109/TSTE.2015.2421447>.
- [68] Dhimish M, Holmes V, Mehrdadi B, Dales M. Comparing Mamdani Sugeno fuzzy logic and RBF ANN network for PV fault detection. *Renew Energy* 2018;117:257–74. <https://doi.org/10.1016/j.renene.2017.10.066>.
- [69] Mekki H, Mellit A, Salhi H. Artificial neural network-based modelling and fault detection of partial shaded photovoltaic modules. *Simul Model Pract Theory* 2016;67:1–13. <https://doi.org/10.1016/j.simpat.2016.05.005>.
- [70] Chine W, Mellit A, Lugh V, Malek A, Sulligoi G, Massi Pavan A. A novel fault diagnosis technique for photovoltaic systems based on artificial neural networks. *Renew Energy* 2016;90:501–12. <https://doi.org/10.1016/j.renene.2016.01.036>.
- [71] Agroui K. Indoor and Outdoor Characterizations of Photovoltaic Module Based on Mulicrystalline Solar Cells. *Energy Procedia* 2012;18:857–66. <https://doi.org/10.1016/j.egypro.2012.05.100>.
- [72] Power systems reliability subcommittee of the power systems engineering committee of the, Society IIA. IEEE Recommended Practice for the Design of Reliable Industrial and Commercial Power Systems. IEEE Stand Board 1990;Std 493-19:1–382.
- [73] Colli A. Failure mode and effect analysis for photovoltaic systems. *Renew Sustain Energy Rev* 2015;50:804–9. <https://doi.org/10.1016/j.rser.2015.05.056>.
- [74] Solmetric. Solmetric PV Analyzer I-V Curve Tracer User's Guide n.d. [http://www.solmetric.net/get/Solmetric PV Analyzer Users Guide_1500_en.pdf](http://www.solmetric.net/get/Solmetric%20PV%20Analyzer%20Users%20Guide_1500_en.pdf) (accessed November 18, 2019).
- [75] Suckow S. 2/3-Diode Fit 2014.
- [76] National Institutes of Health. ImageJ Image Processing and analysis in Java n.d. <https://imagej.nih.gov/ij/>.
- [77] Linear Technology - Design Simulation and Device Models n.d. <http://www.linear.com/designtools/software/> (accessed March 9, 2018).
- [78] Matlab Homepage n.d. <https://www.mathworks.com/> (accessed August 25, 2019).
- [79] Pajares G, de la Cruz JM. A wavelet-based image fusion tutorial. *Pattern Recognit* 2004;37:1855–72. <https://doi.org/10.1016/j.patcog.2004.03.010>.
- [80] Zitová B, Flusser J. Image registration methods: A survey. *Image Vis Comput* 2003;21:977–1000. [https://doi.org/10.1016/S0262-8856\(03\)00137-9](https://doi.org/10.1016/S0262-8856(03)00137-9).
-

- [81] FLIR. FLIR Tools. THERMAL ANALYSIS AND REPORTING (DESKTOP) n.d. <https://www.flir.co.uk/products/flir-tools/> (accessed December 26, 2019).
- [82] Workswell Infrared cameras and systems. Workswell CorePlayer n.d. <https://www.workswell-thermal-camera.com/workswellcoreplayer/> (accessed December 4, 2019).
- [83] Testo. The thermal imager n.d. <https://www.testo.com/en-UK/products/thermal-imager> (accessed January 24, 2020).
- [84] Microsoft. Office 365 n.d. <https://products.office.com/en-us/home> (accessed December 19, 2019).
- [85] Colli A. Extending performance and evaluating risks of PV systems failure using a fault tree and event tree approach: Analysis of the possible application. 38th IEEE Photovoltaics Spec. Conf., 2012, p. 2922–6. <https://doi.org/10.1109/PVSC.2012.6318198>.
- [86] Garoudja E, Harrou F, Sun Y, Kara K, Chouder A, Silvestre S. A statistical-based approach for fault detection and diagnosis in a photovoltaic system. 6th Int. Conf. Syst. Control. ICSC 2017, IEEE; 2017, p. 75–80. <https://doi.org/10.1109/ICoSC.2017.7958710>.
- [87] Perdue M, Gottschalg R. Energy yields of small grid connected photovoltaic system: effects of component reliability and maintenance. IET Renew Power Gener 2015;9:432–7. <https://doi.org/10.1049/iet-rpg.2014.0389>.
- [88] Zini G, Mangeant C, Merten J. Reliability of large-scale grid-connected photovoltaic systems. Renew Energy 2011;36:2334–40. <https://doi.org/10.1016/j.renene.2011.01.036>.
- [89] Collins E, Dvorack M, Mahn J, Mundt M, Quintana M. Reliability and availability analysis of a fielded photovoltaic system. IEEE Photovolt. Spec. Conf., IEEE; 2009, p. 002316–21. <https://doi.org/10.1109/PVSC.2009.5411343>.
- [90] Stember LH. Reliability Considerations in the Design of Solar Photo-Voltaic Power-Systems. Sol Cells 1981;3:269–85. [https://doi.org/10.1016/0379-6787\(81\)90008-9](https://doi.org/10.1016/0379-6787(81)90008-9).
- [91] Golnas A. PV system reliability: An operator's perspective. IEEE J Photovoltaics 2013;3:416–21. <https://doi.org/10.1109/JPHOTOV.2012.2215015>.
- [92] Piantoni G, Araneo R. Reliability and maintenance in high-power grid-connected

-
- photovoltaic systems: A survey of critical issues and failures. 17th IEEE Int. Conf. Environ. Electr. Eng. 2017 1st IEEE Ind. Commer. Power Syst. Eur. IEEEIC / I CPS Eur. 2017, IEEE; 2017, p. 1–4. <https://doi.org/10.1109/IEEEIC.2017.7977870>.
- [93] Cristaldi L, Faifer M, Lazzaroni M, Khalil MMAF, Catelani M, Ciani L. Diagnostic architecture: A procedure based on the analysis of the failure causes applied to photovoltaic plants. *Measurement* 2015;67:99–107. <https://doi.org/10.1016/j.measurement.2015.02.023>.
- [94] Waqar Akram M, Li G, Jin Y, Chen X, Zhu C, Zhao X, et al. Improved outdoor thermography and processing of infrared images for defect detection in PV modules. *Sol Energy* 2019;190:549–60. <https://doi.org/10.1016/j.solener.2019.08.061>.
- [95] Ebner R, Zamini S, Újvári G. Defect analysis in different photovoltaic modules using electroluminescence (EL) and infrared (IR)-thermography. 25th Eur. Photovolt. Sol. Energy Conf. Exhib. / 5th World Conf. Photovolt. Energy Conversion, 6-10 Sept. 2010, Val. Spain, vol. 66, 2010, p. 37–9. <https://doi.org/10.4229/25thEUPVSEC2010-1DV.2.8>.
- [96] Gallardo-Saavedra S, Hernández-Callejo L, Alonso-García M del C, Santos JD, Morales-Aragonés JI, Alonso-Gómez V, et al. Nondestructive characterization of solar PV cells defects by means of electroluminescence, infrared thermography, I-V curves and visual tests: experimental study and comparison. *Energy* 2020.
- [97] Berardone I, Lopez Garcia J, Paggi M. Quantitative analysis of electroluminescence and infrared thermal images for aged monocrystalline silicon photovoltaic modules. 2017 IEEE 44th Photovolt. Spec. Conf., IEEE; 2018, p. 402–7. <https://doi.org/10.1109/pvsc.2017.8366338>.
- [98] Nasr Esfahani S, Asghari S, Rashid-Nadimi S. A numerical model for soldering process in silicon solar cells. *Sol Energy* 2017;148:49–56. <https://doi.org/10.1016/j.solener.2017.03.065>.
- [99] Li G, Akram MW, Jin Y, Chen X, Zhu C, Ahmad A, et al. Thermo-mechanical behavior assessment of smart wire connected and busbarPV modules during production, transportation, and subsequent field loading stages. *Energy* 2019;168:931–45. <https://doi.org/10.1016/j.energy.2018.12.002>.
- [100] Gallardo-Saavedra S, Karlsson B. Simulation, validation and analysis of shading
-

- effects on a PV system. *Sol Energy* 2018;170:828–39. <https://doi.org/10.1016/j.solener.2018.06.035>.
- [101] Rezk H, AL-Oran M, Gomaa MR, Tolba MA, Fathy A, Abdelkareem MA, et al. A novel statistical performance evaluation of most modern optimization-based global MPPT techniques for partially shaded PV system. *Renew Sustain Energy Rev* 2019;115:109372. <https://doi.org/10.1016/j.rser.2019.109372>.
- [102] Chaturvedi P, Hoex B, Walsh TM. Broken metal fingers in silicon wafer solar cells and PV modules. *Sol Energy Mater Sol Cells* 2013;108:78–81. <https://doi.org/10.1016/j.solmat.2012.09.013>.
- [103] Munoz MA, Alonso-García MC, Vela N, Chenlo F. Early degradation of silicon PV modules and guaranty conditions. *Sol Energy* 2011;85:2264–74. <https://doi.org/10.1016/j.solener.2011.06.011>.
- [104] Ruschel CS, Gasparin FP, Costa ER, Krenzinger A. Assessment of PV modules shunt resistance dependence on solar irradiance. *Sol Energy* 2016;133:35–43. <https://doi.org/10.1016/j.solener.2016.03.047>.
- [105] Kim KA, Krein PT. Reexamination of Photovoltaic Hot Spotting to Show Inadequacy of the Bypass Diode. *IEEE J Photovoltaics* 2015;5:1435–41. <https://doi.org/10.1109/JPHOTOV.2015.2444091>.
- [106] Kedzierski M, Wierzbicki D. Radiometric quality assessment of images acquired by UAV's in various lighting and weather conditions. *Meas* 2015;76:156–69. <https://doi.org/10.1016/j.measurement.2015.08.003>.
- [107] Kedzierski M, Wierzbicki D. Methodology of improvement of radiometric quality of images acquired from low altitudes. *Meas* 2016;92:70–8. <https://doi.org/10.1016/j.measurement.2016.06.003>.
- [108] Coello J, Gutierrez P, Velasco A, Cristobal A, Parra V, Rosa M. Implementation of Aerial Thermography Inspection of PV Modules in the O&M Activities in Large PV Plants. 32nd Eur. Photovolt. Sol. Energy Conf. Exhib., WIP; 2016, p. 1730–5. <https://doi.org/10.4229/EUPVSEC20162016-5DO.12.1>.
- [109] Agencia Estatal de Seguridad Aérea Ministerio de Fomento n.d. http://www.seguridadaerea.gob.es/LANG_EN/home.aspx (accessed February 16, 2017).
- [110] IEC TS 62446-3:2017: Photovoltaic (PV) systems - Requirements for testing,
-

- documentation and maintenance - Part 3: Photovoltaic modules and plants - Outdoor infrared thermography. 2017.
- [111] Sieberth T, Wackrow R, Chandler JH. UAV Image Blur - Its Influence and Ways to Correct it. Int. Conf. Unmanned Aer. Veh. Geomatics, Vol. XL-1/W4, Toronto (Canada): n.d., p. 33–9.
- [112] Buerhop C, Schlegel D, Vodermayr C, Nieß M. Quality control of PV-modules in the field using infrared-thermography. 26th Eur. Photovolt. Sol. Energy Conf. Exhib., Hamburg, Germany: n.d., p. 3894 – 3897.
- [113] UNE EN ISO 9712:2012: Non-destructive testing - Qualification and certification of NDT personnel. 2012.
- [114] MacHin G, Simpson R, Broussely M. Calibration and validation of thermal imager. Quant Infrared Thermogr J 2008;6:133–47.
- [115] Budzier H, Gerlach G. Calibration of uncooled thermal infrared cameras. J Sens Sens Syst 2015;4:187–97.

1.8. Abbreviations

<i>AI</i>	Artificial Intelligence
<i>CdTe</i>	Cadmium Telluride
<i>CMMS</i>	Computerized Maintenance Management Systems
<i>DC</i>	Direct Current
<i>EL</i>	Electroluminescence
<i>FOV</i>	Field of View
<i>FMECA</i>	Failure Rate, Effect and Criticality Analysis
<i>GaAs</i>	Gallium Arsenide
<i>Ge</i>	Germanium
<i>IFOV</i>	Instantaneous Field of View

<i>InGaAs</i>	Indium-Gallium-Arsenide
<i>IRT</i>	Infrared Thermography
<i>I-V</i>	Current-Voltage
<i>LOP</i>	Loss of Profit
<i>MTBF</i>	Mean Time Between Failures
<i>MV</i>	Medium Voltage
<i>NETD</i>	Noise-Equivalent Temperature Difference
<i>O&M</i>	Operation and Maintenance
<i>PID</i>	Potential Induced Degradation
<i>PV</i>	Photovoltaic
<i>RPN</i>	Risk Priority Number
<i>RGB</i>	Red, Green Blue
<i>c-Si</i>	Crystalline Silicon
<i>STC</i>	Standard Test Conditions
<i>UAVs</i>	Unmanned Aerial Vehicles

1.9. Index of figures

Figure 1: Temperature and humidity controlled chamber at the EIFAB in Soria, Spain	37
Figure 2: EL and IR imaging capturing system used in the temperature and humidity controlled chamber	37
Figure 3: PV field of the Campus Duques de Soria, University of Valladolid.....	37

Figure 4: Set up of the EL and IRT cameras for the indoor tests at the Photovoltaic Solar Energy Unit of the CIEMAT, in Madrid.....	38
Figure 5: Outdoor IRT testing bench at the Photovoltaic Solar Energy Unit of the CIEMAT, in Madrid.	38
Figure 6: Equipment used in the aerial inspections to the 3 MW PV site, composed by a thermographic camera FLIR TAU 2 640 on board of a hexacopter DJI S900. At the back the STREAM monocrystalline modules with two portrait distribution.....	40
Figure 7: Temperature sensor matrix validation (a) Setup (b) Sensors deployed.	41
Figure 8: Solar panel IRT with drone (a) Cat S60 thermal camera and DJI Mavic Pro drone (b) captured image.	41
Figure 9: String of six modules with bypass diodes at HIG laboratory.	42
Figure 10: One of the shading cases studied (37% of a row shaded in three modules).	42
Figure 11: (a) to (m) Monocrystalline and (n) to (p) Polycrystalline modules tested in the research, presenting different kinds of defects.	43
Figure 12: (a) Front view of the tested module. (b) Back view of the tested module. (c) Defective cells distribution showed in the back view of the tested module.....	44
Figure 13: General view of the PV structures of the 3 MW PV plant analyzed.	46
Figure 14: General view of the PV modules of the 35kWp at the University of Cuenca.	46
Figure 15: 2/3 Diode Fit program screenshot while obtaining the single-diode model of a solar cell equivalent circuit.....	47
Figure 16: Module Windon 265W Mono-crystalline simulated in Ltspice IV with the real single-diode model cells presented in Figure 17.	48
Figure 17: Real single-diode model of a solar cell simulated in Ltspice IV.....	48
Figure 18: (a) RGB of the module under analysis (SE-2). Initial available (b) EL and (c) thermographic images in their original format for the fusion.....	49
Figure 19: EL and thermographic images resized and in grey scale, placed side by side.	50
Figure 20: Average number of failures per kW for the different defined groups (from PV1 to PV5) from 2012 to 2016.....	54

Figure 21: Distribution of the registered failures in each of the PV plants monitored elements, considering data from 2012 to 2016.....	54
Figure 22: Sum of the RPN for each of the groups of elements under study and the accumulated RPN sum	55
Figure 23: EL images taken before (a) and after 96 h of Isc current injection of a Tynsolar 175W monocrystalline module (b).	57
Figure 24: Evolution of the IRT and EL mean value intensities with the current injection in the module (a). Detailed evolution after the initial current injection in two periods are depicted in (b-e).....	58
Figure 25: S-E1 PV module: RGB appearance (a), first and last EL images (b), IR image in the fourth quadrant during the EL test (c), visual (d) and IR (e) outdoor images in ordinary module operation.	59
Figure 26: Merged images using (a) 'diff', (b) "fpde_fusion", (c) "ifm_fusion", and (d) "gff_fusion" algorithms.	61
Figure 27: I-V Curves of the manufacturing defective cells of the first string (string AB) at 1,000 W/m ² , using B9 as the healthy reference cell of the string for comparison.....	62
Figure 28: I-V Curves of the manufacturing defective cells of the first string (string AB) at 100 W/m ² , using B9 as the healthy reference cell of the string for comparison.....	63
Figure 29: EL images of the manufacturing defective cells of the first string (string AB) with an injected current of 8.9 A. Images taken with PCO 1300 camera, with a focal distance of 4 cm and exposure time 40 s.	63
Figure 30: Indoor IRT images of the low efficiency (a and b) and the short-circuited I defective cells of the first string (string AB) during EL tests, injecting a current of 8.9A. Images taken with FLIR SC 640 IR camera. Their maximum and minimum temperatures in these conditions are: a) Tmax=38.8°C and Tmin=29.1°C. b) Tmax=40.6°C and Tmin=30.8°C and c) Tmax=33.0°C and Tmin=27.6°C.	64
Figure 31: Indoor IRT images of the back side of the module (a) and of the C8 cell (b) during EL tests, injecting current of 8.9A. Images taken with FLIR SC 640 IR camera. The maximum and minimum temperatures in C8 cell in these conditions are: Tmax=38.2°C and Tmin=29.6°C.	65

Figure 32: EL and RGB images of the broken defective cells of the third string (string EF) with an injected current of 8.9A. EL images taken with PCO 1300 camera, with a focal distance of 4 cm and exposure time 40s.....	66
Figure 33: Optical micrographs of a crack in F9 solar cell which displayed a dark irregular area in the crack zone in the EL. Images captured with a Nikon SMZ 800 microscope.	66
Figure 34: I-V Curves of the complete module and separate strings at 1,000 W/m ² . The secondary axis presents the P-V curves of the module at this irradiance.	67
Figure 35: EL images of the tested module with an injected current of 8.9 A (a) and 0.89 A (b). EL images taken with PCO 1300 camera, with a focal distance of 4 cm and exposure time 50 s (a) and 15 min (b).....	68
Figure 36: Outdoor IRT images of the module in the lower current step of the I-V curve at 7.3 A-24 V (a) and in the middle current step of the I-V curve at 7.8 A-15 V (b) at 933 W/m ² . Images taken with FLIR SC 640 IR camera. The maximum temperature values of the different hot spots are indicated in the figures.	68
Figure 37: Box chart showing the delta temperature between overheated and healthy areas, ΔT , grouped by defect type for each of the 1,140 defective modules detected. .	73
Figure 38: Temperature difference between the hotspot and the healthy area of the faulty modules detected in the manual inspection (blue), aerial inspection at 30 m (red) and aerial inspection at 80 m (green).	78
Figure 39: Thermographic images of defects 1 (a) to 6 (f). The temperature range in each of the six thermographic images is: (a) 1.3-22.6°C, (b) 8.1-30.3°C, (c) 18.1-35.7°C, (d) 24.6-51.8°C, (e) 9.9-52.6°C, (f) -32.7-86.3°C.....	79
Figure 40: Difference of temperature between the hotspot and the healthy area of the six defects captured at twelve different distances. The secondary horizontal axis shows the pixel size at each distance. The images have been captured manually with the camera Testo 870-2.....	79

1.10. Index of tables

Table 1: Severity ranking intervals calculated from the fixing price and the loss of profit that a failure produces	35
Table 2: Severity ranking criteria.....	35

Detection, classification and characterization of defects in photovoltaic modules through the use of thermography, electroluminescence, I-V curves and visual analysis

Table 3: Detection ranking criteria following [73].	35
Table 4: Cells defects types and codes per string.	45
Table 4: Thermographic defects detected classified by the module affected component	72
Table 5: All defects detected classified by the affected component and in three temperature groups	73
Table 6: Anomalies identified, classified by their temperature.	77

Chapter 2

PUBLISHED PAPERS

'Science knows no country, because knowledge belongs to humanity, and is the torch which illuminates the world. Science is the highest personification of the nation because that nation will remain the first which carries the furthest the works of thought and intelligence.'

Louis Pasteur.

This chapter presents the papers and contributions done throughout this doctoral thesis. It has been structured in three subchapters, corresponding each of them with the publications related to each of the three partial objectives established in section 1.3 Hypothesis and objectives.

2.1. Study of the state of the art (Obj. 1)

This section includes the following articles:

- [2.1.1] Gallardo-Saavedra S, Hernández-Callejo L, Duque-Pérez O. Quantitative failure rates and modes analysis in photovoltaic plants. *Energy* 2019;183:825–36. <https://doi.org/10.1016/j.energy.2019.06.185>.
- [2.1.2] Gallardo-Saavedra S, Pérez-Moreno J, Hernández-Callejo L, Duque-Pérez Ó. Failure rate determination and Failure Mode, Effect and Criticality Analysis (FMECA) based on historical data for photovoltaic plants ISES Conference Proceedings 2017:1-8. <https://doi.org/10.18086/swc.2017.20.04>.
- [2.1.3] Hernández-Callejo L, Gallardo-Saavedra S, Alonso-Gómez V. A review of photovoltaic systems: Design, operation and maintenance. *Sol Energy* 2019;188:426–40. <https://doi.org/https://doi.org/10.1016/j.solener.2019.06.017>.

2.1.1. Quantitative failure rates and modes analysis in PV plants

QUANTITATIVE FAILURE RATES AND MODES ANALYSIS IN PHOTOVOLTAIC PLANTS

Sara Gallardo-Saavedra ^{a,b*}, Luis Hernández-Callejo ^a, Oscar Duque-Pérez ^b

^a **Universidad de Valladolid (UVa), School of Forestry, Agronomic and Bioenergy Industry Engineering (EIFAB), Department of Agricultural and Forestry Engineering, Campus Duques de Soria, 42004, Soria, Spain**

^b **Universidad de Valladolid (UVa), Industrial Engineering School, Department of Electrical Engineering, Paseo del Cauce ,59, 47011, Valladolid, Spain**

***Corresponding autor**

Energy, vol. 183, pp. 825-836 (2019).

<https://doi.org/10.1016/j.energy.2019.06.185>

Abstract

The greater challenge that researchers address and indicate while investigating about photovoltaic (PV) system failures during their Operation and Maintenance (O&M) is the lack of accessible reliable real quantitative data. For this reason, several publications have focused on this problem through a qualitative approach. However, this fact is one of the greater strengths of this paper, in which the quantitative information from the historical data of sixty-three PV plants portfolio in Italy and Spain has been accessible. Results obtained from the research provide essential information for main players involved in PV plants to identify failure modes and rates, in order to reduce investment risk and to focus their maintenance efforts on preventing those failures, improving longevity and performance of PV plants. The paper presents failure rates per PV Site and per kW, considering all portfolio and dividing it regarding five PV plants groups per size, distribution of failures per element, Mean Time Between Failures (MTBF), reparation times per affected element and the main failures modes examining each of the almost 100,000 complete alarms registered during the five years analyzed.

2.1.2. Failure rate determination and Failure Mode, Effect and Criticality Analysis (FMECA) based on historical data for photovoltaic plants

FAILURE RATE DETERMINATION AND FAILURE MODE, EFFECT AND CRITICALITY ANALYSIS (FMECA) BASED ON HISTORICAL DATA FOR PHOTOVOLTAIC PLANTS

Sara Gallardo-Saavedra^{1,2}, Javier Pérez-Moreno², Luis Hernández-Callejo¹ and Óscar Duque-Pérez³

1 Universidad de Valladolid (UVa), School of Forestry, Agronomic and Bioenergy Industry Engineering (EIFAB), Department of Agricultural and Forestry Engineering, Soria (Spain)

2 Solarig, Soria (Spain)

3 Universidad de Valladolid (UVa), Industrial Engineering School, Department of Electrical Engineering, Valladolid (Spain)

Proceedings: ISES Conference Proceedings of the ISES Solar World Conference 2017 and the IEA SHC Solar Heating and Cooling Conference for Buildings and Industry 2017, pp. 1232-1239.

<https://doi.org/10.18086%2Fswc.2017.20.04>

Abstract

It is essential for photovoltaic plants investors, operators and equipment manufacturers to identify the failure modes and rates of the system in order to reduce investment risk, to focus their maintenance efforts on preventing those failures and to improve longevity and performance of the PV Plant. In this paper, it is assessed the importance of the Failure Modes within a real existing portfolio in Spain and Italy of continuous operation since 2008 and it is identified the module level failure modes, which are imperceptible in the standard monitoring systems, through the application of thermographic inspection. The experimental Mean Time Between Failures (MTBF) and the failure rates are calculated and these ratios are used to define the ranking criterion to perform the Failure Mode, Effect and Criticality Analysis (FMECA) and to focus on the module level analysis. The conclusions highlight the most critical sub-system and failure modes within a photovoltaic PV plant.

2.1.3. A review of photovoltaic systems: design, operation and maintenance

A REVIEW OF PHOTOVOLTAIC SYSTEMS: DESIGN, OPERATION AND MAINTENANCE

Luis Hernández-Callejo^{1,*}, Sara Gallardo-Saavedra¹, Víctor Alonso-Gómez²

¹ Department of Agricultural Engineering and Forestry, University of Valladolid (UVa), Campus Universitario Duques de Soria, 42004 Soria, Spain. L.H-C.: luis.hernandez.callejo@uva.es; S.G-S.: s.gallardosaavedra@gmail.com;

² Department of Physics, University of Valladolid (UVa), Campus Universitario Duques de Soria, 42004 Soria, Spain. V.A-G.: victor.alonso.gomez@uva.es

* Correspondence: luis.hernandez.callejo@uva.es ; Tel.: +34-975-129-418; Fax: +34-975-129-401

Solar Energy, 188, pp. 426-440 (2019).

<https://doi.org/10.1016/j.solener.2019.06.017>

Abstract

Nowadays renewable energies are becoming more important in the generation of electricity. Fossil resources do not present a sustainable option for the future since they are non-renewable sources of energy that contribute to environmental pollution.

Within the sources of renewable generation, photovoltaic energy is the most used, and this is due to a large number of solar resources existing throughout the planet. At present, the greatest advances in photovoltaic systems (regardless of the efficiency of different technologies) are focused on improved designs of photovoltaic systems, as well as optimal operation and maintenance. This work intends to make a review of the photovoltaic systems, where the design, operation and maintenance are the key points of these systems. Within the design, the critical components of the system and their own design are revised. Regarding the operation, it is reviewed the general operation and the operation of hybrid systems, as well as the power quality. Finally, in relation to the maintenance of photovoltaic (PV) systems, it has been studied their performance, thermography and electroluminescence, dirt, risks and failure modes.

2.2. Detection, characterization and classification of defects in PV modules through the use of different inspection techniques (Obj. 2)

This section includes the following articles:

- [2.2.1] Gallardo-Saavedra S, Karlsson B. Simulation, validation and analysis of shading effects on a PV system. *Sol Energy* 2018;170:828–39. <https://doi.org/10.1016/j.solener.2018.06.035>.
- [2.2.2] Moretón A, Gallardo S, Jiménez MM, Alonso V, Hernández L, Morales JI, et al. Influence of large periods of dc current injection in c-si photovoltaic panels. 36th Eur. Photovolt. Sol. Energy Conf. Exhib., 2019, p. 1079-108. <https://doi.org/10.4229/eupvsec20192019-4av.1.38>.
- [2.2.3] Gallardo S, Moretón A, Jiménez MM, Alonso V, Hernández L, Morales JI, et al. Failure diagnosis on photovoltaic modules using thermography, electroluminescence, RGB and I-V techniques. 36th Eur. Photovolt. Sol. Energy Conf. Exhib., 2019, p. 1171–5. <https://doi.org/10.4229/eupvsec20192019-4av.2.20>.
- [2.2.4] Gallardo-Saavedra S, Hernández-Callejo L, Escamilla-Ambrosio PJ, Alonso-Gómez V. Merged images for fault detection in photovoltaic panels. II Ibero-American Congr. Smart Cities (ICSC-CITIES 2019), 2019, p. 167-178, ISBN: [978-958-5583-78-8](https://doi.org/10.1016/j.procs.2019.05.038).
- [2.2.5] Gallardo-Saavedra S, Hernández-Callejo L, Alonso-García M del C, Domingo-Santos J, Morales-Aragonés JI, Alonso-Gómez V, et al. Nondestructive characterization of solar PV cells defects by means of electroluminescence, infrared thermography, I-V curves and visual tests: experimental study and comparison. *Energy* 2020.
- [2.2.6] Gallardo-Saavedra S, Hernández-Callejo L, Duque-Perez O. Analysis and characterization of PV module defects by thermographic inspection. *Rev Fac Ing Univ Antioquia* 2019:92–104. <https://doi.org/10.17533/udea.redin.20190517>.

2.2.1. Simulation, validation and analysis of shading effects on a PV system

SIMULATION, VALIDATION AND ANALYSIS OF SHADING EFFECTS ON A PV SYSTEM

Sara Gallardo-Saavedra^{a,b,*} and Björn Karlsson ^a

^a **Faculty of Engineering and Sustainable Development, Department of Building, Energy and Environmental Engineering, University of Gävle, Sweden**

^{b,*} **Universidad de Valladolid (UVA), School of Forestry, Agronomic and Bioenergy Industry Engineering (EIFAB), Department of Agricultural and Forestry Engineering, Campus Duques de Soria, 42004 Soria, Spain**

E-mail address: sara.gallardo@uva.es (S. Gallardo-Saavedra).

Solar Energy, 170, pp. 828-839 (2018).

<https://doi.org/10.1016%2Fj.solener.2018.06.035>

Abstract

A simulation program for calculating the IV-curve for series connected PV-modules during partial shadowing has been developed and experimentally validated. The software used for modelling the modules is LTspice IV. The validation has been done by means of a comparative analysis using the experimental results obtained in a set of tests performed on the mono-crystalline modules of the Gävle University's laboratory in Sweden. Experimental measurements were carried out in two groups. The first group is a string of six modules with bypass diodes while the second one corresponds to a single PV module. The simulation results of both groups demonstrated a remarkable agreement with the experimental data, which means that the designed model can be used for simulating the influence of shading on the power of a string. The model has been used for analysing the performance of strings of PV modules with shadows and the benefits of installing DC-DC optimizers or module inverters, that minimise the impact of shading, have been investigated.

2.2.2. Influence of large periods of DC current injection in c-Si photovoltaic panels

INFLUENCE OF LARGE PERIODS OF DC CURRENT INJECTION IN C-SI PHOTOVOLTAIC PANELS

A. Moretón^{1*}, S. Gallardo², M.M. Jiménez¹, V. Alonso², L. Hernández², J.I. Morales², O. Martínez¹, M. A. González¹ and J. Jiménez¹

¹ **GdS-Optronlab group, Dpto. Física de la Materia Condensada, Universidad de Valladolid, Edificio LUCIA, Paseo de Belén, 19, 47011 Valladolid (Spain);**

***angel.moreton@outlook.es**

² **Department of Agricultural and Forestry Engineering, School of Forestry, Agronomic and Bioenergy Industry Engineering (EIFAB), Universidad de Valladolid, Campus Duques de Soria, 42004 Soria (Spain)**

Proceedings of the 36th European Photovoltaic Solar Energy Conference and Exhibition, pp.1079-1080 (2019).

ISBN: 3-936338-60-4.

Abstract

Nowadays, electroluminescence imaging (ELi) appears as an emerging technique in the maintenance of photovoltaic (PV) plants. There is a concern about how the current injection needed in ELi measurements can affect the PV modules service life, and how these periodical inspections can affect the long term life of the modules. In order to give a practical answer to this problem, a series of tests consisting of long periods of current injection on several monocrystalline silicon modules has been carried out. The modules tested had already fulfilled their useful life and present multiple defects. In order to analyze how the current injection affects the state of the module, images of infrared thermography (IRT) and ELi were acquired during the current injection period. The subsequent analysis of these images shows only a small effect during the heating period in the EL intensity results at the beginning of each test, not affecting the module performance.

2.2.3. Failure diagnosis on photovoltaic modules using visual inspection, thermography, electroluminescence and I-V techniques

FAILURE DIAGNOSIS ON PHOTOVOLTAIC MODULES USING VISUAL INSPECTION, THERMOGRAPHY, ELECTROLUMINESCENCE AND I-V TECHNIQUES

Sara Gallardo-Saavedra^{1*}, Ángel Moretón-Fernández², Marta María Jiménez-Martín², Víctor Alonso-Gómez¹, Luis Hernández-Callejo¹, Óscar Martínez-Sacristán², Miguel Ángel González-Rebollo² and José Ignacio Morales-Aragonés¹.

¹Universidad de Valladolid (UVa), School of Forestry, Agronomic and Bioenergy Industry Engineering (EIFAB), Department of Agricultural and Forestry Engineering, Campus Duques de Soria, 42004 Soria (Spain);

***sara.gallardo@uva.es**

²GdS-Optronlab, Dept. Física de la Materia Condensada, Universidad de Valladolid (UVa), Paseo de Belén, 19, 47011 Valladolid (Spain)

Proceedings of the 36th European Photovoltaic Solar Energy Conference and Exhibition, pp.1171-1175 (2019).

ISBN: 3-936338-60-4.

Abstract

Different techniques can be used to detect and quantify PV modules anomalies, as visual inspections, electrical tests like the I-V curve test, infrared thermography (IRT) or electroluminescence (EL). PV plants operators usually apply only one or two of them within the Operation and Maintenance (O&M) activities. Additionally, researchers usually studied them separately. However, these methods provide complementary results, glimpsing interesting information about the PV site state. The main strength of the research performed is the simultaneous study of all these inspection techniques, studying the correlation between them. Results confirm that, EL and IRT under current injection on modules are closely correlated, while IRT under normal operation (sun exposure) reveals complementary information not detected in EL but existing in the visible spectrum. In conclusion, it is advisable using as many techniques as possible to characterize the actual state of the module and to explain its I-V curve.

2.2.4. Merged images for fault detection in photovoltaic panels

MERGED IMAGES FOR FAULT DETECTION IN PHOTOVOLTAIC PANELS

Sara Gallardo-Saavedra^{1[0000-0002-2834-5591]}, **Luis Hernández-Callejo**^{1[0000-0002-8822-2948]},
Ponciano Jorge Escamilla-Ambrosio^{2[0000-0003-3772-3651]} and **Víctor Alonso-Gómez**^{1[0000-0001-5107-4892]}.

¹ **University of Valladolid, Campus Duques de Soria, 42004 Soria, España**

² **Instituto Politécnico Nacional: Mexico, Distrito Federal, MX**

Proceedings of the II Ibero-American Congress of Smart Cities (ICSC-CITIES 2019), p. 167-178.

ISBN: 978-958-5583-78-8.

Abstract

Photovoltaic systems are of great interest throughout the world. Its installation, operation and maintenance are crucial for achieving energy sustainability worldwide. In recent years, the inspection of defects in photovoltaic modules using images (thermography, electroluminescence, visible, etc.) is increasing considerably. Therefore, this work presents the experience of merging images to detect faults in photovoltaic modules.

2.2.5. Nondestructive characterization of solar PV cells defects by means of electroluminescence, infrared thermography, I-V curves and visual tests: experimental study and comparison

NONDESTRUCTIVE CHARACTERIZATION OF SOLAR PV CELLS DEFECTS BY MEANS OF ELECTROLUMINESCENCE, INFRARED THERMOGRAPHY, I-V CURVES AND VISUAL TESTS: EXPERIMENTAL STUDY AND COMPARISON

Sara Gallardo-Saavedra ^{a*}, Luis Hernández-Callejo ^a, María del Carmen Alonso-García ^b, José Domingo Santos ^b, José Ignacio Morales-Aragón ^a, Víctor Alonso-Gómez ^a, Ángel Moretón-Fernández ^c, Miguel Ángel González-Rebollo ^c and Oscar Martínez-Sacristán ^c.

^a **Universidad de Valladolid (UVa), School of Forestry, Agronomic and Bioenergy Industry Engineering (EIFAB), Department of Agricultural and Forestry Engineering, Campus Duques de Soria, 42004, Soria, Spain.**

^b **Photovoltaic Solar Energy Unit (Energy Department, CIEMAT), Avda. Complutense 40, 28040 Madrid, Spain.**

^c **Universidad de Valladolid (UVa), Department of Condensed Matter Physics, GdS Optronlab Group, Paseo de Belen 19, 47011, Valladolid, Spain.**

***Corresponding author.**

Energy. (2020).

Abstract

Photovoltaic (PV) modules are the core of every PV system, representing the power generation and their operation will affect the overall plant performance. It is one of the elements within a PV site with the higher failure appearance, being essential their proper operation to produce reliable, efficient and safety energy. Quantitative analysis and characterization of manufacturing, soldering and breaking PV defects is performed by a combination of electroluminescence (EL), infrared thermography (IRT), electrical current voltage (I-V) curves and visual inspection. Equivalent-circuit model characterization and microscope inspection are also performed as additional techniques when they contribute to the defects characterization. A 60-cells polycrystalline module has been ad hoc manufactured for this research, with different defective and non-defective cells. All cells are accessible from the backside of the module and the module includes similar kinds of defects in the same bypass string. This paper characterizes different defects of PV modules to control, mitigate or eliminate their influence and being able to do a quality assessment of a whole PV module, relating the individual cells performance with the combination of defective and non-defective cells within the module strings, with the objective of determining their interaction and mismatch effects, apart from their discrete performance.

2.2.6. Analysis and characterization of PV module defects by thermographic inspection.

ANALYSIS AND CHARACTERIZATION OF PV MODULE DEFECTS BY THERMOGRAPHIC INSPECTION.

Sara Gallardo-Saavedra^{1,2} (0000-0002-2834-5591), Luis Hernández-Callejo¹ (0000-0002-8822-2948) and Óscar Duque-Pérez² (0000-0003-2994-2520)

¹Departamento de Ingeniería Agropecuaria y Forestal, Facultad de Ingeniería Forestal, Ingeniería Agronómica y de la Industria de la Bioenergía (EIFAB), Campus Duques de Soria, Universidad de Valladolid (UVa). Calle Universidad, C.P. 42004, Soria, España.

² Departamento de Ingeniería Eléctrica, Escuela de Ingeniería Industrial, Universidad de Valladolid (UVa). Paseo del Cauce, 59, C.P. 47011, Valladolid, España.

Facultad de Ingeniería Universidad de Antioquía, no.93, pp. 92-104, Oct-Dec 2019.

<https://doi.org/10.17533/udea.redin.20190517>

Abstract

Being able to detect, to identify and to quantify the severity of defects that appear within photovoltaic modules is essential to constitute a reliable, efficient and safety system, avoiding energy losses, mismatches and safety issues. The main objective of this paper is to perform an in-depth, onsite study of 17,142 monocrystalline modules to detect every single existing defect, classifying them in different groups, studying the variance of the same kind of defect in different modules and the patterns of each group of thermal defects. Results can be useful in a subsequent development of a software to automatically detect if a module has an anomaly and its classification. Focusing on the results obtained, all faults detected have been classified in five different thermographic defects modes: hotspot in a cell, bypass circuit overheated, hotspot in the junction box, hotspot in the connection of the busbar to the junction box and whole module overheated. An analysis of patterns of the different defects is included, studying location within the module, size and temperature statistical results, as average temperature, standard deviation, maximum temperature, median and first and third quartile.

Resumen

Ser capaz de detectar, identificar y cuantificar la gravedad de los defectos que aparecen en los módulos fotovoltaicos es esencial para constituir un sistema fiable, eficiente y seguro, evitando pérdidas de energía, desajustes y problemas de seguridad. El objetivo principal de esta investigación es realizar un estudio de 17.142 módulos monocristalinos para detectar cada defecto existente, clasificándolos en diferentes grupos, estudiando la varianza del mismo tipo de defecto en diferentes módulos y los patrones de cada grupo de defectos térmicos. Los resultados obtenidos pueden ser útiles en el desarrollo posterior de un software de detección automática de anomalías en módulos y su clasificación. Atendiendo a los resultados obtenidos, los defectos detectados se han clasificado en cinco modos de fallo termográficos: sobrecalentamiento en celdas, en circuito bypass, en la caja de conexiones, en la conexión entre la barra colectora (busbar) y la caja de conexiones y en el módulo completo. Se incluye un análisis de patrones de los diferentes defectos, estudiando su ubicación dentro del módulo, tamaño y resultados estadísticos de temperatura, como temperatura promedio, desviación estándar, temperatura máxima, mediana y primer y tercer cuartil.

2.3. Analysis of aerial thermography as a novel inspection technique (Obj. 3)

This section includes the following articles:

- [2.3.1]** Gallardo-Saavedra S, Hernández-Callejo L, Duque-Perez O. Technological review of the instrumentation used in aerial thermographic inspection of photovoltaic plants. *Renew Sustain Energy Rev* 2018;93:566–79. <https://doi.org/10.1016/J.RSER.2018.05.027>.
- [2.3.2]** Gallardo-Saavedra S, Alfaro-Mejia E, Hernández-Callejo L, Duque-Pérez Ó, Loaiza-Correa H, Franco-Mejia E. Aerial thermographic inspection of photovoltaic plants: analysis and selection of the equipment. *ISES Conference Proceedings 2017:1-9* <https://doi.org/10.18086/swc.2017.20.03>.
- [2.3.3]** Dávila-Sacoto M, Hernández-Callejo L, Alonso-Gómez V, Gallardo-Saavedra S, González-Morales L. Low-cost infrared thermography in aid of photovoltaic panels degradation research. *Fac Ing Univ Antioquía* 2020.
- [2.3.4]** Gallardo-Saavedra S, Hernandez-Callejo L, Duque-Perez O. Image Resolution Influence in Aerial Thermographic Inspections of Photovoltaic Plants. *IEEE Trans Ind Informatics* 2018;14:5678–86. <https://doi.org/10.1109/TII.2018.2865403>.

2.3.1. Technological review of the instrumentation used in aerial thermographic inspection of photovoltaic plants

TECHNOLOGICAL REVIEW OF THE INSTRUMENTATION USED IN AERIAL THERMOGRAPHIC INSPECTION OF PHOTOVOLTAIC PLANTS

Sara Gallardo-Saavedra ^{a,b,*}, Luis Hernández-Callejo ^a, Oscar Duque-Pérez ^b

^{a,*} Universidad de Valladolid (UVa), School of Forestry, Agronomic and Bioenergy Industry Engineering (EIFAB), Department of Agricultural and Forestry Engineering, Campus Duques de Soria, 42004, Soria, Spain

^b Universidad de Valladolid (UVa), Industrial Engineering School, Department of Electrical Engineering, Paseo del Cauce ,59, 47011, Valladolid, Spain

Renewable and sustainable energy reviews, 93, pp. 566-579 (2018).

<https://doi.org/10.1016%2Fj.rser.2018.05.027>

Abstract

Photogrammetric studies performed with Unmanned Aerial Vehicles (UAV) have recently become more popular as they present an interesting low-cost alternative. A novel application of thermography with UAVs has been validated during the last years: aerial thermography for inspection of photovoltaic plants as a useful diagnostic technique to assess performance of photovoltaic modules, superseding time-consuming traditional manual methods. This paper describes the current state of thermographic cameras and UAV technology, with the aim of examining the general principles of aerial thermographic measurement and required instrumentation, detailing the most important system aspects, discussing new developments and future trends in aerial thermography sensors and instrumentation, and evaluating them for specific application of aerial thermographic inspection of photovoltaic plants.

2.3.2. Aerial thermographic inspection of photovoltaic plants: analysis and selection of the equipment

AERIAL THERMOGRAPHIC INSPECTION OF PHOTOVOLTAIC PLANTS: ANALYSIS AND SELECTION OF THE EQUIPMENT

Sara Gallardo-Saavedra¹, Estefanía Alfaro-Mejía² Luis Hernández-Callejo¹, Óscar Duque-Pérez³, Humberto Loaiza-Correa² and Edinson Franco-Mejía²

- 1 Universidad de Valladolid (UVa), School of Forestry, Agronomic and Bioenergy Industry Engineering (EIFAB), Department of Agricultural and Forestry Engineering, Soria (Spain)**
- 2 Universidad del Valle, Escuela de Ingeniería Eléctrica y Electrónica, Santiago de Cali (Colombia)**
- 3 Universidad de Valladolid (UVa), Industrial Engineering School, Department of Electrical Engineering, Valladolid (Spain)**

Proceedings: ISES Conference Proceedings of the ISES Solar World Conference 2017 and the IEA SHC Solar Heating and Cooling Conference for Buildings and Industry 2017, pp. 1223-1231.

<https://doi.org/10.18086%2Fswc.2017.20.03>

Abstract

In recent times, more and more countries are choosing the alternative of generating clean energy. The photovoltaic (PV) energy installed is rapidly increasing around the World. PV cells are made with semiconductor materials such as Si, GaAs, among others. Despite the quality controls in the manufacture and manipulation of the panels, damages occur during their manufacturing, installation, use or of wear due to environmental factors, doing it necessary a periodic review. Manual inspections become expensive and largely inefficient due to the big extensions of PV plants. For this reason, it is necessary to automate the inspection task. This paper presents a methodology for the selection of equipment used to make inspections of faults in solar panels using aerial thermography, based on the review of the state of the art and the latest equipment technology available.

2.3.3. Low-cost infrared thermography in aid of photovoltaic panels degradation research

LOW-COST INFRARED THERMOGRAPHY IN AID OF PHOTOVOLTAIC PANELS DEGRADATION RESEARCH

Miguel Dávila-Sacoto¹, Luis Hernández-Callejo², Víctor Alonso-Gómez³, Sara Gallardo-Saavedra² and Luis González-Morales¹

¹ Ingeniería Eléctrica, Facultad de Ingeniería, Universidad de Cuenca, Campus Central, 010104 Cuenca, Ecuador

² Departamento de Ingeniería Agrícola y Forestal, Universidad de Valladolid, Campus Universitario Duques de Soria, 42004 Soria, Spain

³ Departamento de Física Aplicada, Universidad de Valladolid, Campus Universitario Duques de Soria, 42004 Soria, Spain

Facultad de Ingeniería Universidad de Antioquía, (2020).

Abstract

The analysis of PV solar panels deterioration allows researchers to know the health status of a panel in order to determine the overall functioning of a PV solar farm. A part of this analysis is performed by thermography, generally using professional and expensive equipment. This article presents a validation for the use of low-cost thermal imaging cameras, reviewing the relative error that can be obtained through scattering, contour analysis and three-dimensional meshes. The procedure is validated by analysis of I-V/P-V curves and a temperature sensor matrix, reaching errors less than 10% with cameras with less than 500USD.

Resumen

El análisis del deterioro de paneles fotovoltaicos permite a los investigadores conocer el estado de salud de un panel con el objetivo de determinar el funcionamiento global de una granja fotovoltaica. Una parte de este análisis se realiza mediante termografía, utilizando generalmente equipos profesionales y de costos elevados. Este artículo se presenta una validación para el uso de cámaras termográficas de bajo costo, revisando el error relativo que se puede obtener mediante análisis de dispersión, contorno y mallas tridimensionales. El procedimiento es validado mediante análisis de curvas I-V/P-V y una matriz de sensores de temperatura, llegando a errores menores del 10% con cámaras con inferiores a 500USD.

**2.3.4. Image Resolution Influence in Aerial
Thermographic Inspections of Photovoltaic Plants.**

**IMAGE RESOLUTION INFLUENCE IN AERIAL
THERMOGRAPHIC INSPECTIONS OF PHOTOVOLTAIC
PLANTS.**

Sara Gallardo-Saavedra ^{a,b*}, Luis Hernández-Callejo ^a, Oscar Duque-Pérez ^b

^a **Universidad de Valladolid (UVa), School of Forestry, Agronomic and Bioenergy
Industry Engineering (EIFAB), Department of Agricultural and Forestry
Engineering, Campus Duques de Soria, 42004, Soria, Spain**

^b **Universidad de Valladolid (UVa), Industrial Engineering School, Department of
Electrical Engineering, Paseo del Cauce ,59, 47011, Valladolid, Spain**

***Corresponding autor**

**IEEE Transactions on Industrial Informatics, vol. 14, no. 12, pp. 5678-5686,
december 2018.**

<https://doi.org/10.1109%2Ftii.2018.2865403>

Abstract

Photovoltaic energy is the renewable energy with the greatest growth and use. The tendency of the last years is directed towards the formation of increasingly larger plants, which implies that optimizing their maintenance is becoming extremely important. Aerial thermography has become a convenient quality assessment tool for photovoltaic power plants, being reliable, cost-effective and time-saving. However, it is essential to be aware of its strengths and limitations in order to apply and interpret the results correctly. This paper presents a study about the influence of Spatial Resolution of thermographic images on the severity of failures, evaluating the results obtained in a set of experimental aerial and manual inspections performed in a 3 MW PV plant in Spain. The research analyzes how aerial thermography should be arranged as a function of the thermographic camera and lens used with the aim of satisfying the resolution requirements. Indications about the correct procedure to perform aerial thermographic inspections are also provided.

Chapter 3

CONCLUSIONS AND FUTURE WORK

'Our imagination is the only limit to what we can hope to have in the future.'

Charles F. Kettering.

This chapter presents the conclusions of the research described in the thesis and the main contributions. The aim and objectives of the research, outlined in the Introduction, are reviewed and their achievement addressed. Finally, proposals for future work are suggested.

3.1. Conclusions and PhD contributions

In this dissertation, it has been presented an **analysis of the detection, characterization and classification of defects in PV modules through the use of IRT, EL, I-V curves and visual analysis**, which is the aim of the research. To achieve this **main objective**, the research has been focused on three main threads, coinciding with the **three partial objectives** of the thesis: the study of the state of the art, the detection, characterization and classification of defects in PV modules through the use of different inspection techniques and the analysis of aerial IRT as a novel inspection technique. The main contributions of the thesis on these three areas are presented in this section.

Firstly, regarding the **study of the state of the art**, the failure rates and modes in PV plants and the design, operation and maintenance of these sites have been analyzed. It has been proved how PV production is never faultless, like any other technology, quantifying the failure rates corresponding to each of the elements in a PV plant. It has been seen how although PV plants are getting older each year, a proper maintenance can be responsible of keeping the defects ratio or even reducing it. Accurately performed predictive, preventive and corrective maintenance include improvements in PV plants, which reduces the failure ratio in the long term. It has been notice how there are defects that do not depend on the plant size or the plant number of elements or components; therefore, the failure number per power unit is higher in smaller plants. At the front of the list of elements with more failures are the monitoring and communication systems, followed by the MV elements, the inverter and the PV generator (including the PV modules). Each defect involves each own repairing time to fix a defect, and excluding the elements that usually require the presence of the manufacturer or outsourcing for their reparation and have a higher reparation time, the PV generator is the element with the higher fixing value. Studying the failure ratios occurrence combined with their severity and detection probability, it is seen how inverter, MV, auxiliary services and PV modules are the most relevant systems. It has been notice that the module is

the key element on a PV system, but, even so, it has limited access to local monitoring alarms, which are not frequently automatically generated, being specially complicated the detection of failures at this level and even more difficult the recognition of the failure cause and mode. From the study of the state of the art, it is highlighted the importance of the research on PV modules failures detection, classification and characterization in order to produce reliable, efficient and safety energy.

Secondly, concerning the **detection, characterization and classification of defects in PV modules through the use of different inspection techniques**, it has been addressed three different aspects. The first deals with the detection of PV defects using different techniques and the comparison of the information obtained with each of them. From an experimental point of view, our contribution lies in the simultaneous application of these inspection techniques to several PV modules with different failures. These experiments were performed for studying the correlation between them. Results show that EL and IRT under current injection on modules are closely correlated, while IRT under normal operation (sun exposure) reveals complementary information not detected in EL but existing in the visible spectrum. It has been concluded, it is advisable using as different techniques as possible to characterize the actual state of the module and to explain its I-V curve. It has been studied the possibility to use different algorithms to generate merged images of frames captured by means of EL and IRT in the fourth quadrant, with the objective of exploring how using image processing techniques to align multiple scenes in a single integrated image simplifies the analysis and reporting of results of inspections of PV plants, resulting to be a very interesting and promising field. Regarding the I-V curves, several electrical circuits which model a PV system have been simulated using LTspice and validated with experimental measurements. We have obtained successful results, both on simulation and on real experimentation, showing that the designed model is a very useful tool that can be used to study the performance of shaded or defective PV systems, allowing the simulation of numerous faults. Regarding the analysis of the EL current injection in modules, the main focus of this thesis was on answering to the generalized concern about how this current injection can affect the PV modules service life. In the research it is not appreciated that this current has any negative effect on the performance of damaged modules. In the second investigation, a quantitative analysis and characterization of manufacturing, soldering and breaking PV defects by a combination of the inspection techniques previously analyzed was performed for the characterization of PV cells and modules as an important part of the search process. Equivalent-circuit model characterization and microscope inspection have also been performed as additional techniques when they contribute to

the defects characterization. Our contribution in this part was to study in detail and characterize different defects and their combination within a module. In particular, regarding the manufacturing defects, it has been seen that there is a tendency to decrease the light emission during EL tests with the efficiency drop. Short-circuited cell does not emit any light during EL and it is seen colder than the rest in IRT, which authors propose to denominate as *cold spot*, defining it as cell or group of cells at abnormal low temperature in a PV system. Low-efficiency defects are seen as a tire imprint in the cell EL images and can be originated due to inhomogeneity during the firing process or in the transportation belt in the cell production and they can experiment almost a 50% power loss. Soldering defective cells present smaller parameter deviations than the rest of defects studied. It has been proved that there are more losses when there is a local soldering defect in just a part of the bus, as the series resistance is considerably increased. Conversely, having all (or some) tabs loose does not interrupt the electrical contact despite not being welded, and its influence is not disastrous. However, this could be altered after some years of operation of the module in which the encapsulation is exposed to thermal cycles. It has also been seen that the greatest danger of bad welds are usually the electric arcs, since that bad contact causes the tab to warm up and it can come out to disconnect it. A relevant tension difference between two points very close can generate micro arcs. That ends up burning the back sheet behind, or if they are generated in broken cells, the edges of the cell are usually burned and also depending on the composition of the paste together with the permeability of the back sheet, the humidity causes the fingers to blacken, being easily identifiable the cell breakages, which is commonly known as snail trails. Concerning broken cells, it has been analyzed how the shape of the I-V curves of the affected cells is very similar to the one of the nominal equivalent cell but decreasing the current proportionally. Alternatively, if a piece of other cell over placed in the front part of a cell generates a parallel electrical path which is responsible of a small R_{sh} in the cell, turning the I-V curve into a straight line. The third point presents the classification of PV defects attending to failure patterns. A discussion on the different thermographic defects have been presented. Our contribution here is the classification of defects in five different modes base on an experimental database generated with numerous on-site measurements and the study of their patterns: hotspot in a cell or in a group of cells, bypass circuit overheated, hotspot in the junction box, hotspot in the connection of the busbar to the junction box and whole module overheated, with more than three quarters of the affected modules correspond to cell hotspots and being this the defect type that shows higher temperature differences, achieving up to

77.4°C between the overheated hotspot and the healthy area in one of the tested modules. This study results can be useful as a base to develop the patterns of the different kind of defects in a software to automatically detect if a module has an anomaly and its classification.

Thirdly, aerial IRT has been proposed to address the drawbacks of traditional inspection techniques by using thermal cameras onboard of UAVs. Up-to-date traditional techniques have been applied to diagnose and assess the performance of PV modules resulting in costly and time-consuming inspections. The use of thermographic cameras and UAVs has been analyzed in detail. Regarding the **analysis of aerial IRT as a novel inspection technique** the main contributions of the work are three: to review the available equipment focusing on their desirable characteristic for their application on aerial thermographic inspection of PV sites, to review the most important aspects in the tests that should be taken into account in order to obtain valid results and to study the influence of the resolution of IRT images. Although there are several researchers developing this novel technique, there were no clear guidelines for selection of involved instrumentation meeting the needs of PV inspections. The research presented aims to present a clear review and discussion of available equipment and its main characteristics applied to PV plants, as well as to review the equipment already used in this application as reported in the related bibliography. The most important aspects on this regard are reviewed, such as resolution, thermal sensitivity, accuracy, lens and the corresponding FOV, radiometric functionality, visual or RGB images, frame rate or temperature range for the thermographic camera, as well as stability of the system, maximum altitude, flight duration and maximum payload, full compatibility between instruments and duration of batteries for UAVs. The second contribution relies in the review of the most important aspects in the tests that should be taken into account in order to make them valid, as the presence of steady state conditions, minimum irradiance value of at least 600 W/m², maximum wind speed of 28 km/h, maximum UAV moving speed of 3 m/s, clean modules, accurate angle of view to avoid reflections, setting the correct emissivity, reflected temperature, relative humidity, temperature and distance between the sensor and the object values in the camera, correctly select the temperature range and properly calibrating the camera. Finally, it has been proved that the images resolution will strongly influence the results by means of the particular case of one manual and two aerial inspections at 30 and 80 m, respectively, of a 3 MW site. Important anomalies can be hidden or disdained if the inspection is not well planned. Therefore, it has been seen that the aerial IRT should be arranged as a function of the thermographic camera and lens that will be used, selecting a flight height that satisfies the Spatial and the Measurement

Detection, classification and characterization of defects in photovoltaic modules through the use of thermography, electroluminescence, I-V curves and visual analysis

Resolutions, understanding how the resolution affects the results and how to interpret them and considering the important factors previously mentioned.

Thus, it is considered that the main objective of the doctoral thesis, which is the **analysis of the detection, characterization and classification of defects in PV modules through the use of IRT, EL, I-V curves and visual analysis** have been satisfactorily achieved by means of the suitably completion of the three partial objectives established.

3.2. Future work

Although it is considered that the goal of the thesis has been accomplished, there are plenty of advances that could be done in order to achieve supplementary results. In this section are detailed some of the open issues that could deserve further research for some of the aspects related to this thesis (some of which we are already working on).

- **Aerial inspection with EL sensors**

It has been seen how the detection accuracy of IRT is limited by many aspects, as the weather conditions, and to faults causing a sufficient increase in temperature. Another alternative fast and accurate automatic UAV-based inspection system for PV plants can be based on EL sensors. This technique could be a significant leap forward in PV plant inspection technologies, combining the speed of UAV-based inspections with the in-depth analysis of EL, detecting a wider range of PV panel failures. This automation of the EL imaging process can be done through a bidirectional PV inverter, which will require full coordination with the UAV planning.

- **Bidirectional inverters for PV maintenance**

With respect to EL, as mentioned, it is a limitation to have to disconnect the PV solar modules and connect them to an external power supply. In line with the development of aerial inspections using EL sensors, it is essential the research on bidirectional inverters. This kind of inverters can be used in aerial EL inspections to feed electricity to the strings of modules that are going to be inspected without the necessity of disconnecting the strings from the inverter neither having an external DC source that would slow down the inspection process as well as raise the price. Actually, in utility scale PV plants this kind of inverters can be already used to regulate and monitor the flow of power between a DC bus and an AC grid and to restrict the voltage expense at

the former to only a certain permissible range of voltages. A bidirectional inverter is the one that not only performs the DC to AC conversion, but also performs the conversion of AC power to DC, with the major advance of giving the flexibility to the user to decide when to buy power from an electrical grid and when to sell so as to make the maximum profit based on the price of electricity at a particular point in time.

- **Advanced measures in PV plants**

It has been seen that many different failure modes can appear at the module level. However, typically the monitoring system trails the string series current of multiple modules connected, or even the inverter current, which is the sum of the parallel string current, and does not track the performance of the individual PV modules. Therefore, PV module alarms are not frequently automatically generated being specially complicated the detection of failures at this level and even more difficult the recognition of the failure cause and mode. The need for advanced and intelligent devices to apply to PV solar modules is a necessity to turn them into plants of the future. Up to now, I-V curves is a process totally dependent on the human operator, who needs to interrupt a PV solar string to measure a single module, with the partial loss of production due to the disconnection. An element of intelligence associated with a PV solar plant of the future, could consist on a centralized / decentralized measurement of I-V curves measurement of all PV solar modules in a string, and in a coordinated and simultaneous way, minimizing the energy losses during the measures. It would allow the simultaneous electrical parameters acquisition of all modules in a string, making easier the PV plant assessment.

- **Characterization of soldering defects in the front of the module**

It is proposed the analysis of the same soldering defects performed on the front site of the cells instead of on the back site as a future work, in order to characterize them and compare the effect of the soldering defect location within the cell. It could be interesting seeing if they are detectable with EL and if the lack of this metal sheet in the front site generates heat differences in the front soldering defects, as well as comparing the power production changes in case the defects are in the front or in the back of cells. Additionally, as it has been seen that having all tabs loose may not interrupt the current in a new manufactured module, it would also be interesting to study its influence after some years of operation or after several thermal cycles.

- **Characterization of combination of PV defects by simulations**

The defects characterization performed within this thesis in combination with the electrical circuits developed, which model a PV system using LTspice, could be used to simulate the module behavior depending on the defects combination and location within a module. With this research, it could be possible predicting the PV modules behavior according to their defects without the necessity of physically having them, and to determine the impact of different defects combinations or patterns.

- **Image processing automation and PV defects detection and classification**

Something that seems to fit in the advances in O&M is the use of techniques based on AI, to be able to guarantee the early detection of failures, or the increase of the energy efficiency of PV solar plants. Once a discussion on the different thermographic defects has been provided within the thesis objectives, these results can be useful as a base to set the patterns of the different kind of defects in a software to automatically detect if a module has an anomaly and its classification.

Annex A

ADDITIONAL PUBLICATIONS

'A winner is a dreamer who never gives up.'

Nelson Mandela.

This annex includes other publications in which the author of this thesis has also contributed, although they have not been included in the “compendium of articles” of the doctoral thesis.

- Hernández-Callejo L, Gallardo-Saavedra S, Diez-Cercadillo A, Alonso-Gómez V. Analysis of the influence of DC optimizers on photovoltaic production. *Rev Fac Ing* 2020:43–55. <https://doi.org/10.17533/udea.redin.20190521>.
- Hernández-Callejo L, Gallardo-Saavedra S, Diez-Cercadillo A, Alonso-Gómez V. Study of the Influence of DC-DC Optimizers on PV-Energy Generation. *Smart Cities. Commun. Comput. Inf. Sci.*, 2019, p. 1–17. https://doi.org/https://doi.org/10.1007/978-3-030-12804-3_1.
- Hernández-Callejo L, Gallardo-Saavedra S, Diez-Cercadillo A, Alonso-Gómez V. Study of the Influence of DC-DC Optimizers on PV-Energy Generation. *Ibero-American Congr. Smart Cities (ICSC-CITIES 2018)*, Soria (Spain): 2018, p. 616–33.
- Gallardo-Saavedra S, Hernández-Callejo L, Duque-Pérez Ó. Analysis and Characterization of Thermographic Defects at the PV Module Level. In: Nesmachnow S, Hernández Callejo L, editors. *Smart Cities. Commun. Comput. Inf. Sci.*, vol. 978, Cham: Springer International Publishing; 2019, p. 80–93. https://doi.org/https://doi.org/10.1007/978-3-030-12804-3_7.
- Gallardo-Saavedra S, Hernández-Callejo L, Duque-Pérez Ó. Analysis and characterization of thermographic defects at the PV module level. *Ibero-American Congr. Smart Cities (ICSC-CITIES 2018)*, Soria (Spain): 2018, p. 487–502.
- Dávila-Sacoto M, Hernández-Callejo L, Alonso-Gómez V, Gallardo-Saavedra S, González LG. Detecting Hot Spots in Photovoltaic Panels Using Low-Cost Thermal Cameras. *Smart Cities. Commun. Comput. Inf. Sci.*, vol. 1152 CCIS, Springer; 2020, p. 38–53. https://doi.org/10.1007/978-3-030-38889-8_4.
- Dávila-Sacoto M, Hernández-Callejo L, Alonso-Gómez V, Gallardo-Saavedra S, González LG. Detecting Hot Spots in Photovoltaic Panels Using Low-Cost Thermal Cameras. *II Ibero-American Congr. Smart Cities (ICSC-CITIES 2019)*, 2019, p. 151–166.
- Hernández-Martínez B, Gallardo-Saavedra S, Hernández-Callejo L, Alonso-Gómez V, Morales-Aragónés JI. General Purpose I-V Tester Developed to Measure a Wide Range of Photovoltaic Systems. *Smart Cities. Commun. Comput. Inf. Sci.*, vol. 1152 CCIS, Springer; 2020, p. 135–45. https://doi.org/10.1007/978-3-030-38889-8_11.

- Hernández-Martínez B, Gallardo-Saavedra S, Hernández-Callejo L, Alonso-Gómez V, Morales-Aragonés JI. General purpose I-V tester developed to measure a wide range of photovoltaic systems. II Ibero-American Congr. Smart Cities (ICSC-CITIES 2019), 2019, p. 33–44.
- Hernández-Martínez B, Hernández-Callejo L, Gallardo-Saavedra S, Alonso-Gómez V, Morales-Aragones JI. Low-cost illumination system for photovoltaic devices validation at the control and constant irradiance. II Ibero-American Congr. Smart Cities (ICSC-CITIES 2019), 2019, p. 842–851.
- Ballestín-Fuertes J, Muñoz-Cruzado-Alba J, Sanz-Osorio JF, Hernández-Callejo L, Alonso-Gómez V, Morales-Aragones I, Gallardo-Saavedra S, et al. Novel Utility-Scale Photovoltaic Plant Electroluminescence Maintenance Technique by Means of Bidirectional Power Inverter Controller. Appl Sci 2020: 3084. <https://doi.org/10.3390/app10093084>.